Magnetoencephalography to image the influence of different spinal cord stimulation paradigms on somatosensory evoked responses

MSc Technical Medicine
Janne Luijten

TU Delft

Erasmus MC
Universitair Medisch Centrum Rotterdam

This page was intentionally left blank.

Magnetoencephalography to image the influence of different spinal cord stimulation paradigms on somatosensory evoked responses

Janne Luijten

Student Number: 4460855

12 December 2023

To obtain the degree of Master of Science in Technical Medicine from Leiden University, Delft University of Technology, and Erasmus University Rotterdam.

Supervisors:

- Dr. ir. Cecile de Vos
- Laurien Reinders, MSc
- Prof. dr. ir. Alfred Schouten
- Dr. Sander Frankema

Thesis committee members:

- Dr. ir. Cecile de Vos, EMC
- Prof. dr. ir. Alfred Schouten, TU Delft (Chair)
- Dr. Sander Frankema, EMC
- Dr. ir. Mark van Ruit, TU Delft

Universiteit Leiden The Netherlands

TU Delft Delft University of Technology

Erasmus University Rotterdam

This page was intentionally left blank.

Preface

This master thesis concludes my time as a student at the Delft University of Technology, Erasmus University Rotterdam, and Leiden University. During my Bachelor in Clinical Technology, I developed a preference for the more technical-oriented courses, particularly those focused on signal analysis. Additionally, I have always been interested in the human brain. After my bachelor's, I completed a bridging year in Mechanical Engineering to explore the more technical aspects of the clinical-technical spectrum, because I figured that the Technical Medicine master was too clinically oriented for my preferences. However, during the bridging year, I was still hesitating so I also followed the Technical Medicine course on Advanced Signal Processing to see whether I did like the Technical Medicine master. This course made me decide to return to Technical Medicine again because, to me, it represented the perfect combination and integration of technical and clinical aspects.

For this master thesis, I found this combination and integration of technical and clinical aspects again in the shape of a challenging project. In the last year, I have learned a lot about patients suffering from chronic pain, the functioning of the brain, and signal analysis. I hope that my research efforts contributed, albeit minimal, to this interesting field.

Thank you, **Cecile**, for your help with this thesis and beyond. Your enthusiasm and attitude to go above and beyond for your students inspires me both academically and on a personal level. A prime example of this was ensuring that I could attend the e-INS congress in Hamburg. Thank you, **Laurien**, for the help and friendship. It was fun to have you as a friend c.q. supervisor this past year to discuss this project, and everything else. Having worked together on so many projects since the start of our bachelor's, it is special to finish my master's working together again. Thank you, **Alfred**, for the birds-eye view and for making sure we did not overlook anything. You often asked sharp questions about issues I hadn't noticed myself. Thank you, **Sander**, for your feedback on the medical aspects of this thesis. Our conversations often strayed from the scope of the project, but were always interesting. Thank you, **everyone in Na-17**, for your friendship throughout the year. Thanks to my friends and housemates for the fun times outside of my thesis.

Mom, Dad, *, Kars, and Halithan, thank you for your endless belief in me and your unconditional help and support.

Janne Luijten
Rotterdam, December 2023

Abstract

Introduction

Chronic pain is an increasing problem in terms of prevalence and disease-related costs. Due to its complexity, it is difficult to treat. Spinal cord stimulation (SCS) is a neurostimulation therapy with a relatively good success rate for patients with severe, intractable chronic pain. The mechanisms of action (MOAs) of SCS are considered to rely on spinal and supraspinal mechanisms. It has been suggested that newer SCS paradigms, such as burst SCS, may act through different MOAs than the traditional tonic SCS paradigm. Tonic and burst SCS are both postulated to act on the lateral pain pathway, which is associated with the location and character of a stimulus, whereas burst SCS is postulated to additionally act on the medial pain pathway, which is associated with the emotional/attentional processing of a stimulus. Somatosensory evoked responses (SERs) can be used to evaluate the processing of somatosensory stimuli and may aid in the unraveling of the MOAs of SCS.

Aim

The aim of this thesis is to assess how burst and tonic SCS affect the supraspinal SERs elicited by non-painful transcutaneous electrical stimulation of the tibial nerve as well as of the median nerve. The two distinct SERs are evaluated using magnetoencephalography (MEG).

Methods

26 chronic pain patients treated with SCS underwent MEG sessions after receiving tonic and burst SCS for one week. Four of these patients additionally underwent a MEG session before SCS treatment. During each session, approximately 200 non-painful electrical stimuli were applied to the median nerve as well as to the tibial nerve to elicit SERs. The SERs were compared in various cortical and subcortical regions of interest (ROIs). The following comparisons were made: 1) SERs in chronic pain patients before SCS implantation versus SERs in the same individuals during SCS, 2) SERs elicited by tibial nerve stimulation versus SERs elicited by median nerve stimulation, 3) SERs during tonic SCS versus SERs during burst SCS, and 4) the SERs in four case studies of two good and two poor responders to the tonic and/or burst SCS paradigms.

Results

22 patients were included for analysis. The number of patients varied among comparisons to facilitate within-patient comparisons. The results suggested an inhibitory effect of SCS on the SER elicited by tibial nerve stimulation, whereas the amplitude of the SER elicited by median nerve stimulation tended to increase during SCS. For both the SERs elicited by tibial nerve and by median nerve stimulation, the SER amplitudes were predominantly higher during burst SCS compared to tonic SCS. Differences in SER amplitude that were observed in the case studies did not correlate with pain relief.

Conclusion

The results suggested a spinal MOA of SCS on the SER, however, supraspinal MOAs likely play a role as well. The results did not suggest that burst SCS additionally acts on the emotional/attentional processing compared to tonic SCS. No evidence was found to support a correlation between the effect of SCS on the SER and the effect of SCS on the pain, underscoring the complexity of the relationship between somatosensory processing and pain perception in the context of SCS.

Contents

List of Abbreviations

AAL2	automated anatomical labelling atlas 2
AAL3	automated anatomical labelling atlas 3
ACC	anterior cingulate cortex
pgACC	pregenual anterior cingulate cortex
AUC	area under the curve
CRPS	complex regional pain syndrome
DC	direct current
DNP	diabetic neuropathy
ECG	electrocardiogram
EEG	electroencephalography
FBSS	failed back surgery syndrome
IC	insular cortex
MCC	middle cingulate cortex
MEG	magnetoencephalography
MN	Minimum Norm
MOA	mechanism of action
MRI	magnetic resonance imaging
NRS	numerical rating scale
PAG	periaqueductal gray
PCC	posterior cingulate cortex
PSD	power spectral density
PSPS	persistent spinal pain syndrome
ROI	region of interest
SCS	spinal cord stimulation
SER	somatosensory evoked response
SSP	signal-space-projection
S1	primary somatosensory cortex
S2	secondary somatosensory cortex
TTL	transistor-transistor logic

1 Introduction

1.1. Chronic Pain: an Increasing Problem

The International Association for the Study of Pain (IASP) defines pain as ”an unpleasant sensory and emotional experience associated with, or resembling that associated with, actual or potential tissue damage” [1]. The ability to feel pain is the body’s defense mechanism to maintain its integrity and protect itself. Usually, this pain subsides once healing of an injury or treatment of an illness has occurred [2]. Chronic pain is defined as pain that persists or recurs for more than three months, which is considered the period of healing of an acute injury [1, 3, 4].

Chronic pain imposes a vast personal and economic burden [5]. Chronic pain affects most domains of quality of life, primarily physical and emotional functioning, and is associated with other chronic comorbidities, such as coronary heart disease and depression [6]. The prevalence of chronic pain is high, affecting approximately 11% to 40% of the global population [5, 7]. Low back pain was the main cause of years lived with disability in 2020, and projections through to 2050 suggest that its prevalence will increase [8]. It is expected that both the total disability burden and disease-related costs will further increase in the coming decades [9]. This emphasizes the importance of achieving effective treatment for chronic pain.

1.2. Chronic Pain: a Complex Concept

Chronic pain is a complex concept with limited understanding. It often arises due to a disease or injury, but chronic pain is not solely a symptom; rather, it is a distinct condition with its own etiologies, medical definition, and classification [10]. Despite its complexity, some pathways and key structures in the processing and experience of chronic pain have been identified. According to De Ridder et al., chronic pathological pain can be anatomically as well as symptomatically separated into three distinct yet interacting pathways, consisting of an ascending lateral, an ascending medial, and a descending pathway, as shown in Figure 1.1 [4].

The lateral “painfulness” pain pathway comprises the lateral thalamic nuclei [11], the primary somatosensory cortex (S1), and the secondary somatosensory cortex (S2) [4, 11]. This pathway encodes the discriminatory/sensory component of pain, such as painfulness, pain localization, and pain character (burning, aching, etc.) [4, 12]. The medial “suffering” pain pathway comprises the medial thalamus [11], the (anterior) cingulate cortices [4, 11], and the insular cortices [4]. This pathway processes the affective motivational aspect (in other words: the unpleasant emotional component) of pain [4, 12, 13]. The medial pain pathway has been considered to be slower compared to the lateral pain pathway [11]. The descending pain pathway involves the rostral and pregenual anterior cingulate cortex (ACC) and the periaqueductal gray (PAG), and is considered to be a pain inhibitory pathway [4, 12, 13].

Chronic pain may be explained by an imbalance between the two ascending “pain input” pathways and the descending “pain suppression” pathway [4, 12–14]. Based on this imbalanced triple pathway model to explain chronic pain, an effective treatment method should target both the ascending pathway(s) and the descending pathway to reduce the imbalance [13]. Spinal cord stimulation (SCS) is considered a treatment method to achieve this [12, 13].

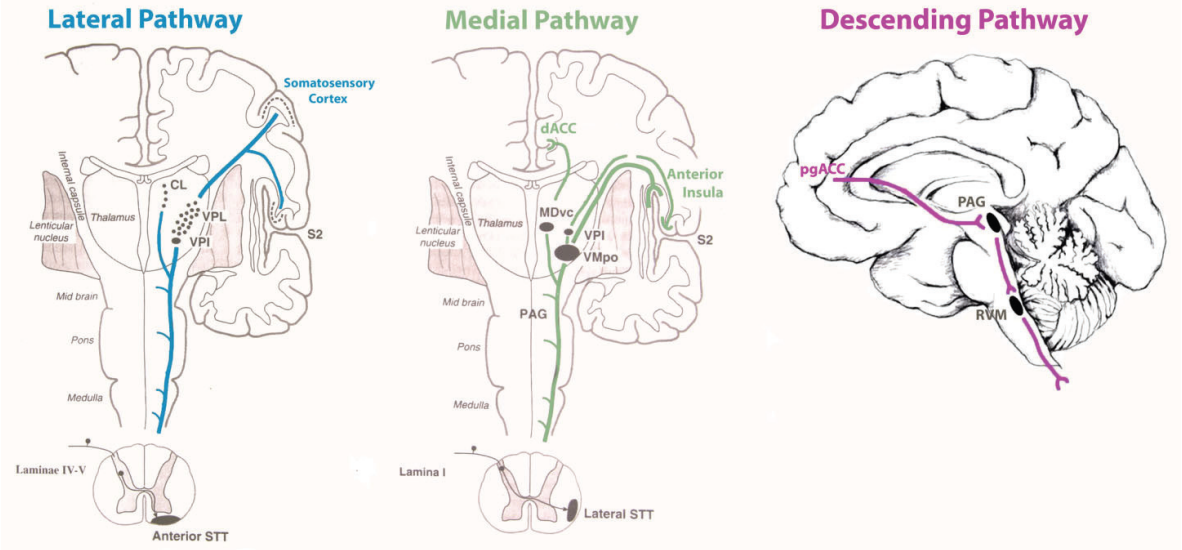

Figure 1.1: An overview of the structures comprising the ascending lateral, ascending medial, and descending pain pathway. The ascending lateral pathway processes the discriminatory components of pain, whereas the ascending medial pathway processes the motivational, affective, and attentional components of pain. The descending, pain inhibitory pathway suppresses ongoing pain. Figure from De Ridder et al. [12]

1.3. Spinal Cord Stimulation

SCS is a neurostimulation therapy for patients with severe, otherwise intractable chronic pain [15]. SCS has a long-term success rate of 47% to 74% for various chronic pain conditions, such as complex regional pain syndrome (CRPS) and persistent spinal pain syndrome (PSPS), formerly known as failed back surgery syndrome (FBSS), where success is generally defined as pain relief of $\geq$ 50% [16–18]. The conventional SCS paradigm consists of a tonic waveform applied to the dorsal column, which causes paresthesias in the area innervated by the stimulated nerve fibers [19, 20]. In the last decade, paresthesia-free SCS paradigms were developed, such as burst SCS. The burst SCS paradigm consists of groups of five pulses at a high frequency and at amplitudes much lower than tonic stimulation, mimicking physiological thalamocortical firing [19, 21–23]. The tonic and burst SCS waveforms are shown in Figure 1.2 and Figure 1.3, respectively.

Traditionally, the mechanism of action (MOA) of SCS relied on the Gate Control Theory as proposed by Melzack and Wall in 1965 [24]. The Gate Control Theory is a spinal mechanism that states that nociceptive signals, carried by C- and Aδ-fibers, are inhibited by stimulating non-nociceptive Aβ-fibers. These Aβ-fibers activate inhibitory neurons in the substantia gelatinosa of the dorsal horn of the spinal cord, thereby ”closing the gate” for incoming nociceptive input from C- and Aδ-fibers [25, 26]. The ”closed gate” prevents transmission of nociceptive signals to the brain and, thus, inhibits pain sensation. SCS is targeted at the activation of these same Aβ-fibers in the dorsal column of the spinal cord.

Besides the Gate Control Theory, additional MOAs are considered to be involved in SCS with interactions at spinal and supraspinal levels. These interactions include activation of the descending pain inhibitory pathways and activation of supraspinal structures [25–28]. Moreover, it has been suggested that newer SCS paradigms, such as burst SCS, may act through different MOAs than the traditional tonic SCS [22, 29–35]. Tonic SCS is suggested to modulate the ascending lateral pain pathway as well as the descending pain inhibitory pathway, whereas burst SCS is suggested to additionally modulate the ascending medial pain pathway [12, 13]. This indicates that tonic SCS may merely modulate the somatosensory ”painfulness” processing of pain, while burst SCS may additionally modulate the emotional ”suffering” aspect of pain [12, 13].

To research the differences in the MOAs of the tonic and burst SCS paradigms, the thalamus as a brain structure is particularly interesting because both the lateral and medial ascending pathways include (a substructure of) the thalamus. The thalamus is a key relay station for the transmission of sensory information and is involved in acute and chronic pain functions [36]. Based on anatomical,

electrophysiological, cognitive, and clinical evidence, the thalamus can be broadly divided into lateral and medial subdivisions, both associated with pain processing [4, 26, 36–39]. The lateral thalamic pain pathway includes the ventral posterior nuclei (VP) and the posterior nuclei (PO), the medial thalamic pain pathway includes the intralaminar nuclei (ILN), medial dorsal nuclei (MD), and midline nuclei [36]. In the context of the thalamus, it is suggested that burst SCS activates both the medial and lateral spinothalamic tracts whereas tonic SCS only activates the lateral spinothalamic tract, which renders the thalamus an interesting structure to research the differences in the MOAs of tonic and burst SCS [40].

Despite the relatively high success rate of SCS, a group of chronic pain patients that does not benefit from SCS remains. To understand why SCS is not effective in all chronic pain patients, to identify this group of chronic pain patients before unnecessary implantation, and to improve outcomes for patients that do benefit from SCS, it is crucial to further unravel the mechanisms of action of SCS.

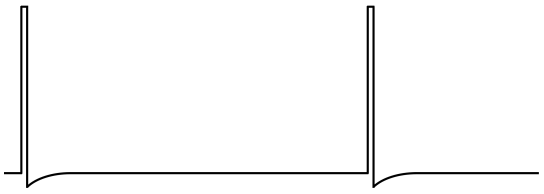

Figure 1.2: Tonic spinal cord stimulation waveform

Figure 1.3: Burst spinal cord stimulation waveform

1.4. Somatosensory Evoked Responses

To obtain more insights into the MOAs of SCS, somatosensory evoked responses (SERs) can be used to evaluate somatosensory processing, and combined with SCS, how somatosensory processing is affected by SCS. A somatosensory evoked response (SER) is the neuronal activity that results from somatosensory input, such as touch or electrical stimulation [41, 42]. Similar to the process of system identification in engineering, which necessitates perturbation of a system to estimate its properties [43], using stimuli to elicit SERs can assist in illustrating an individual's somatosensory processing. The stimulus to elicit the SER can be painful or non-painful. SERs elicited by painful stimuli mainly travel through Aδ- and C-fibers, whereas SERs elicited by non-painful stimuli mainly travel through Aβ-fibers [42]. For this thesis, non-painful stimuli were used to elicit the SERs; assessing how SCS affects these non-painful SERs is of interest because SCS stimulates these same Aβ-fibers on the dorsal column.

SERs can generally be divided into early, middle, and late latency components. The expected latency, especially for the early component, is associated with the stimulation site and the recording location. In this thesis, the stimulation sites were the median nerve at the wrist and the tibial nerve at the ankle. The recording location was supraspinal (on the brain). Following non-painful tibial nerve stimulation at the ankle, the early component of the SER occurs in the foot area of the S1 around 40 to 60 milliseconds after stimulation [44, 45]. The early component is associated with the ascending lateral pathway, which encodes somatosensory processing, such as the localization and character of the stimulus [4, 46]. The middle latency component of the SER elicited by tibial nerve stimulation occurs around 130 to 170 milliseconds after stimulation in the S2, the thalamus, the cingulate cortices, and the insular cortices [45, 47–50]. The middle latency component is associated with both the ascending lateral and medial pathways. The late latency component of the SER elicited by tibial nerve stimulation occurs around 250 to 300 milliseconds after stimulation in the somatosensory cortices, the cingulate cortices, the thalamus, and the insular and opercular cortices [45, 46, 50–52]. The late latency component is associated with the ascending medial pathway and reflects the attentional/emotional processing of a stimulus [4, 46].

For the SER elicited by non-painful median nerve stimulation at the wrist, the early component occurs around 20 to 60 milliseconds after stimulation in the hand area of the S1 [53, 54]. This component has also been recorded from the thalamus at 15 milliseconds following painful and non-painful median nerve stimulation in chronic pain patients, using intracerebral electrodes [48, 55, 56]. The middle latency component occurs around 80 to 150 milliseconds after stimulation in the S2, the cingulate cortices, the insular cortices, and the thalamus [47, 48, 53]. The late latency component occurs around 250 to 300 milliseconds after stimulation in the somatosensory cortices, the cingulate cortices, the thalamus, and the insular and opercular cortices [48, 51, 52].

1.4.1. Somatosensory Evoked Responses in Chronic Pain Patients

In chronic pain patients, the SERs may be altered; Pinheiro et al. reported a decrease in the amplitude of the SER elicited by various stimuli in chronic pain patients compared to healthy controls [57]. Next to this, research has been conducted on assessing the influence of SCS on the supraspinal SER elicited by non-painful as well as painful stimuli in patients with chronic pain [45, 46, 48, 49, 54, 58–75].

Most studies assessed the influence of tonic SCS on non-painful stimulation and the majority reported decreased or complete loss of the early SER amplitude [45, 59, 61, 66–69, 72–74], whereas some studies reported no difference [46, 62, 66, 75]. A small set of studies examined the influence of paresthesia-free SCS paradigms on the early component of the non-painful SER and the reported results were inconclusive [46, 54, 60, 68, 73]. For the middle latency components of the SER, Polácek et al. reported a decrease of the SER amplitude [45], whereas Blair et al. reported no change [66] during tonic SCS. For the late components of the SER, the effect of tonic SCS on the SER amplitude was not conclusive; studies found a decrease [45, 66], an increase [62] as well as no change [62, 75] of the SER amplitude. One study, by Niso et al., reported a decreased late SER amplitude during tonic SCS and burst SCS while participants were not paying attention to the stimuli, whereas burst SCS also decreased the SER while participants were paying attention to the stimuli [46].

Various MOAs have been hypothesized in these studies regarding the inhibitory effect of SCS on the SER. These MOAs can be categorized into segmental spinal, spinal, and supraspinal mechanisms. Hypothesized theories for segmental spinal mechanisms include a conduction block at the site of stimulation [54, 66, 73], decreasing neuronal hyperexcitability in the dorsal horn [74], and the Gate Control Theory [45, 74]. An often-cited spinal mechanism for tonic SCS is the mechanism of interference, also called the collision of impulses theory, which posits that the ascending volley generated by the somatosensory stimulus and the descending action potentials induced by SCS collide and mutually nullify one another. A schematic representation of this theory is illustrated in Figure 1.4. However, these (segmental) spinal theories do not explain selective inhibition of SER components, which were reported in multiple studies [45, 46, 62, 75]. Hypothesized supraspinal mechanisms for SCS include decreased somatosensory processing resulting from input from lemniscal neurons [45], modulation of somatosensory processing at the thalamic level [45], and descending inhibitory controls [54, 74]. For burst SCS specifically, an inhibitory drive involving both the GABAergic and glutamatergic networks [54, 71] and for the late SER component specifically reduction of the capacity for cortical attention directed to somatosensory stimuli are hypothesized [46]. These specific MOAs for burst are based on reduced attentional processing through activation of the medial pathway, in alignment with the triple pathway model (section 1.2).

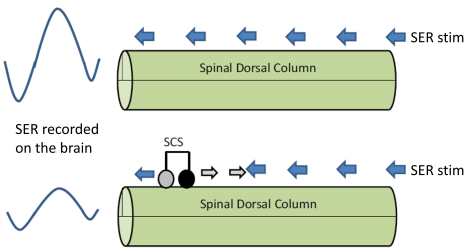

Figure 1.4: Schematic representation of the collision of impulses theory, adjusted from Urasaki et al. [67]. Electrical stimulation pulses elicited by tibial nerve stimulation travel along the dorsal column of the spinal cord and elicit supraspinal somatosensory evoked responses (SERs). Due to the collision between ascending SER impulses and antidromic spinal cord stimulation pulses, the amplitude of the SER is attenuated.

The abovementioned studies share a commonality in not attempting to assess the specific MOAs involved by eliciting the SERs at various locations. In each study, the SERs were elicited either within the area innervated by the spinal cord stimulator or in an area where the propagating SER entered the spinal cord below the SCS electrodes. To differentiate between the hypothesized spinal and supraspinal effects, and predominantly to assess the spinal MOAs, SERs elicited at two distinct locations should be compared; SERs that enter the dorsal column both *above* and *below* the SCS electrode. In this thesis, SERs were elicited at two different locations, on the median nerve and the tibial nerve, while all patients were treated with SCS for chronic pain in the back and/or the lower extremities. Consequently, the SERs elicited on the median nerve enter the dorsal column *above* the SCS electrode on the dorsal column, whereas the SERs elicited on the tibial nerve enter the dorsal column *below* the SCS electrode or at the same level, allowing for the exploration of spinal effects.

Additionally, the vast majority of studies utilized a limited number of recording electrodes ($\leq$ 10) to capture the SER, which complicates the detection of supraspinal mechanisms [54, 59–62, 66–69, 72–75]. Contrarily, studies that utilized numerous electroencephalography (EEG) electrodes or whole-head magnetoencephalography (MEG) generally hypothesized both spinal and supraspinal mechanisms [45, 46, 63]. For this thesis, whole-head MEG was employed as a measurement technique, facilitating the assessment of supraspinal effects as well.

1.5. Magnetoencephalography

As described in the previous section, the SERs are assessed using magnetoencephalography (MEG), which is a non-invasive imaging technique that detects brain activity. An electric current, such as neuronal activity, is always associated with a magnetic field perpendicular to its direction, following the right-hand rule [76]. These small magnetic fields can be detected by MEG using very sensitive magnetometers [76]. A schematic overview of the neuronal magnetic fields that can be detected using MEG is shown in Figure A.1. To perform a MEG measurement, the patient is situated with its head in a MEG ”helmet”, as is shown in Figure A.2. These measurements must be performed in a magnetically shielded room to shield out the earth’s relatively strong magnetic field [76, 77].

Research into SERs frequently employ EEG as measurement modality due to its affordability, accessibility and mobility [42, 78]. Both MEG and EEG can detect brain activity with a temporal resolution in the sub-millisecond range, which is useful for research into SERs [76–81]. EEG signals are strongly affected by differences in electrical conductivity between different tissues, such as the scalp, skull, cerebrospinal fluid and the brain [76, 81]. In contrast, MEG signals are homogeneous across all tissue compartments, including the air between the scalp and sensors, because the magnetic permeability of biological tissues is almost the same as that of empty space [81]. Consequently, MEG provides better spatial resolution of source localization (2-3mm) than EEG (7-10mm) at the cortical surface [76, 78, 80, 81]. For deeper structures, the signal to noise ratio decreases with source depth [81]. This is because superficial cortical sources produce MEG signals up to 100 times stronger than deeper subcortical structures at equivalent current strengths, resulting in uneven sensitivity and spatial resolution of MEG source imaging across the brain [81]. However, both modeling and growing experimental evidence suggest that optimized paradigm designs and signal extraction techniques enable MEG resolution of deeper subcortical brain regions like the insula and thalamus [81].

1.6. Thesis Aim

The primary objective of this thesis is to assess how various spinal cord stimulation (SCS) paradigms affect the supraspinal somatosensory evoked response (SER) elicited by a non-painful peripheral stimulus. To fulfill this objective, supraspinal SERs elicited by non-painful transcutaneous electrical stimulation of the tibial nerve as well as of the median nerve are evaluated in chronic pain patients treated with SCS, utilizing magnetoencephalography (MEG) as a measurement technique. The utilized SCS paradigms are tonic and burst SCS. The supraspinal SERs are compared among various groups, namely:

1) SERs in chronic pain patients before SCS implantation versus SERs in the same individuals during both SCS paradigms,
2) SERs elicited by tibial nerve stimulation versus SERs elicited by median nerve stimulation in patients before SCS implantation and during tonic and burst SCS,
3) SERs during tonic SCS versus SERs during burst SCS, and
4) four case studies of two responders and two non-responders to the tonic and/or burst SCS paradigms.

1.7. Hypotheses

The influence of SCS on the SERs will primarily be assessed concerning the amplitude of the SER. To date, none of the studies examining changes in the latency of the SER during SCS have observed any changes [45, 63, 69, 72, 74]. The influence of SCS on the SERs will primarily be assessed concerning the amplitude of the SER, as, to date, none of the studies examining SER latency changes during SCS have observed any changes [45, 63, 69, 72, 74]. Overall, based on the available literature, I anticipate an inhibitory effect of SCS on the amplitude of the supraspinal SERs elicited by tibial nerve stimulation. Regarding the supraspinal SERs elicited by median nerve stimulation, to date, no literature is available describing the effect of SCS on these SERs while the SCS electrode was positioned on the spinal cord *below* the entrance level of the SERs elicited by median nerve stimulation. Consequently, for the SERs elicited on the median nerve, the hypotheses stated below are not necessarily based on similar research. In the sections below, the specific hypotheses for all comparisons are described.

1.7.1. Before SCS and During SCS (Aim 1)

In this comparison, the SERs elicited by tibial nerve stimulation as well as by median nerve stimulation in chronic pain patients before SCS treatment will be compared to the SERs in the same individuals when treated with tonic and burst SCS.

Tibial Nerve

For the SERs elicited by tibial nerve stimulation, based on the available literature, I expect decreased SER amplitudes during SCS compared to without SCS. Regarding the early component, according to the majority of studies that reported on this, I expect a SER amplitude decrease during tonic SCS compared to before SCS implantation [45, 59, 61, 66–69, 72–74]. This corresponds to the hypothesis that tonic SCS operates on the lateral pain pathway (section 1.3), thereby inhibiting the somatosensory processing represented by the early SER component. For burst SCS, the results in the literature are less conclusive. Urasaki et al. did not find a decreased SER amplitude during burst SCS at paresthesia threshold compared to SCS off. However, when burst SCS was employed at the maximum paresthesia threshold, the SER amplitude was decreased [68]. I would anticipate that burst SCS inhibits the early SER amplitude compared to before SCS as well, as burst SCS is also postulated to act on the lateral pathway, similar to tonic SCS. For the middle latency component, I expect decreased SER amplitudes for tonic SCS [45, 66]. For burst SCS, I expect decreased amplitudes as well, as burst SCS is postulated to act on both the medial and lateral pathways, which are both associated with the middle latency component. Concerning the late component, I expect decreased SER amplitudes for tonic SCS [45, 66] as well as for burst SCS [46], compared to before SCS.

Median Nerve

For the SERs elicited by median nerve stimulation, anticipating the effect of SCS is more challenging due to the abovementioned research gap. If the mechanism of action of SCS on the SER is primarily spinal, this would result in less or no attenuation of the SERs elicited on the median nerve during SCS compared to before SCS. However, particularly for the late latency SER component, supraspinal MOAs of SCS have also been hypothesized, as was described in subsection 1.4.1. Supraspinal MOAs of SCS

should, in theory, apply to the SERs elicited on the median nerve similarly to the SERs elicited on the tibial nerve. Consequently, taking into account that the MOA of SCS is most probably a combination of both spinal and supraspinal mechanisms, I anticipate attenuation of the SERs elicited on the median nerve as well, albeit less compared to the SERs elicited on the tibial nerve.

1.7.2. Tibial Nerve and Median Nerve (Aim 2)

In this comparison, the SERs elicited on the tibial nerve will be compared to the SERs elicited on the median nerve in patients before SCS treatment, as well as during tonic and burst SCS, to assess whether a spinal MOA possibly contributes to the effect of SCS on the SER. Initially, this comparison will be performed in the subpopulation of patients treated with tonic and burst SCS who were also included in the study before SCS treatment, as described in subsection 1.7.1. In this manner, the differences or similarities between the SERs elicited on the median nerve and on the tibial nerve before SCS treatment can be compared with the differences or similarities between the SERs elicited on the median nerve and on the tibial nerve during treatment with tonic and burst SCS in these same individuals. Subsequently, the measurements before SCS treatment from this subpopulation will be compared to the population of all included patients during both SCS paradigms to assess whether a potential trend within the subpopulation subsides or fortifies in a larger population.

Based on a frequently cited theory for the observed SER amplitude decrease during tonic SCS, called the collision of impulses theory, I expect differences in the decrease of the two distinct SERs during SCS [61, 67–69, 72, 74]. However, this theory has not been evaluated yet using two distinct SER stimulation locations during SCS. In the patients included in this thesis, the SCS electrode is located on the dorsal column below the entrance level of the SERs elicited by median nerve stimulation and above or at the entrance level of the SERs elicited by tibial nerve stimulation, as is schematically illustrated in Figure 1.5. Consequently, this theory postulates an exclusive or greater decrease of the SER amplitude elicited by tibial nerve stimulation compared to the SER amplitude elicited by median nerve stimulation during SCS.

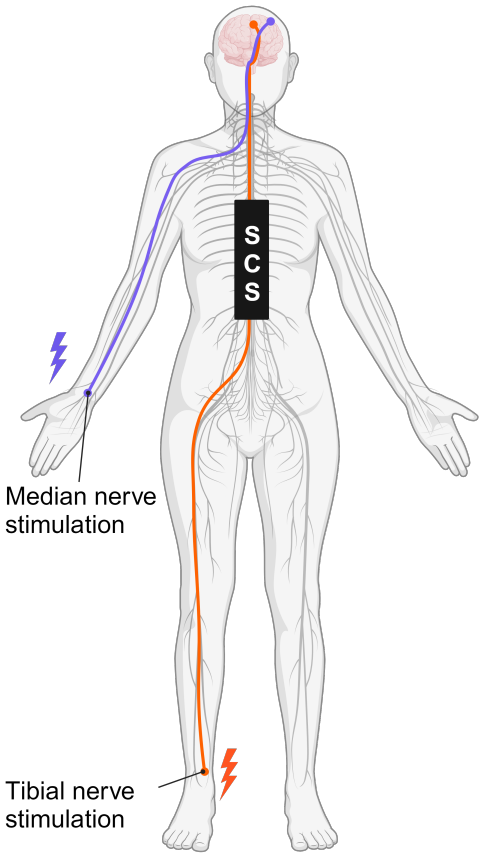

Figure 1.5: The spinal cord stimulation electrodes are located on the dorsal column *below* the entrance level of the somatosensory evoked responses (SERs) elicited by median nerve stimulation and *above* the entrance level of the SERs elicited by tibial nerve stimulation. This figure was created with BioRender.com.

1.7.3. Tonic SCS and Burst SCS (Aim 3)

In this comparison, the SERs elicited by tibial nerve stimulation as well as by median nerve stimulation will be compared during tonic and burst SCS. For this comparison in particular, the thalamus will be useful as a region of interest (ROI), divided into a medial and a lateral part. This specific brain structure will help assess whether both burst and tonic SCS exhibit similar effects on the lateral pain pathway, and whether burst SCS additionally acts on the medial pain pathway.

Tibial Nerve

For tibial nerve stimulation, I do not expect differences in the early components of the SER amplitudes between the two SCS paradigms, as has been reported by Niso et al. [46]. Both tonic and burst SCS are considered to act on the lateral pathway, suggesting that both paradigms might affect the early SER component similarly. Based on the same study, I expect a greater decrease of the late SER amplitude during burst SCS compared to tonic SCS [46]. Niso et al. reported a decreased amplitude of the late component of the SER elicited on the tibial nerve during burst SCS, compared to tonic SCS, when patients focused on the applied SER stimuli. In alignment with this, during the measurements performed for this thesis, patients focused on the applied stimuli as well; therefore, I anticipate similar results.

Median Nerve
For median nerve stimulation, no literature is available comparing various SCS paradigms. However, for the late component specifically, the supraspinal mechanism of burst SCS acting on the medial pathway as opposed to tonic SCS, thereby attenuating this attentional/emotional processing component of the SER, should apply to SERs elicited by median nerve stimulation as well. Consequently, I hypothesize a decreased late SER amplitude that is more pronounced during burst SCS compared to tonic SCS, similar to the SERs elicited by tibial nerve stimulation.

1.7.4. The Effect of Pain Reduction (Aim 4)

For this comparison, four patient cases are examined: one patient is a non-responder to both tonic SCS and burst SCS, one patient is a responder to both tonic SCS and burst SCS, one patient is a non-responder to tonic SCS and a responder to burst SCS, and one other patient is a responder to tonic SCS and a non-responder to burst SCS. An overview of this is provided in Table 1.1.

Table 1.1: An overview of the patients selected for the case studies aimed at exploring the potential correlation between the effect of spinal cord stimulation on the somatosensory evoked response and on chronic pain.

	Tonic	Burst
PT05	NR	NR
PT06	R	R
PTN05	NR	R
PTN08	R	NR

NR, non-responder;
R, responder.

Using these patients' MEG data, it is possible to explore a potential correlation between the effect of SCS on the SER amplitude and the effect of SCS on chronic pain. The differences for the SERs elicited by median nerve and tibial nerve stimulation can be assessed within each patient, comparing the two paradigms. Additionally, the difference between the two responders and the two non-responders to tonic SCS and burst SCS can be assessed within the paradigms. To date, available literature has not revealed a correlation between SER amplitude reduction and pain reduction, although it has been researched [67, 69, 74]. Therefore, based on the literature, differences in the effect of SCS on the SER amplitude correlating with pain reduction due to SCS are not expected. This expectation applies to both the SERs elicited on the tibial nerve and the SERs elicited on the median nerve.

2

Methods

2.1. Data Acquisition

Data acquisition for this study was performed at two institutions: the Montreal Neurological Institute (MNI) in Canada and the Donders Institute Nijmegen in the Netherlands. The study was approved by the Institutional Review Board of the Montreal Neurological Institute and the CMO (Dutch: Commissie Mensgebonden Onderzoek) region Arnhem-Nijmegen. All patients included in the study provided written informed consent.

2.1.1. Patients

The dataset encompassed recordings from a total of 26 chronic pain patients who were treated with SCS, with 11 patients recorded in Montreal and 15 in Nijmegen. Four of these patients had also previously participated in the study as chronic pain patients before treatment with SCS. Their recordings before SCS treatment were included in this thesis as well to facilitate the comparison between before SCS and during SCS. All patients reported chronic pain in their low back and/or lower extremity. An overview of the patient population is provided in Table F.1.

2.1.2. Study Protocol

At the start of each measuring session, the current pain score on the numerical rating scale (NRS, 0-10) attributed to the chronic pain condition was assessed. Each MEG measuring session lasted approximately 40 minutes and consisted of several measurements: a resting state recording, a recording acquired during non-painful transcutaneous electrical stimulation of the median nerve, a recording acquired during non-painful transcutaneous electrical stimulation of the tibial nerve, and three recordings acquired during a conditioned pain modulation test. For this thesis, the measurements during non-painful stimulation of the median and tibial nerve were used.

Spinal Cord Stimulation

The patients underwent three measuring sessions, during each of which they were treated with a different SCS paradigm: tonic SCS, burst SCS, or a sham SCS paradigm created for this study. The order of SCS paradigms was randomized and counterbalanced among the patients. The SCS was active during the measurements. At the end of each measuring session, the SCS settings were adjusted to the new SCS paradigm. The visits were separated by a one-week interval in which the new SCS paradigm was used, acting as a washout period for the previous SCS paradigm setting. The patients as well as the researchers performing the measurements were blinded to the SCS settings. However, the difference between the tonic SCS paradigm, which elicits paresthesias, and the burst and sham SCS paradigms, which do not produce paresthesias, is perceivable for the patients. Therefore, the patients could not be completely blinded.

The sham SCS paradigm is a modified version of the burst SCS paradigm designed to deliver minimal energy, existing of groups of two pulses at the same frequency as burst SCS and at the lowest possible amplitude. The sham SCS waveform is shown in Figure H.1. Because the therapeutic efficacy of the sham SCS paradigm is unknown, and because it is not clinically used, the analysis in this thesis focuses on the tonic and burst SCS paradigms. For the sham SCS paradigm, the results are presented and discussed in Appendix H.

Somatosensory Evoked Responses
As stated in subsection 2.1.2, the recordings acquired during non-painful transcutaneous electrical stimulation of the median nerve as well as of the tibial nerve were used for this thesis. The median nerve was stimulated at the right wrist; the tibial nerve was stimulated at the right ankle. During the measurements, patients sat comfortably in a chair positioned within the magnetically shielded room of the MEG scanner. Throughout the recording session, the patients were asked to relax and keep their eyes open looking at a fixation cross. The stimulation to elicit the SERs was delivered via transcutaneous electrical stimulation with Ag-AgCl surface electrodes. Square wave pulses with a duration of 0.2 milliseconds (constant current stimulator model DS7A, Digitimer Limited, UK) were delivered with the anode positioned distally. Stimuli were delivered at an average frequency of 0.9 Hertz, with the inter-stimulus interval randomly varying from 0.7 to 1.5 seconds.

To determine the stimulation intensity in milliamperes, first, the stimulation intensity was increased to the perception threshold. Subsequently, stimulation was increased to achieve a non-painful yet stable muscle twitch caused by the muscle innervated by the motor counterpart of the sensory nerve that needed to be stimulated. For tibial nerve stimulation, this twitch should be visible for the big toe; for median nerve stimulation, this twitch should be visible for the thumb. The identification of the muscle twitch was conducted because motor fibers have a higher threshold than the sensory fibers, implying that all sensory Aβ-fibers are stimulated at this point. The stimulation intensity for the muscle twitch was used to elicit the SERs. The stimulation intensities for the perception threshold and the muscle twitch, as well as a pain score on the numerical rating scale (NRS) attributed to the applied stimuli, were reported. During each SER recording, around 200 stimuli were applied, varying from 196 to 204. The patients were asked to silently count the applied stimuli and report the number to the researcher afterward. An overview of the study protocol is shown in Figure 2.1.

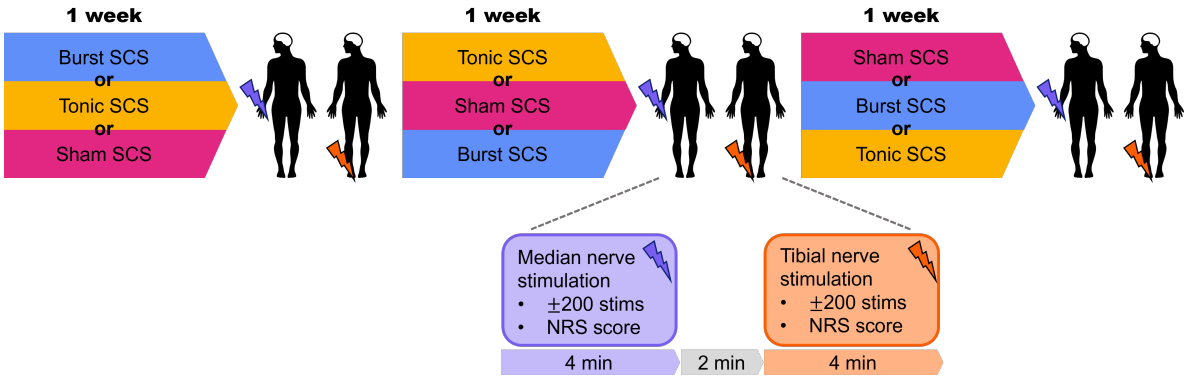

Figure 2.1: An overview of the study protocol: each session consisted of non-painful stimulation of the median nerve as well as of the tibial nerve to elicit somatosensory evoked responses. Each session was during one of the alternated spinal cord stimulation (SCS) paradigms, namely tonic, burst, or sham, after one week of this stimulation paradigm. The order of SCS paradigms was randomized and counterbalanced among the patients; each patient underwent each paradigm for one week in a randomized order. NRS, numerical rating scale

2.1.3. Recordings
At both institutions, measurements were performed in the same manner. MEG measurements were performed using a 275-channel whole-head CTF MEG scanner in a magnetically shielded room. Data acquisition was done using a sampling rate of 2400 Hertz, with a hardware anti-aliasing low-pass filter applied at a cut-off frequency of 600 Hertz. The data files were saved with CTF 3rd-order gradient compensation.

In addition to the MEG recording to capture brain activity, various other electrodes were used to capture either physiological signals or other signals crucial to the research. Cardiac activity was collected using electrodes capturing the electrocardiogram (ECG). Ocular movements were collected using electrodes that captured the vertical electro-oculogram (VEOG) and the horizontal electro-oculogram (HEOG). Next to this, for the chronic pain patients treated with SCS, an electrode was placed on their back over the implanted SCS electrode to capture the SCS pulses applied to the dorsal column. To acquire the timing of the peripherally applied SER stimulation pulses, a transistor-transistor logic (TTL) signal was recorded. For each separate measuring day, empty-room recordings were performed to estimate the instrument and environmental noise in the room.

2.1.4. Anatomy

Because magnetic resonance imaging (MRI) scans of the patients' anatomies were not available, the solution is to use a template anatomy and "warp" (deform) this template based on the head shapes of the patients [82]. The head shapes were digitized using the Polhemus system [83]. This system collects head localization coils (HPI), three anatomical landmarks (nasion (NAS), left ear (LPA), and right ear (RPA)) to match the patient's anatomy to the default anatomy, and scalp points to define the patient's head shape.

2.2. Data Analysis

Data analysis was performed with Brainstorm, which is documented and freely available for download online under the GNU general public license [84]. Brainstorm is a free, open-source Matlab and Java application for multimodal electrophysiology data analytics and source imaging. Brainstorm was used with Matlab 2023a.

2.2.1. Data Preprocessing

Anatomy

For each patient, the ICBM152 (2019) default anatomy was warped to match the individual, digitized head shape, creating a pseudo-individual anatomy. MNI normalization was performed to facilitate processes that work with MNI coordinates in the future [82, 85]. The quality of the source analysis later on is highly dependent on the quality of the co-registration between the patient's anatomy and the MEG sensors. The co-registration is initially done based on three anatomical landmarks (NAS/LPA/RPA) and is improved using the patient's digitized head shape by an iterative algorithm that finds a better fit, improving the co-registration between the MEG sensors and the MRI [86].

Patients remained as still as possible during measurements, yet it remains crucial to assess and account for any head motion, which can particularly affect the analysis of subcortical, deeper structures. Accounting for head motion can be done using the head localization coils (HPI); the distances from a fixed reference position, which is the position just before the recording starts, are saved along the MEG data. Using this signal, sudden head movements were detected and the corresponding segments of recording were labeled as "bad" to be excluded from further analysis [87]. Next, the MEG-MRI co-registration was improved by changing the reference position to the median head position during the recording to better represent the position throughout the recording [88]. The steps in Brainstorm are described in subsection C.1.1.

MEG Data Cleaning

Power spectral density (PSD) plots were made for each recording, including the empty-room recordings, using Welch's method. Bad channels were identified and deleted using the PSDs along with the MEG recordings in the time domain and their corresponding 2D topographies [89].

We decided to not apply filtering because the removal of artifacts inevitably results in the loss of valuable information alongside noise [90]. Frequency filtering of the powerline and spinal cord stimulator noise was omitted because this should only be done if certain frequencies are expected to cause a problem in the analysis, which was not the case [91]. Both the powerline and spinal cord stimulator operate on a constant frequency, whereas the SER stimulation frequency varied randomly. Consequently, the noise introduced by the powerline and the spinal cord stimulator is not time-locked to the stimulus and can be effectively attenuated with the averaging of multiple trials [91]. Further cleaning was initially explored on a subset of the data before an informed decision regarding the cleaning process was made and applied to the entire dataset. As a result, we have chosen not to use specific artifact cleaning methods (frequency filtering, signal-space-projection) to reduce physiological noise introduced by respiration, heartbeats, and ocular movements as well as the noise introduced by the electrical stimulation of peripheral nerves to elicit the SERs. A more detailed rationale and justification are described in subsection C.1.2.

Subsequently, the MEG data was visually inspected again, and additional bad channels and bad segments were identified and deleted. The cause of all bad segments was assessed; bad segments were mainly caused by head motion, eye blink artifacts, and SER stimulation artifacts.

2.2.2. Epoching and Averaging

To assess the SERs elicited by peripheral nerve stimulation, the continuous signal is segmented into epochs of uniform length, using the onset of the SER stimuli as the onset (t=0) of each epoch [92]. The SER stimuli were detected based on the TTL signal. An event marker was assigned to the onset of each stimulus [93]. The accuracy of detection was verified; event markers were assigned to the onset of each SER stimulus with sample-level precision. The SER stimuli in the TTL pulse are subject to a hardware delay: the TTL pulse is saved when the stimulation computer requests a stimulus, but the path through the equipment to deliver the stimulus to the patient takes some time. To estimate the accurate timing of the brain response, the hardware delay was removed using 2.5 milliseconds for Montreal and 1.7 milliseconds for Nijmegen [94].

The signal was segmented into epochs using a broad window of 500 milliseconds before to 1000 milliseconds after a SER stimulus [92]. This window was chosen to allow for filtering after averaging if needed, without introducing filtering edge effects at the time segment of interest. For each epoch, for each channel, the direct current (DC) offset was removed using the average of the time range of 200 to 5 milliseconds before the SER stimulus. The window was chosen following this rationale: the stimulation pulses were separated by at least 700 milliseconds, and the evoked brain activity was expected to last for approximately 500 milliseconds. For this reason, 200 milliseconds before each SER stimulation pulse should consist of ”baseline” activity suitable to be used for baseline removal. The 5 milliseconds before the pulse was selected to allow some time before any part of the stimulation artifact may occur.

All epochs containing (part of) a ”bad” event are automatically excluded from further processing steps. To preserve as much data as possible, these ”bad” epochs were reviewed and accepted as ”good” if the ”bad” segment occurred more than 200 milliseconds before the stimulus or more than 700 milliseconds after the stimulus. The first boundary was chosen to leave a sufficient buffer between the ”bad” segment and the subsequent SER stimulus; the second boundary was chosen because, from 700 milliseconds onwards, a new stimulus may occur, which means that the epochs will not be analyzed for more than 700 milliseconds.

For each recording separately, the epochs were averaged using the arithmetic average; for each patient, for each session, for median nerve stimulation as well as for tibial nerve stimulation, a sensor average was calculated. The steps in Brainstorm are described in section C.2.

2.2.3. Head Models and Source Estimation

For MEG recordings, the sensor locations with respect to the patient’s head can differ between recordings. This precludes averaging at the sensor level across patients or recordings, as one sensor does not necessarily correspond to the same brain region [95, 96]. For further analysis of brain activity, a model is needed that explains how the neural electric currents, called the ”source space”, produce magnetic fields at external sensors, called the ”sensor space”, taking into account the different tissues between the brain and the MEG helmet [97]. This is called ”forward modeling” and results in a ”head model” that describes an approximation of the head geometry based on the patient’s anatomy and the locations of the MEG sensors, represented as a set of thousands of vertices. The subsequent process, the ”source estimation”, estimates the brain activity at these vertices based on much fewer sensor locations; it is an ill-posed inverse problem [95]. The head model and source estimation processes can be done for the cortical surface, as well as for the entire brain volume. As mixed models are not recommended, both approaches were employed separately [98].

For the head model, the ”Overlapping spheres” approach is used, which is the recommended model for MEG. It simplifies the head geometry as multiple overlapping spheres, one for each MEG sensor [97]. For source estimation, the Minimum Norm (MN) imaging approach is used [95]. This method is recommended because it is a simple and robust approach that is less sensitive to approximations of the head model, compared to other methods [95]. MN imaging requires a noise covariance matrix to specify the noise statistics. This is provided using the empty-room recordings. The current at each vertex is modeled by the orientation of an equivalent current dipole. For surface source estimation, the orientation of these dipoles can be set to be normal to the cortex (”Constrained”) or can consist of three orthogonal dipoles along the Cartesian directions of the coordinate system for each vertex (”Unconstrained”). The unconstrained option is recommended when using the template anatomy instead of individual MRI scans, as this may account for some of

the model uncertainties [95]. For volume source estimation, only the unconstrained orientation is available. Therefore, unconstrained current density maps were used for both the surface and volume source estimation.

To compensate for the inhomogeneous sensitivity of MEG with depth and orientation of the current flow, the use of standardized maps is recommended. Standardization of MN imaging can be done either with respect to the noise covariance or with respect to a time segment of no interest. For an analysis of evoked activity, it is more appropriate to employ normalization relative to a time segment without evoked activity rather than noise covariance [95]. For this normalization, the used time segment was the same as the baseline window used to remove the DC offset with epoching, which was 200 milliseconds to 5 milliseconds before SER stimulation. For the volume source models, some additional steps to enable averaging of the source models later on are required in Brainstorm. These steps, as well as a more detailed rationale and background on the head models and source estimation, are described in section C.3.

2.2.4. Data Exclusion

Recordings were excluded based on the following criteria:

- Use of an SCS paradigm other than tonic, burst, or sham;
- Absence of the TTL pulse, preventing SER stimulus detection with sample-level precision;
- Severe data contamination causing poor data quality.

The data quality of each recording was assessed using the sensor space data and their corresponding 2D topographies as well as the source space data. Additionally, the recording notes were used for information on the measurements. Recordings that appeared clean in the sensor space and the source space, and did not contain any warnings in the recording notes, were included. Conversely, recordings that appeared contaminated in one or both of the spaces, and had an explanatory note in the recording notes, were excluded. To assess the remaining cases, two regions of interest (ROIs) were defined in the surface source space for a more detailed examination of the data. These were the hand and foot area of the primary somatosensory cortex, corresponding to the early component of the SERs elicited by, respectively, median nerve and tibial nerve stimulation. These ROIs were selected because they are relatively constant among individuals; in literature, these early components are often assessed when only two EEG electrodes are used [54, 58–60, 62, 64, 67–69, 72–74]. If the signals from these ROIs were evidently contaminated, the recording was excluded. This approach resulted in minimal data exclusion.

2.2.5. Regions of Interest

Several ROIs were identified in both the surface model and the volume model, each representing a subset of dipoles [99]. The ROIs were defined based on the lateral ascending pathway, representing the discriminatory-sensory component of pain, and the medial ascending pathway, representing the motivational-affective component of pain (Figure 1.1, [12]). The ROIs corresponding to the lateral pathway were the areas of the primary somatosensory cortex (S1) related to the hand and the foot, the secondary somatosensory cortex (S2), and the lateral thalamus. The ROIs corresponding to the medial pathway comprised the insular cortices, the anterior cingulate cortex (ACC), the middle cingulate cortex (MCC), the posterior cingulate cortex (PCC), and the medial thalamus.

Surface Model

To identify the ROIs on the S1, an averaged source map of all included recordings was used, separately for the SERs elicited on the median nerve and on the tibial nerve. The ROIs were identified as the region of activation seen in the hand area at approximately 20 to 40 milliseconds after median nerve stimulation and in the foot area at approximately 40 to 60 milliseconds after tibial nerve stimulation. The regions of activation are shown in Figure D.1 for the median nerve stimulation and in Figure D.2 for the tibial nerve stimulation. As stimulation was applied to the right wrist and right ankle, the S1 ROIs were defined solely for the left hemisphere. The ROIs on the S2 were based on the Mindboggle atlas and adjusted based on the activity observed on the averaged source maps [100]. The S2 ROIs were defined on both hemispheres, as evoked responses were expected on both hemispheres [45]. The insular cortices were defined on both hemispheres using the Mindboggle atlas. These ROIs were retained in their entirety and were additionally subdivided into an anterior insular cortex and a posterior insular cortex based on the anatomical subdivision [101, 102]. The cingulate cortex ROIs were identified

and adjusted from the Mindboggle atlas on both hemispheres. The caudal ACC and the rostral ACC were merged into one ACC ROI. The MCC and PCC were adjusted by extending them slightly forward, allowing the edges of the ACC, MCC, and PCC ROIs to adjoin. For all cingulate cortices, the left and right ROIs were merged due to their close anatomical proximity. An overview of all defined ROIs on the cortical surface is shown in Figure D.3 in Appendix D.

Volume Model
For the volume source models, ROIs were defined using the automated anatomical labelling atlas 2 (AAL2) and 3 (AAL3). The difference between the two atlases is that a number of areas defined in the AAL2 atlas, including the thalamus and the ACC, are divided into subregions in the AAL3 atlas [103]. It is recommended by the developers of the atlases to run both atlases if users wish to include an area that is available in AAL2, but also want to research what happens in its subareas. The bilateral ACC, MCC and PCC as well as the bilateral insula were defined using the AAL2 atlas. In accordance with De Ridder's theory, emphasizing the predominant contribution of the pregenual anterior cingulate cortex (pgACC) in the descending pathway, this substructure of the ACC was additionally defined using the AAL3 atlas [4].

The thalamus was defined for both hemispheres using the AAL2 atlas. For the subdivision of the thalamus into a medial and a lateral part, all thalamic nuclei defined in the AAL3 atlas were regrouped into a lateral and medial thalamic subarea based on the sizes of the ROIs and the thalamus anatomy [36–39, 104–106]. The exact subdivision of the thalamus along with a more detailed rationale is shown in Table E.1 and Figure E.1 in Appendix E.

2.2.6. Comparisons

For each comparison separately, within-patient comparisons were facilitated by excluding patients who were missing a recording in any of the groups involved in that particular comparison. Next, to compare SERs between groups, the *source* models of the included patients in all groups needed to be averaged. This is done for both the surface and volume source models. Before averaging across patients, the unconstrained source maps are reduced to one dimension per source location ('flattened'), using the norm of the three unconstrained orientations [96, 107]. For all groups, unweighted arithmetic averages and the standard error were calculated. The steps in Brainstorm are described in section C.5.

Somatosensory Evoked Responses
To evaluate the SERs for each ROI in the averaged source models, the mean of each ROI was used; the ROI signal is the mean of all vertices of the ROI. The time traces for the ROIs were extracted from the averaged source maps (average $\pm$ standard error) and processed into graphs using the IBM colorblind palette [108]. The graphs were interpreted from 0 to 700 milliseconds after stimulus. In accordance with other MEG research on somatosensory evoked responses, the SER components are referred to using "M". This is different from EEG research, which uses "N" and "P" to refer to the polarity of the EEG signal [109].

Area Under the Curve Ratio
For the comparison between the SERs elicited on the tibial nerve and the SERs elicited on the median nerve in patients before SCS and during tonic and burst SCS, an area under the curve (AUC) ratio was defined to quantify the difference between the SERs elicited on the tibial nerve and the SERs elicited on the median nerve. The AUC ratio is defined as:

$$\text{AUC ratio} = \frac{\text{AUC of median nerve SER}}{\text{AUC of tibial nerve SER}}$$

To account for the differences in latency between the SERs elicited on the tibial nerve and the SERs elicited on the median nerve, as well as for the differences in latency across the various ROIs, different time windows to calculate the AUCs were defined for each ROI, for the SERs elicited on the tibial nerve and the SERs elicited on the median nerve separately. The time windows were defined using the before SCS recordings, ensuring that the component of the SER elicited on the tibial nerve was accurately captured in the AUC for the tibial nerve and likewise for the SER elicited on the median nerve. The time windows for both SERs were equally broad; the time window for the SER elicited on the tibial nerve was only delayed relative to the time window for the SER elicited on the median nerve. The utilized time windows are displayed in Table 2.1. Because the baseline signal before SER stimulation was not at zero, this was corrected for in the AUC using the average of the baseline just before stimulation (50 to 5 milliseconds before stimulation). This approach allows for the comparison of the SERs elicited on the tibial nerve and the SERs elicited on the median nerve between before and during SCS.

Table 2.1: The time windows used to calculate the areas under the curves for the somatosensory evoked responses elicited by median nerve and tibial nerve stimulation.

	Window MN [ms]	Window TN [ms]
S1 foot area	15 - 75	30 - 90
S1 hand area	15 - 75	30 - 90
S2 left	40 - 155	65 - 180
S2 right	40 - 155	65 - 180
ACC	20 - 240	45 - 265
MCC	20 - 240	45 - 265
PCC	20 - 240	45 - 265
IC left	40 - 155	65 - 180
IC right	40 - 155	65 - 180
Thalamus left	20 - 130	45 - 155
Thalamus right	20 - 130	45 - 155

MN, median nerve; TN, tibial nerve; ms, milliseconds; S1, primary somatosensory cortex; S2, secondary somatosensory cortex; ACC, anterior cingulate cortex; MCC, middle cingulate cortex; PCC, posterior cingulate cortex; IC, insular cortex.

Statistics

Due to the explorative nature of this research, no statistical analyses were employed. The standard error was utilized as an indicator of the spread of the mean. When the means of two compared groups overlapped, this was defined as no difference between groups. When the mean of one group did not overlap with the standard error of another group, this was defined as a difference. In intermediate cases, the word 'slightly' was used to indicate that the observed difference was marginal.

The AUC ratios as well as the graphs (average $\pm$ standard error) of the SERs elicited by tibial nerve stimulation and the SERs elicited by median nerve stimulation across different conditions were assessed. Based on the changes that were observable from the graphs, a change of $\geq$ 0.4 in AUC ratio was defined as a difference. Using this cut-off value, only evident differences from the graphs were defined as changes.

3 Results

3.1. Patient Population

Twenty-six patients treated with SCS were enrolled in this study. Two patients were excluded due to data contamination caused by dental implants; one patient was excluded because he completed only the first MEG recording session. For one patient, only median nerve stimulation recordings were available as tibial nerve stimulation was not perceptible for this patient. For two patients, one median nerve stimulation recording was excluded due to bad channels in the hand area of the S1. For two patients, one session was excluded because the employed SCS paradigm was not tonic, burst, or sham. For one patient, one session was excluded because the TTL pulse signal was missing. For one patient, only one session remained after data exclusion based on the set criteria (subsection 2.2.4). This remaining session was excluded as well because it was not usable in any of the comparisons, due to the data selection ensuring within-patient comparisons.

An overview of the excluded recordings as described is shown in Table F.3. Four of the included patients treated with SCS were also previously enrolled in this study before SCS treatment. An overview of all patient characteristics is shown in Table F.1. An overview of the characteristics of all included patients is Table 3.1. The groups of included patients differed slightly between comparisons based on the available data to allow for within-patients comparisons; an overview of the included patients for each comparison is provided in Table F.2.

Table 3.1: Characteristics of all included patients.

Characteristics	
Number of patients	22
Age [yrs $\pm$ std]	56 $\pm$ 10
Sex [Male/Female]	11/11
Years lived with chronic pain [yrs $\pm$ std]	18 $\pm$ 12
Pain location	
Back	14/22
Left buttock/hip/leg/foot	9/22
Right buttock/hip/leg/foot	12/22
Pain condition	
FBSS	19/22
DNP	3/22
CRPS	1/22

yrs, years; std, standard deviation; FBSS, failed back surgery syndrome; DNP, diabetic neuropathy; CRPS, complex regional pain syndrome.

3.2. Somatosensory Evoked Responses

The insula and the cingulate cortices were defined as ROIs in both the surface and volume models. Possible differences between the surface and volume ROIs were examined, however, no differences were observed. Consequently, the ROIs from the surface model were utilized for data interpretation, as these align more closely with other published research in this field, which typically employs surface models. Additionally, the anterior and posterior insular cortices, the pregenual anterior cingulate cortex, and the medial and lateral thalamus were defined as substructures within larger ROIs. No differences were observed between these substructures and their respective encompassing structures. Consequently, solely the results of the encompassing structures are presented.

The observed SER components that occurred within 90 milliseconds after SER stimulation were defined as early latency components, the components that occurred between 90 and 180 milliseconds after SER stimulation were defined as middle latency components, and the components that occurred later than 180 milliseconds after SER stimulation were defined as late latency components. Additionally, components that occurred after 450 milliseconds were defined as very late latency components. An overview of the observed latencies following from tibial nerve and median nerve stimulation is provided in Table 4.1.

3.2.1. Before SCS and During SCS

The SERs elicited on the tibial nerve as well as on the median nerve before SCS treatment were compared to the SERs in the same individuals when treated with tonic and burst SCS to assess the influence of SCS on the SER. All recordings from these patients could be used, meaning that all groups consisted of four measurements. An overview of the included patients is shown in Table F.2, and a summary of the included patients' characteristics is provided in Table F.5.

Tibial Nerve

The amplitude of the early component (M45) of the SER in the foot area of the S1 was slightly higher before SCS compared to the SCS paradigms, where the amplitude during the SCS paradigms was lowest for tonic SCS, as is shown in Figure 3.1. The amplitude of the middle latency component (M120) in the left S2 was slightly higher during burst SCS compared to tonic and before SCS. In the right S2, the amplitude of the M120 was slightly higher before SCS compared to during tonic and burst SCS, this is shown in Figure 3.2.

In the ACC, no differences were observed for the M120. The late latency component (M220) was not visible; no changes or differences in amplitude were observed for all conditions. In the MCC and PCC, the amplitude of the M120 was slightly higher before SCS compared to during both SCS paradigms, whereas no differences were observed for the M220. In the left insular cortex, the amplitude of the M120 was slightly higher during burst SCS compared to before SCS. In the right insular cortex, the amplitude of the M120 was slightly higher before SCS and during burst SCS, compared to during tonic SCS. In both the left and right insular cortices, the M220 was not evident; no changes or differences in amplitude were observed for all conditions. For the left thalamus, no differences were observed for the M120, whereas the amplitude of the late latency component (M200) was higher during burst SCS compared to before SCS. In the right thalamus, the amplitude of the M120 was slightly higher before SCS compared to during tonic and burst SCS. The amplitude of the M200 was higher during burst SCS compared to tonic and before SCS.

In the cingulate cortices, the insular cortices, and the thalamus, a very late latency component (M550) was visible. In the ACC, the cingulate cortices, and the thalamus, no differences were observed among conditions. In the MCC and PCC, the SER amplitude was higher before SCS compared to during burst SCS, while the amplitude during tonic SCS was intermediate. An overview of these results, consisting of a table of the findings and the SERs in all ROIs, is provided in subsection G.1.1.

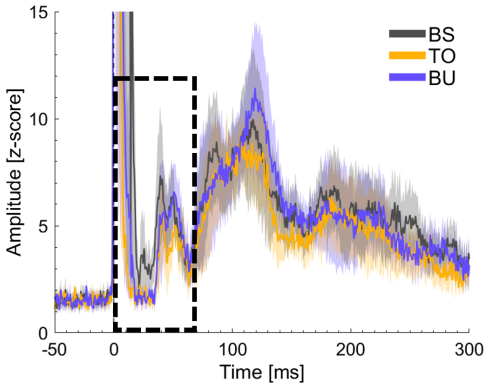

(a) An overview of the SER up to 300 milliseconds. The dotted box represents the area of the zoomed-in plot on the right.

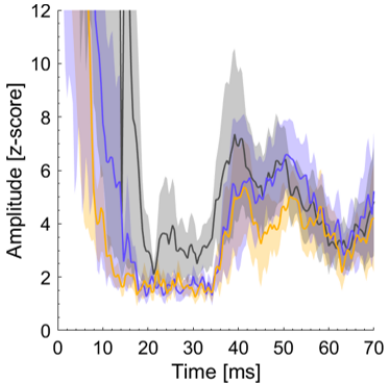

(b) Zoomed-in view of the early latency component (M45) of the SER.

Figure 3.1: The somatosensory evoked response (SER) elicited by tibial nerve stimulation before spinal cord stimulation (SCS) treatment, during tonic SCS, and during burst SCS in the foot area of the primary somatosensory cortex (S1). The shaded areas represent the standard error (SE). The amplitude of the early latency component (M45) of the SER was slightly higher before SCS treatment compared to during SCS. The amplitude was lowest during tonic SCS.
BS, before spinal cord stimulation treatment; TO, tonic spinal cord stimulation; BU, burst spinal cord stimulation.

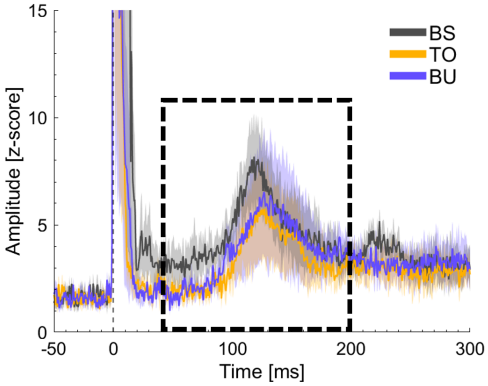

(a) An overview of the SER up to 300 milliseconds. The dotted box represents the area of the zoomed-in plot on the right.

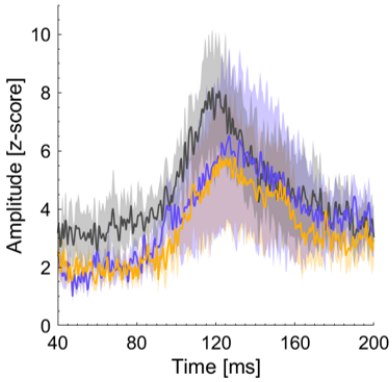

(b) Zoomed-in view of the middle latency component (M120) of the SER.

Figure 3.2: The somatosensory evoked response (SER) elicited by tibial nerve stimulation before spinal cord stimulation (SCS) treatment, during tonic SCS, and during burst SCS in the right secondary somatosensory cortex (S2). The shaded areas represent the standard error (SE). The amplitude of the middle latency component (M120) of the SER was slightly higher before SCS treatment compared to during SCS.
BS, before spinal cord stimulation treatment; TO, tonic spinal cord stimulation; BU, burst spinal cord stimulation.

Median Nerve

The amplitude of the early component (M30) of the SER in the hand area of the S1 was higher during both SCS paradigms compared to before SCS, as is shown in Figure 3.3. Within the SCS paradigms, the amplitude was higher for burst SCS compared to tonic SCS. The amplitude of the middle latency component (M100) in the left S2 was higher during burst SCS compared to tonic SCS and before SCS. No differences were observed in the right S2.

In the ACC, the M100 was higher during burst SCS, compared to tonic SCS and before SCS, whereas no differences were observed for the late latency component (M200). In the MCC, no differences were observed for the M100, whereas the M200 was slightly higher during burst SCS compared to during tonic SCS and before SCS. In thePCC, no differences were observed for the M100 and the M200. In the left insular cortex, the amplitude of the M100 was slightly higher during burst SCS compared to tonic SCS and before SCS. In the right insular cortex, no differences were observed in the amplitude of the M100. In both the left and right insular cortices, no differences were observed for the M200. In both the left and right thalamus, no differences were observed for the

M100. In the left thalamus, the amplitude of the M200 was slightly higher during burst SCS compared to tonic SCS and before SCS. For the right thalamus, no differences were observed for the M200.

Predominantly in the ACC and left and right thalamus, but also in the MCC, the PCC, and the insular cortices, a very late latency component (M500) was visible. In the cingulate cortices, this component was higher before SCS compared to during SCS. For the ACC, this is shown in Figure 3.4. In the left and right thalamus, this component was higher during burst SCS and before SCS, compared to tonic SCS. An overview of these results, consisting of a table of the findings and the SERs in all ROIs, is provided in subsection G.1.2.

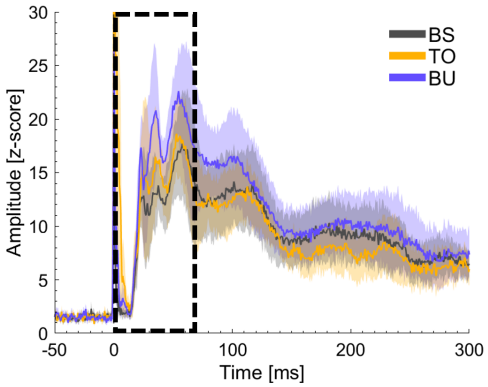

(a) An overview of the SER up to 300 milliseconds. The dotted box represents the area of the zoomed-in plot on the right.

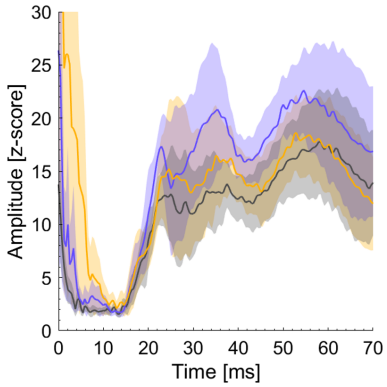

(b) Zoomed-in view of the early latency component (M30) of the SER.

Figure 3.3: The somatosensory evoked response (SER) elicited by median nerve stimulation before spinal cord stimulation (SCS) treatment, during tonic SCS, and during burst SCS in the hand area of the primary somatosensory cortex (S1). The shaded areas represent the standard error (SE). The amplitude of the early latency component (M30) of the SER was (slightly) higher during both SCS paradigms compared to before SCS. The amplitude was highest during burst SCS.
BS, before spinal cord stimulation treatment; TO, tonic spinal cord stimulation; BU, burst spinal cord stimulation.

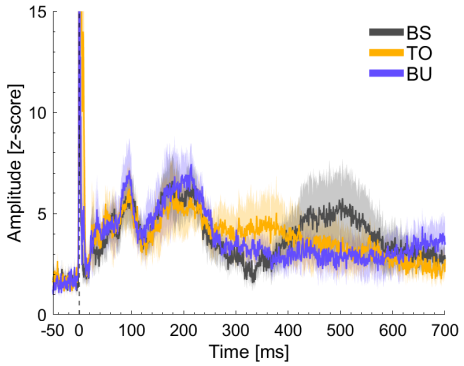

Figure 3.4: The somatosensory evoked response (SER) elicited by median nerve stimulation before spinal cord stimulation (SCS) treatment, during tonic SCS, and during burst SCS in the anterior cingulate cortex (ACC) shown for 700 milliseconds. The shaded areas represent the standard error (SE). The amplitude of the very late latency component (M500) was higher before SCS compared to during SCS.
BS, before spinal cord stimulation treatment; TO, tonic spinal cord stimulation; BU, burst spinal cord stimulation.

3.2.2. Tibial Nerve and Median Nerve

The SERs elicited by tibial nerve stimulation were compared to the SERs elicited by median nerve stimulation in patients before SCS and during tonic and burst SCS. The difference between the two SERs was quantified using the AUC ratio, and the AUC ratios before SCS treatment were compared to the AUC ratios during SCS. The comparison between AUC ratios was initially performed in the subpopulation of patients who were also previously included in the study before SCS treatment, comparing the AUC ratios before SCS to the AUC ratios during tonic and burst SCS in the same individuals. Subsequently, the AUC ratios of the patients before SCS treatment were compared to the AUC ratios during tonic and burst SCS in the patient population consisting of all included patients treated with SCS. For all SCS paradigms, the same patients were included; if a patient was missing one recording in one of the paradigms, this patient was excluded from the comparison. An overview of the included patients is shown in Table F.2, a summary of the included patients' characteristics is provided in Table F.5 (n=4) and Table F.6 (n=19).

Before SCS Treatment

The AUC ratios of the patients before SCS treatment (n=4) and the AUC ratios of the same individuals (n=4) during tonic and burst SCS are shown in Table 3.2. A higher AUC ratio indicates a greater difference between the median nerve and tibial nerve SER. In the S1 hand and foot area as well as in the right S2, the AUC ratios were higher during tonic and burst SCS. In the right insular cortex and right thalamus, the AUC ratios were higher during tonic SCS. In the MCC and PCC, the AUC ratios were higher during burst SCS. An overview of the graphs showing the AUCs for the SERs elicited by tibial nerve and median nerve stimulation in all ROIs is provided in subsection G.2.1.

All Patients

After observing these differences in the patients that participated before SCS treatment and during SCS, the same comparison was made between these patients before SCS treatment (n=4) and all included patients that were treated with SCS (n=19). The AUC ratios for the patients before SCS treatment and all patients during SCS treatment are shown in Table 3.3. In the S1 hand area, the right S2, and both the left and right thalamus, the AUC ratio was higher during tonic and burst SCS. For the right thalamus, the AUCs that were used to determine the AUC ratios are shown in Figure 3.5. In the right insular cortex, the AUC ratio was higher during tonic SCS. In the MCC, the AUC ratio was higher during burst SCS. An overview of the graphs showing the AUCs for the SERs elicited by tibial nerve and median nerve stimulation in all ROIs is provided in subsection G.2.2.

Table 3.2: The area under the curve ratios of the patients before spinal cord stimulation (SCS) treatment and of the same individuals (n=4) during tonic and burst SCS

	Before SCS (n=4)	Tonic SCS (n=4)	Burst SCS (n=4)
S1 foot area	1,5	**2,7**	**2,5**
S1 hand area	5,9	**7,3**	**8,3**
S2 left	1,9	1,8	1,8
S2 right	0,9	**1,8**	**1,4**
ACC	1,4	1,5	1,7
MCC	1,6	1,9	**2,4**
PCC	1,3	1,5	**1,8**
IC left	1,7	1,6	1,5
IC right	1,1	**1,6**	1,0
Thalamus left	1,3	1,3	1,4
Thalamus right	1,1	**1,5**	1,3

Table 3.3: The area under the curve ratios of the patients before spinal cord stimulation (SCS) treatment (n=4) and of all included patients (n=19) during tonic and burst SCS.

	Before SCS (n=4)	Tonic SCS (n=19)	Burst SCS (n=19)
S1 foot area	1,5	1,7	1,7
S1 hand area	5,9	**7,2**	**6,8**
S2 left	1,9	2,0	1,9
S2 right	0,9	**1,9**	**1,5**
ACC	1,4	1,5	1,5
MCC	1,6	1,6	**2,0**
PCC	1,3	1,3	1,5
IC left	1,7	1,6	1,4
IC right	1,1	**1,8**	1,4
Thalamus left	1,3	**1,8**	**1,8**
Thalamus right	1,1	**2,2**	**1,5**

S1, primary somatosensory cortex; S2, secondary somatosensory cortex; ACC, anterior cingulate cortex; MCC, middle cingulate cortex; PCC, posterior cingulate cortex; IC, insular cortex.

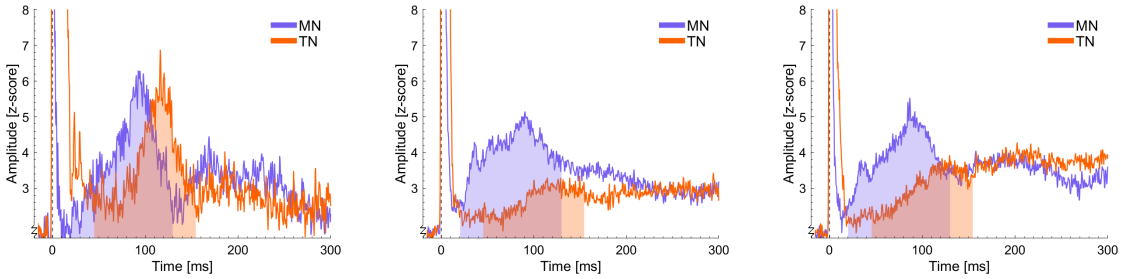

(a) AUC before SCS (n=4). **(b)** AUC during tonic SCS (n=19). **(c)** AUC during burst SCS (n=19).

Figure 3.5: Overview of the areas under the curves (AUCs) for the somatosensory evoked responses (SERs) elicited by tibial nerve and median nerve stimulation in the right thalamus before spinal cord stimulation treatment (n=4), during tonic spinal cord stimulation (n=19), and during burst spinal cord stimulation (n=19). The shaded areas represent the AUCs that were used to determine the AUC ratio for each condition. MN, median nerve; TN, tibial nerve.

3.2.3. Tonic SCS and Burst SCS

The SERs elicited by tibial nerve as well as by median nerve stimulation were be compared during tonic and burst SCS.

Tibial nerve

In the foot area of the S1, no differences were observed for the early component (M45), as is shown in Figure 3.6. In the left and right S2, the middle latency component (M120) was higher during burst SCS. In the cingulate cortices, no differences were observed for the M120 and the late latency component (M220). In the left and right insular cortices, the amplitudes of the M120 and M220 were higher during burst SCS. In the left thalamus, no difference was observed for the M120, whereas this component was higher during burst SCS in the right thalamus. In both the left and right thalamus, the M220 was higher during burst SCS. In the ACC and PCC, the insular cortices, and the thalamus, a very late latency component (M550) was visible with a higher amplitude during burst SCS. An overview of these results, consisting of a table of the findings and the SERs in all ROIs, is provided in subsection G.3.1.

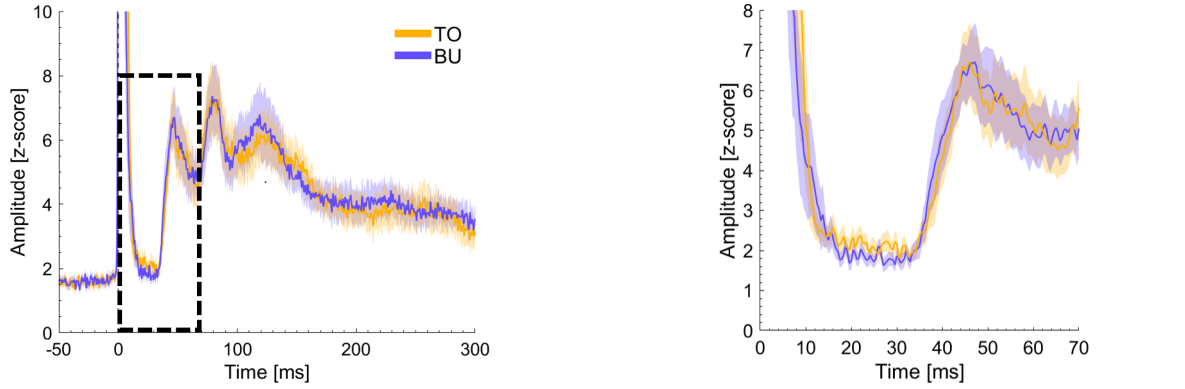

(a) An overview of the SER up to 300 milliseconds. The dotted box represents the area of the zoomed-in plot on the right.

(b) Zoomed-in view of the early latency component (M45) of the SER.

Figure 3.6: The somatosensory evoked response (SER) elicited by tibial nerve stimulation during tonic and burst spinal cord stimulation in the foot area of the primary somatosensory cortex (S1). The shaded areas represent the standard error (SE). No difference was observed for the amplitude of the early latency component (M45) of the SER.
TO, tonic spinal cord stimulation; BU, burst spinal cord stimulation.

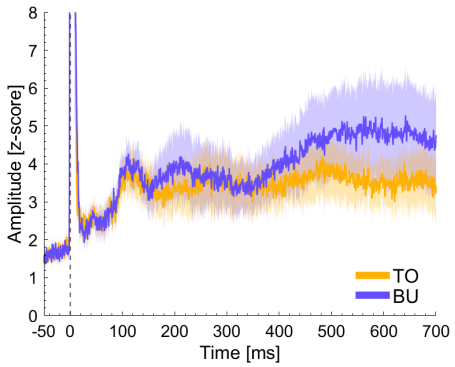

Figure 3.7: The somatosensory evoked response (SER) elicited by tibial nerve stimulation during tonic and burst spinal cord stimulation (SCS) in the left thalamus shown for 700 milliseconds. The shaded areas represent the standard error (SE). The amplitude of the very late latency component (M550) was higher during burst SCS.
TO, tonic spinal cord stimulation; BU, burst spinal cord stimulation.

Median Nerve

In the hand area of the S1, no differences were observed for the early component (M30), as is shown in Figure 3.8. In the left S2, the amplitude of the middle latency component (M100) was higher during burst SCS, whereas no differences were observed in the right S2. In the ACC, the amplitudes of the M100 and the late latency component (M200) were higher during burst SCS. In the MCC, no difference was observed for the M100, whereas the amplitude of the M200 was higher during burst SCS. In the PCC, no differences were observed for both the M100 and M200. In the left insular cortex, the M100 was higher during burst SCS, whereas no difference was observed for this component in the right insular cortex. In the left and right insular cortices, the amplitude of the M200 was higher during burst SCS. In both the left and right thalamus, no differences were observed in the M100, whereas the amplitude was higher during burst SCS for the M200. In the cingulate cortices, the insular cortices, and the thalamus, a very late latency component (M500) was visible with a higher amplitude during burst SCS. An overview of these results, consisting of a table of the findings and the SERs in all ROIs, is provided in subsection G.3.2.

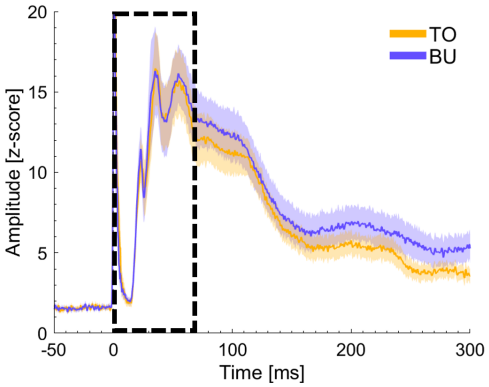

(a) An overview of the SER up to 300 milliseconds. The dotted box represents the area of the zoomed-in plot on the right.

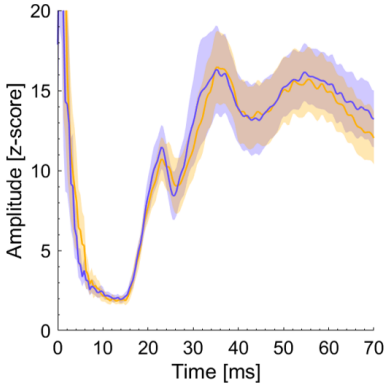

(b) Zoomed-in view of the early latency component (M330) of the SER.

Figure 3.8: The somatosensory evoked response (SER) elicited by median nerve stimulation during tonic and burst spinal cord stimulation in the hand area of the primary somatosensory cortex (S1). The shaded areas represent the standard error (SE). No difference was observed for the amplitude of the early latency component (M30) of the SER.
TO, tonic spinal cord stimulation; BU, burst spinal cord stimulation.

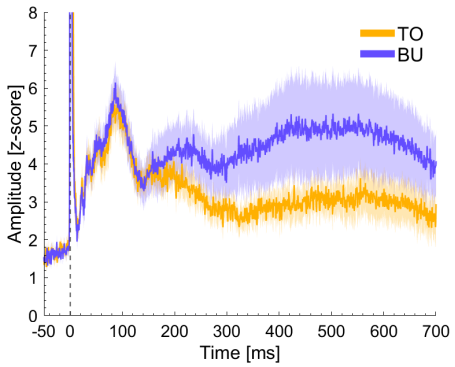

Figure 3.9: The somatosensory evoked response (SER) elicited by median nerve stimulation during tonic and burst spinal cord stimulation (SCS) in the left thalamus shown for 700 milliseconds. The shaded areas represent the standard error (SE). The amplitude of the late (M200) as well as the very late latency component (M500) of the SER was higher during burst SCS.
TO, tonic spinal cord stimulation; BU, burst spinal cord stimulation.

3.2.4. The Effect of Pain Reduction

Four patients, as is shown in Table F.2, were selected for this comparison to explore a possible correlation between the effect of SCS on the SER amplitude and the effect of SCS on chronic pain. The selected patients and their characteristics are shown in Table F.1 (denoted with ‡). First, the SERs elicited on the median nerve as well as on the tibial nerve were compared within the selected patients during tonic and burst SCS. Secondly, the SERs were compared between two responders and two non-responders within tonic and burst SCS.

Within Patient Comparison

For the two patients that were a responder or a non-responder to both paradigms, no differences between SERs were expected between the paradigms if a correlation between pain relief and effect on SER amplitude exists. However, for the non-responder to both paradigms, differences were observed in the SER amplitudes following from tibial nerve stimulation in the right insular cortex; the amplitude was higher during tonic SCS. Following from median nerve stimulation, the SER amplitudes were higher during burst SCS in the cingulate cortices as well as in the hand area of the S1. For the S1, this is shown in Figure 3.10. For the responder to both paradigms, the amplitude of the SER elicited by tibial nerve stimulation was higher during burst SCS in the right insular cortex and slightly in the left S2. For the SER elicited by median nerve stimulation, the amplitude was higher during tonic SCS in the left thalamus. Overall, the responder to both paradigms had very low amplitudes for all SER components; the early component in the foot area of the S1 was even missing after stimulation of the tibial nerve. This is shown in Figure G.9a.

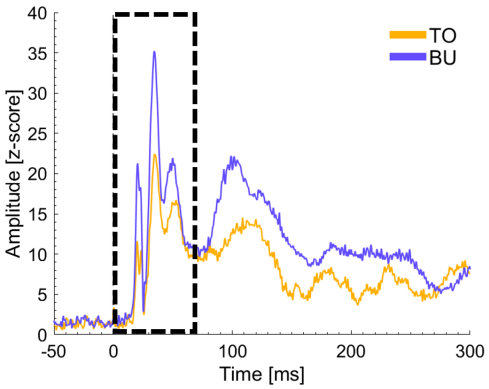

(a) An overview of the SER up to 300 milliseconds. The dotted box represents the area of the zoomed-in plot on the right.

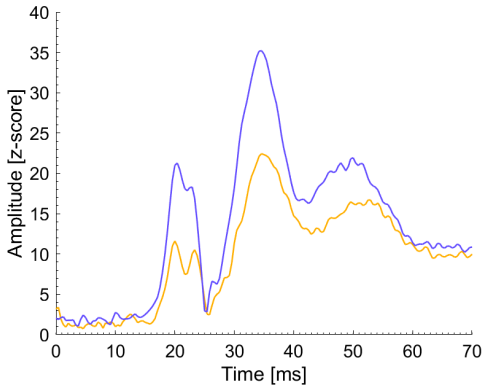

(b) Zoomed-in view of the early latency component (M30) of the SER.

Figure 3.10: The somatosensory evoked response (SER) elicited by median nerve stimulation during tonic and burst spinal cord stimulation (SCS) in the hand area of the primary somatosensory cortex (S1) for the non-responder to both tonic and burst SCS (PT05). The amplitude of the early latency component (M30) of the SER was higher during burst SCS.
TO, tonic spinal cord stimulation; BU, burst spinal cord stimulation.

For the two patients who were a responder to one of the paradigms and a non-responder to the other paradigm, opposite differences between tonic and burst SCS were expected if a correlation between pain relief and effect on SER amplitude exists. For the responder to burst SCS, the SERs elicited by both tibial nerve and median nerve stimulation were higher during burst SCS in the left insular cortex and in, respectively, the foot and hand area of the S1. For the SER elicited by median nerve stimulation in the hand area of the S1, this is shown in Figure 3.11. Additionally, the SER elicited by median nerve stimulation was higher in the left S2 during burst SCS. For the responder to tonic SCS, the SER elicited by tibial nerve stimulation was slightly higher during tonic SCS in the left thalamus. For the SER elicited by median nerve stimulation, the amplitude was higher during tonic SCS in the ACC, in the right insular cortex, and in the thalamus. However, conversely, the SER was higher during burst SCS in the hand area of the S1. The SERs in all ROIs for all case studies are provided in section G.4.

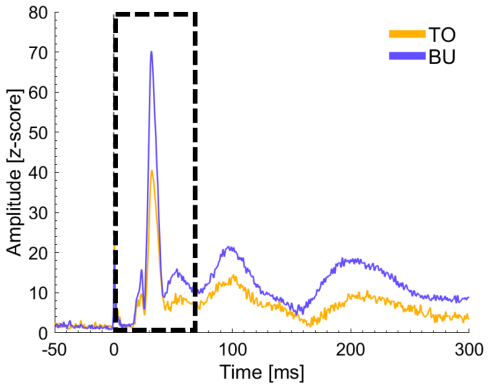

(a) An overview of the SER up to 300 milliseconds. The dotted box represents the area of the zoomed-in plot on the right.

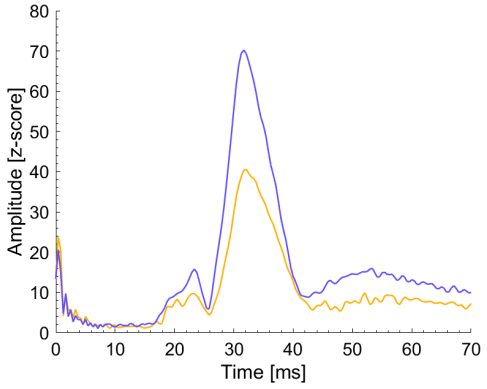

(b) Zoomed-in view of the early latency component (M30) of the SER.

Figure 3.11: The somatosensory evoked response (SER) elicited by median nerve stimulation during tonic and burst spinal cord stimulation (SCS) in the hand area of the primary somatosensory cortex (S1) for the responder to burst SCS (PTN05). The amplitude of the early latency component (M30) of the SER was higher during burst SCS. Note the high range of the vertical axis.
TO, tonic spinal cord stimulation; BU, burst spinal cord stimulation.

Within Paradigm Comparison

Subsequently, the four patients were divided into two sets of two for both tonic and burst SCS, comparing the two responders to each paradigm to the two nonresponders for each paradigm separately. No trends were observed that could differentiate between responders and nonresponders within tonic SCS as well as within burst SCS.

4

Discussion

The primary objective of this thesis was to assess how various SCS paradigms affect the supraspinal SER elicited by a non-painful peripheral stimulus. To fulfill this objective, supraspinal SERs elicited by non-painful transcutaneous electrical stimulation of the median nerve as well as the tibial nerve were evaluated in chronic pain patients treated with SCS, utilizing MEG as a measurement technique. The influence of SCS on the SER was assessed concerning the amplitude of the SER.

4.1. Observed Components

The early latency components in the S1 and the middle latency components in the S2 and the thalamus are considered to be associated with the lateral ascending pathway and reflect the somatosensory processing of the SER stimulus, such as the localization and character of the stimulus. The middle and late latency components in the cingulate cortices, the insular cortices, and the thalamus are considered to be correlated with the medial ascending pathway and reflect the attentional/emotional processing of the stimulus. Consequently, the middle latency components in the thalamus were considered to be correlated with both the lateral and medial ascending pathways.

Table 4.1: An overview of the generally observed latencies for the early, middle, late, and very late latency components for the somatosensory evoked responses elicited by tibial nerve and median nerve stimulation.

	TN	MN
Early component [ms]	45	30
Middle component [ms]	120	100
Late component [ms]	220	200
Very late component [ms]	550	500

ms, milliseconds;
TN, tibial nerve; MN, median nerve.

The early latency components of the SER were observed in the foot area of the S1 around 45 milliseconds after stimulation of the tibial nerve and in the hand area of the S1 around 30 milliseconds after stimulation of the median nerve. These observed latencies correspond to the literature [44, 45, 53, 54]. The early latency components were occasionally observed in the cingulate cortices and thalamus as well. However, these components were presumably far-field signals originating from the S1, because the latency corresponded perfectly and the amplitude was considerably lower in these other structures.

The middle latency components of the SER were observed in the S2, the cingulate cortices, the insular cortices, and the thalamus around 120 milliseconds after stimulation of the tibial nerve and around 100 milliseconds after stimulation of the median nerve. The late latency components of the SER were observed in the cingulate cortices, the insular cortices, and the thalamus around 220 milliseconds after stimulation of the tibial nerve and around 200 milliseconds after stimulation of the median nerve. The middle and late latency components were observed slightly later than anticipated based on the literature, which is primarily based on EEG research [45–47, 51, 52]. Latency differences between EEG and MEG have previously been reported and may stem from a delayed radial source that is detectable by EEG, but not by MEG [45].

Additionally, a very late latency SER component was observed around 550 milliseconds after tibial nerve stimulation and around 500 milliseconds after median nerve stimulation in the cingulate cortices, the insular cortices, and the thalamus. For the thalamus, a component with similar latency has previously been reported using intracerebral electrodes and has been hypothesized to reflect pain-related activity mediated via Aδ and C-fibers [48–50]. For the cingulate cortex, a similar latency component was reported by Hylands-White et al. following painful stimulation at the hand [58].

4.2. Comparisons

The supraspinal SERs were compared among various groups, namely: 1) SERs in chronic pain patients before SCS implantation versus SERs in the same individuals during tonic and burst SCS, 2) SERs elicited on the tibial nerve versus SERs elicited on the median nerve in patients before SCS implantation and during tonic and burst SCS, 3) SERs during tonic SCS versus SERs during burst SCS, and 4) four case studies of two responders and two non-responders to the tonic and/or burst SCS paradigms.

4.2.1. Before SCS and During SCS

The SERs elicited on the tibial nerve as well as on the median nerve before SCS treatment were compared to the SERs in the same individuals when treated with tonic and burst SCS to assess the influence of SCS on the SER.

Tibial Nerve

For the early component in the S1 and for the middle latency components in the left S2 and the left and right thalamus, the SER amplitude was either unchanged or decreased during SCS. Conversely, in the left S2, the SER amplitude was increased during burst SCS. These results are somewhat inconsistent and the observed differences were small. However, these results suggest a potential inhibitory effect of SCS on the somatosensory processing of the SER elicited by tibial nerve stimulation, aligning with literature [45, 59, 61, 66–69, 72–74].

For the middle latency components in the cingulate cortices, the right insular cortex, and the thalamus, the SER amplitude was either unchanged or decreased during SCS. Conversely, in the left insular cortex, the amplitude of the middle latency component was higher during SCS. The late latency component was unchanged in the cingulate cortices and the insular cortices, whereas this component was increased during burst SCS in the thalamus. The very late latency component was unchanged in the ACC, the insular cortices, and the thalamus, whereas this component was decreased during SCS in the MCC and PCC. These results predominantly indicate either no or an inhibitory effect of SCS on the SER amplitude, however, the results are somewhat inconsistent and the observed differences were small. This aligns with the literature; for the middle and late latency components of the SER, the effect of SCS on the SER amplitude was not conclusive [45, 62, 66, 75]

Median Nerve

For the early components in the S1 and the middle latency components in the S2 and the thalamus, the amplitude of the SER either remained unchanged or increased during SCS. Similarly, for the middle latency and late latency components of the SER in the cingulate cortices, the insular cortices, and the thalamus, the amplitude of the SER either remained unchanged or increased during SCS. These results indicates that both the somatosensory and the attentional/emotional processing of the SER stimulus were not inhibited during SCS. However, for the very late latency component, the amplitude of the SER was either unchanged or decreased during SCS. This selective inhibition of the very late latency component could indicate a supraspinal inhibitory MOA of SCS on theattentional/emotional processing of the SER stimulus.

Considerations and Limitations

An important limitation of the comparison between the SERs in patients before SCS treatment and during SCS is the substantial change that occurs within these patients between the measurements before and during SCS. Inherent to the comparison of patients before and during SCS is the fact that multiple variables change. Firstly, between the before SCS and during SCS conditions, patients change from chronic pain patients with severe, intractable chronic pain to patients receiving treatment that may partly relieve their pain. In other words, the chronic pain condition itself may change. Secondly, the electrical activation that is introduced by SCS may lead to both long-term and immediate physiological changes in the patients, which may or may not be correlated with the therapeutic effect. Lastly, this electrical activation may lead to potential electrical effects concerning the MEG measurements that were previously absent. These variables, amongst possible other factors, collectively contribute to the observed differences and thus complicate the interpretation of these differences. The predominantly increased amplitude of the SER elicited by median nerve stimulation during SCS may indicate a restoration of the somatosensory system in these chronic pain patients during SCS treatment. Pinheiro et al. reported decreased amplitudes of the SER in chronic pain patients compared to healthy controls. Therefore, an increased SER amplitude may indicate restoration of the somatosensory system, approximating the SERs observed in healthy controls.

Overall, the differences observed between the SERs before and during SCS in this group of four patients were quite small. This raises the question of whether these observed differences would be more pronounced or less pronounced in a larger group of patients. Within this thesis, the comparison between tonic and burst SCS may serve as an indication for this question. The group of patients utilized for the comparison between tonic and burst SCS consisted of, respectively, 22 and 21 patients for the SERs elicited by median nerve and tibial nerve stimulation. In these larger groups, no differences were observed for the early component of the SER in the S1 between tonic and burst SCS, whereas this smaller group of four did exhibit some differences for the early component of the SER in the S1 between tonic and burst SCS. This indicates that at least part of the observed difference in this comparison may be attributed to noise or other variabilities between measurements due to the small group of patients. The impact of the patient group size in research on both SERs and patients with chronic pain is further elaborated on in subsection 4.3.1.

4.2.2. Tibial Nerve and Median Nerve

The SERs elicited by tibial nerve stimulation were compared to the SERs elicited by median nerve stimulation in patients before SCS and during tonic and burst SCS. This comparison was employed to assess whether a spinal MOA may contribute to the effect of SCS on the SER, such as the collision of impulses theory (Figure 1.4). The AUC ratio was used to quantify the difference between the SER elicited by tibial nerve stimulation and the SER elicited by median nerve stimulation across different conditions.

For the patients that were included in the study before SCS treatment as well as during SCS treatment with tonic and burst SCS, the AUC ratio was higher during both tonic and burst SCS for the hand and foot area of the S1 and for the right S2. For the comparison between patients that were included in the study before SCS treatment and all included patients during tonic and burst SCS, the AUC ratio was higher during both tonic and burst SCS for the hand area of the S1, the right S2, and the left and right thalamus.

The observed increased AUC ratios during both SCS paradigms support the possibility of a spinal MOA of SCS on the SER amplitude. If the collision of impulses theory is indeed one of the MOAs of SCS on the SER, its effect would be primarily expected on the lateral pathway, because the theory is hypothesized based on early components of the SER, which correspond to the lateral pathway [61, 67–69, 72, 74]. This expectation aligns with the structures that predominantly exhibited an increase in AUC ratio during SCS, namely the S1, the S2, and the thalamus, which constitute the lateral pathway.

Considerations and Limitations

An important limitation of this possible MOA is that the collision of impulses of SCS on the non-painful SER is based on interference of the ascending and descending volleys that travel through the Aβ-fibers of the spinal cord. Pain, however, travels through C- and Aδ-fibers. This means that this MOA of SCS *on the SER* should not be confused with the MOA of SCS *on the chronic pain condition*. This complicates the translation of the MOA of SCS on the non-painful SER to the MOA of SCS on (chronic) pain.

The amplitudes of the SERs elicited by median nerve stimulation were, in general, higher compared to the amplitudes of the SERs elicited by tibial nerve stimulation. This difference cannot be attributed to a higher SER stimulation intensity, as, on average, the stimulation intensity was slightly higher for the tibial nerve stimulation, as is shown in Table 4.2. The difference may be explained by the cortical representation of both stimulated limbs in the S1, known as the sensory homunculus. The hand/wrist area, corresponding with the median nerve stimulation, has a more extensive cortical representation compared to the foot/ankle area, corresponding with the tibial nerve stimulation. This difference in cortical representation was primarily evident in the S1. For instance, the SER component in the thalamus was of similar amplitude for both SERs in the patients before SCS treatment (Figure 3.5).

The AUC ratio was an acceptable indicator for the change in differences between the two distinct SERs before and during SCS. It was a reasonably adequate solution to incorporate the differences in latencies between the two SERs. However, it was sensitive to the absolute amplitude of the SERs. For the relatively high SER amplitudes in the S1 compared to, for example, a deeper brain structure such as the thalamus, differences of ≥ 0.4 in AUC ratio were more easily obtained.

Another important limitation of this comparison is the possible effect of stimulation in the painful area of the patients. For approximately half of the patients (2/4 in the population of patients included before SCS treatment, 9/19 in the bigger SCS population), the chronic pain area included the right hip, leg, and/or foot (Table F.5, Table F.6). As the SERs on the tibial nerve were elicited on the right ankle, this suggests that in half of the patients, the SERs on the tibial nerve were elicited in the chronic pain area. Conversely, none of the patients experienced pain in the upper extremity and, thus, the SERs elicited on the median nerve were not elicited in the chronic pain area. Morgalla et al. have reported that painful SERs elicited either within versus outside of the chronic pain area may differ in chronic pain patients treated with dorsal root ganglion stimulation [110, 111]. The impact of SER stimulation within or outside of the chronic pain area is further elaborated on in subsection 4.4.2.

4.2.3. Tonic SCS and Burst SCS

The SERs elicited by tibial nerve as well as by median nerve stimulation were compared during tonic and burst SCS.

Tibial Nerve

No difference was observed for the early component in the S1, which aligns with the expectations based on the study by Niso et al. [46]. For the middle latency components in the S2 and the right thalamus, the amplitude was higher during burst SCS, whereas this component was unchanged in the left thalamus. These results suggest that the somatosensory processing of the non-painful SER elicited by tibial nerve stimulation is either similar during both paradigms, or decreased during tonic SCS compared to burst SCS. For the middle, late, and very late latency components in the cingulate cortices, the insular cortices, and the thalamus, the results were similar; the amplitude of the SER was either higher during burst SCS compared to tonic SCS, or no difference was observed. This indicates that the emotional/attentional processing of the SER elicited by tibial nerve stimulation was not decreased during burst SCS compared to tonic SCS, which is contrary to the expected results based on literature [4, 46]. In particular for the very late latency component, the higher SER amplitude during burst SCS was accompanied by an increase in standard error for the signal during burst SCS. This very late latency difference between burst and tonic SCS was additionally observed in the somatosensory cortices (S1, S2). However, in these ROIs, it resembled a baseline shift during burst SCS instead of a very late latency SER component and was also accompanied by an increase in standard error for the burst SCS signal.

Median Nerve

No differences were observed for the early component in the S1. No differences were observed for the middle latency components in the right S2 and the thalamus, whereas this component was higher during burst SCS in the left S2. This suggests that the somatosensory processing of the non-painful SER elicited by median nerve stimulation is either similar for both paradigms, or decreased during tonic SCS compared to burst SCS. For the middle, late, and very late latency components in the cingulate cortices, the insular cortices, and the thalamus, the observed results were similar; the amplitude of the SER was either higher during burst SCS compared to tonic SCS, or no difference was observed. This indicates that the emotional/attentional processing of the SER elicited by median nerve stimulation was not decreased during burst SCS compared to tonic SCS, which is contrary to the expected results based on literature [4, 12]. Similar to the SERs elicited by tibial nerve stimulation, the higher SER amplitude during burst SCS for the very late latency component was accompanied by an increase in standard error for the signal during burst SCS. Additionally, this very late latency difference between burst and tonic SCS was also observed in the somatosensory cortices and, similarly, resembled a baseline shift accompanied by an increase in standard error for the burst SCS signal.

Considerations and Limitations

Contrary to the expected results, the late latency SER amplitudes were higher during burst SCS [46]. Two potential contributing factors to these unexpected results were explored: the average stimulation intensity during each paradigm and the level of noise resulting from the electrical stimulation of the spinal cord stimulator. Firstly, a higher stimulation intensity during burst SCS may provide an explanation for the higher amplitudes during burst SCS. However, the average stimulation intensity did not differ between the paradigms, as is shown in Table 4.2. Secondly, the level of noise resulting from the electrical stimulation of the spinal cord stimulator was assessed, because a recording more affected by noise leads to lower z-scores after baseline normalization, and, thus, to lower SER amplitudes. The noise levels introduced by both tonic and burst SCS were evaluated for a subset of

patients using the signal of the EEG electrode on the patients' backs. This specific sensor was used, because the SCS-induced noise that might have affected the MEG signal would presumably be most pronounced in this sensor. No differences were observed between tonic and burst SCS, for both paradigms the artifact was effectively attenuated with the averaging of trials. Consequently, neither factors appear to explain the unexpected results. Moreover, the fact that the early components of the SER did not differ between paradigms supports the indication that neither the stimulation intensity of the SER nor the noise induced by SCS may explain the observed differences in the later SER components.

A limited amount of studies have researched the effect of multiple SCS paradigms on the painful or non-painful SER [46, 68, 71, 73]. To date, only one study with a similar protocol exists, using non-painful SERs, assessing not only the early component but the later SER components as well, using multiple (EEG) channels [46]. It is remarkable that the results in this thesis, showing *higher* SER amplitudes during burst SCS for the later SER components, differ from this study by Niso et al. [46]. To assess the feasibility of comparing these results to the study by Niso et al. in the condition where patients paid attention to the SER stimuli, the difference between counted and applied SER stimuli was examined [46]. This is important because no differences between tonic and burst SCS were observed in the condition where patients were *not* attentive to the SER stimuli. In this thesis, the difference between counted and applied SER stimuli was approximately 1 across all SCS paradimgs, for the SERs elicited by both tibial nerve and median nerve stimulation. This suggests that, on average, the patients were attentive to the stimuli. In addition, the patient populations were similar. Niso et al. [46] included 12 patients diagnosed with failed back surgery syndrome (FBSS), suffering from chronic pain in the lower back and one or two legs; 19 out of the 22 patients included in this thesis were also diagnosed with FBSS (Table 3.1), suffering from chronic pain in the lower back and/or one or both legs.

However, a crucial difference between this thesis and the study by Niso et al. is the fact that Niso et al. applied the SER stimuli to the affected leg. In this thesis, the SER stimuli were applied to the right leg in all patients and in only approximately half of the patients this corresponded to their pain area (10/21 for the SERs elicited by tibial nerve stimulation, Table F.7; 11/22 for the SERs elicited by median nerve stimulation, Table F.8). This difference may explain the discrepancy in results between this thesis and the study by Niso et al. [46]. This difference is proposed as opportunity for further research in subsection 4.4.2.

Table 4.2: Average stimulation intensity during each spinal cord stimulation paradigm for the somatosensory evoked responses elicited by tibial nerve (TN) and by median nerve (MN) stimulation.

	Tonic	**Burst**
TN stim [mA] [mean ($\pm$ std)]	27.4 ($\pm$ 11.4)	28.0 ($\pm$ 13)
MN stim [mA] [mean ($\pm$ std)]	17.3 ($\pm$ 8.2)	16.3 ($\pm$ 9.0)

std, standard deviation; mA, milliamperes.

4.2.4. The Effect of Pain Reduction

Based on the patients who were a responder or a non-responder to both paradigms, a correlation between the effect of SCS on the SER amplitude and the effect of SCS on chronic pain was improbable. These patients did not experience a difference in pain relief between both SCS paradigms, while they did exhibit differences in SER amplitude. Based on the patients who were a responder to one of the paradimgs and a non-responder to the other, a subtle trend was observed towards higher SER amplitudes during the paradigm to which they were a responder. However, these results were not consistent: the SER amplitude following from median nerve stimulation in the hand area of the S1 was higher during burst SCS in the responder to tonic SCS (Figure G.14a). Additionally, the SER amplitudes of the patient who was a responder to both paradimgs were notably low compared to the other patients. In the comparison within the paradigms, no trends were observed that could differentiate between responders and non-responders within tonic SCS as well as within burst SCS for both the SERs elicited by tibial nerve and median nerve stimulation. These results align with the literature and may be attributed to the fact that the MOA of SCS on the SER may differ from the MOA of SCS on chronic pain [67, 69, 74].

4.3. General Strengths and Limitations

In this section, the general strengths and limitations of the research are discussed.

4.3.1. Patient Group Size

In this thesis, different patient group sizes were utilized for different comparisons: the cases studies involved analyses within individual patients and between two sets of two patients, the group of patients included in the study before SCS and during SCS consisted of four patients, and the groups of patients during the various SCS paradigms consisted of 19 to 22 patients (Table F.2).

In particular the group sizes for the case studies and for the comparison between before SCS and during SCS were small. However, these group sizes are comparable to the group sizes typically observed in this field of research. For studies that examined the influence of SCS on the painful or non-painful SER, the majority of studies are case studies based on one or two patients [48, 49, 54, 58, 60, 63, 73] or studies with not more than 10 included patients [45, 61, 62, 66, 68, 69, 72, 75, 110]. Research on SERs is subject to substantial between- and within-patient variability in amplitude [42], which was observed for the case studies in this thesis: differences between SER amplitudes were occasionally very large in these individual patients, as was evident from Figure 3.11. Next to the variability in SER research, the heterogeneity of chronic pain as a concept contributes to this variability as well [112].

As described, the observed differences between SERs in patients before SCS treatment and during SCS were small and somewhat inconsistent, therefore not completely aligning with the majority of literature. This discrepancy with both smaller and larger study groups could possibly be attributed to both the high variability of SERs and the heterogeneity of chronic pain. Additionally, the possibility of publication bias in published case studies may have affected the existing literature. For studies with small patient group sizes, it is possible that the published results were observed by chance and thus reported, rather than reflecting a consistent trend that would be observed in a larger patient group. Contrary to other studies with small patient groups, often case studies, the group of patients included for this thesis for the comparison between before and during SCS did not consist of selected patients based on the effect of SCS on the SER amplitude; it included all patients who had coincidentally already been included in the study before SCS treatment.

In contrast, the group size of patients treated with SCS used to compare between various SCS paradigms, was relatively large compared to other studies in the research field, even after exclusion of unusable data (n=19 - n=22, Table F.2). The impact of a larger patient group was observable in, for instance, the standard error of the first component in the S1. The standard error was smaller in the groups of approximately 20 patients (Figure 3.6) compared to the group of four patients (Figure 3.1). In a generalized overview, summarizing the relationship between group size, observed difference in amplitude, and the accompanying standard error, the SER amplitudes of the case studies (n=1) demonstrated large differences, while the group of patients that were also included before SCS treatment (n=4) showed smaller differences with relatively large standard errors. In the larger patient groups (n=19 - n=20), the difference in amplitude was either small accompanied by a small standard error (early component S1) or large accompanied by a large standard error (later latency components).

4.3.2. Interpretation of Somatosensory Evoked Responses

The performed analysis was exploratory in nature. For this reason, no statistical methods were employed to analyze the statistical significance of observed differences. To interpret differences, the standard error of the mean was utilized as an indication. Due to the absence of a statistical analysis, no compensation was done for the performance of multiple comparisons; performing multiple comparisons increases the likelihood of observing differences, which necessitates compensation. Implementing a standardized approach to analyze the SERs in this thesis was challenging due to the numerous comparisons and the inherent large variability in SER research. It would be challenging to define specific latencies of SER components that apply to all comparisons and cross all ROIs where these components should be observable to be able to perform statistical analysis for specific SER components. Because latencies may differ slightly due to the variability in SERs, this would possibly lead to skewed results.

When interpreting the results, one must consider that the graphs displaying the SERs in the ROIs are the result of multiple averaging processes. Firstly, approximately 200 SERs are averaged for each recording. Secondly, the averaged SERs of approximately 20 patients per group are averaged using the source maps (average $\pm$ standard error). Lastly, the vertices of the ROIs that were defined on the averaged source maps are averaged to produce the final graphs. Consequently, these graphs are sensitive to the methodological steps. This supports the choice for minimal filtering of the MEG data, because this enhanced the chance of observing genuine results that are not affected by filtering. For instance, low-pass filtering of the data before normalization relative to a time segment without evoked activity ("the baseline") yields a cleaner baseline, and consequently higher z-scores, potentially exaggerating differences.

The mean function for the ROIs was selected due to its intuitive nature and ease of interpretation by other researches in the primarily medical field, particularly when combined with the standard error. Alternative approaches such as Principal Component Analysis (PCA) or using the maximum value could potentially highlight differences by focusing on the extremer values within the ROIs. However, these approaches are more sensitive to outliers than using the mean of the ROI. In addition to the mean function for the resultant ROI signal, the size and location of the ROIs is of importance as well. In the case of using the mean, an overly large ROI results in a diminished response, whereas an excessively small ROI may miss a portion of relevant activity. For this reason, the ROIs were primarily adjusted or copied from existing atlases or otherwise based on the average activation of all included recordings (seperately for the SERs elicited by tibial nerve and median nerve stimulation).

Outliers
Outliers concerning the SER amplitude that were observed in the data were not removed unless a specific explanation could be identified, such as an evident artifact or an explanation in the recording notes. Given that SER research is subject to substantial between- and within-subject variability in amplitude [42], and the heterogeneity of chronic pain as a concept [112], outliers without explanation were considered part of the patient group. The variability within groups was accounted for by using the standard error of the mean. Since compared groups consisted of the same patients, the observed differences were assumed to be genuine differences within patients.

4.3.3. Somatosensory Evoked Responses as a Method

The SERs in this thesis were elicited in patients with chronic pain and SCS treatment with the ultimate, overarching goal of researching the possible MOAs of SCS on chronic pain. However, eliciting SERs is not equivalent to eliciting (chronic) pain; in fact, it is not possible to simulate chronic pain by a transient trigger. The SERs were used to evaluate the patients' processing of a somatosensory stimulus, and combined with SCS, how this processing is affected by SCS.

The stimuli to elicit the SERs for this thesis were, on average, not perceived as painful. This is shown in Table 4.3. On the numerical rating scale, scores of 5 or below are typically considered to represent, at most, mild pain [113]. It may thus be assumed that the stimuli to elicit the SERs were not painful. This means that the SERs mainly traveled through Aβ-fibers. These same Aβ-fibers in the dorsal column are stimulated by the spinal cord stimulator. Pain, however, travels through C- and Aδ-fibers. This complicates the translation of the possible MOAs of SCS on the non-painful SERs to the MOAs of SCS on chronic pain.

Table 4.3: Average pain intensity on the numerical rating scale (NRS) attributed to the stimuli to elicit the SERs during each paradigm, for the SERs elicited by tibial nerve (TN) stimulation and by median nerve (MN) stimulation.

	Tonic	**Burst**
TN NRS [mean ($\pm$ std)]	3.3 ($\pm$ 1.8)	3.6 ($\pm$ 1.9)
MN NRS [mean ($\pm$ std)]	3.2 ($\pm$ 1.6)	2.8 ($\pm$ 1.4)

std, standard deviation.

4.3.4. The Triple Pathway Model

The triple pathway model, as introduced in section 1.2, is a theory hypothesized by De Ridder et al. to explain the mechanism of chronic pain. It provides a plausible summary and explanation for the complex mechanisms of chronic pain and, based on these mechanisms, provides potential treatment methods. For instance, the triple pathway model is used to support the additional value of the newer burst SCS paradigm over the conventional tonic SCS paradigm. Based on the results in this thesis, which were based on a relatively large group of patients, no new evidence was found to substantiate this theory.

An important caveat regarding this theory is the fact that a relatively small group of researchers, particularly De Ridder and several co-authors who frequently publish together, are actively publishing evidence for this theory. This is evident when using `connectedpapers.com` for one of their recently published studies [4, 13]. Moreover, De Ridder himself has a significant conflict of interest as the patent holder to the first burst SCS waveform with one of the major companies in neurostimulation. Abbott's BurstDR, which was used in this thesis as well, means Burst-De-Ridder [114]. This could be considered a motivating factor to promote belief in the triple pathway model.

Furthermore, another limitation of this theory lies in the practical challenges of distinguishing the specified structures of the separate pathways using neuroimaging techniques such as MEG and EEG. In this thesis, using state-of-the-art 275-channel MEG, differentiating between the medial and lateral thalamus was not feasible. Nor was it possible to assess the descending pathway based on the pregenual anterior cingulate cortex (pgACC) because this structure could not be distinguished from the ACC in its entirety.

4.4. Directions for Further Research

In this section, several directions for further research are described, based on the observed results in this thesis.

4.4.1. Spinal Effects of SCS

The comparison of the SERs elicited by tibial nerve stimulation to the SERs elicited by median nerve stimulation before and during SCS supported the possibility of a spinal MOA of SCS on the SER amplitude, as was described in subsection 4.2.2. This potential MOA of SCS on the SER amplitude should be further explored to confirm its existence, given that only four patients that were included before SCS treatment were available for comparison.

Further research on this potential spinal mechanism should employ recordings during SCS and without SCS, preferably using SCS-ON and SCS-OFF conditions as opposed to the before and during SCS conditions in this thesis. If collision of impulses is a MOA of SCS on the SER, this should initiate immediately with turning SCS on and cease immediately with turning SCS off. Similar to this thesis, the SERs should be elicited on two peripheral locations to enter the spinal cord both above and below the SCS electrode (Figure 1.5). This is most feasible in patients with pain in one of the lower extremities because for these patients, the spinal cord stimulator electrodes are located in the lower part of the back. Additionally, a group of patients suffering from chronic pain in one of the upper extremities should be included to serve as a control group. In both patient groups, SERs should be elicited on the affected limb and the other ipsilateral limb, because the largest effect of SCS is expected on the affected area. In the group with unilateral *lower* limb pain, greater differences in the two distinct SERs are expected during SCS-ON compared to SCS-OFF, similar to this thesis. In the group with unilateral *upper* limb pain, *no* greater differences are expected based on collision of impulses; the SERs elicited on the lower limb should be equally affected by SCS as the SERs elicited on the upper limb, because both SERs travel through the part of the spinal cord that is stimulated by SCS.

A possible addition to the research on spinal mechanisms of SCS on the SER is the use of SCS leads that are capable of recording from the spinal cord, such as the closed-loop SCS systems as developed by Saluda Medical [115] and Medtronic [116]. Confirmation of a spinal effect could potentially be achieved through the combination of measurements on the spinal cord as well as supraspinally using MEG or EEG.

However, the clinical relevance of researching the effect of SCS on the SER remains uncertain, as no correlation has yet been established between the effect of SCS on the SER and the effect of SCS on chronic pain. Furthermore, this direction for further research focuses on a potential spinal mechanism of SCS, but a supraspinal mechanism of SCS on the SER or on chronic pain should not be ruled out. In fact, it is highly unlikely that the MOA of SCS on either the SER or on chronic pain is solely spinal. If the MOAs of SCS were solely spinal, we would have a more comprehensive understanding of these MOAs today than is currently the case.

4.4.2. Pain Area

For the patients treated with SCS who were included in this thesis, approximately half experienced pain in the right lower extremity (Table 3.1). Consequently, for this subgroup of patients, the SERs elicited by tibial nerve stimulation were elicited within the chronic pain area. This may have affected, in particular, the results of two comparisons, namely the comparison between SERs elicited by tibial nerve stimulation and median nerve stimulation before and during SCS, and the comparison between SERs during tonic and burst SCS. Using the data for this thesis, further research could be done exploring the influence of eliciting SERs within or outside of the pain area.

For the comparison between SERs elicited by tibial nerve stimulation and median nerve stimulation before and during SCS, the group should be divided into two subgroups based on pain area (right side versus left side). The changes in AUC ratios between the different conditions (before SCS, during tonic SCS, during burst SCS) should be compared between these two subgroups. In theory, the greatest effect of SCS would be expected in the pain area, because this area is innervated by the SCS. Consequently, in the subpopulation of patients with pain in the right leg, the changes in AUC ratio during SCS compared to before SCS may be larger, compared to the subpopulation of patients without pain in the right leg.

For the comparison between SERs during tonic and burst SCS, the subpopulation of patients experiencing pain in the right lower extremity should be selected. Using the results from this subpopulation for the SERs elicited by tibial nerve stimulation during tonic and burst SCS allows for a more accurate comparison with the results reported by Niso et al. [46]. The results from this subpopulation might align more closely with the results reported by Niso et al. [46].

4.4.3. Pain Relief

Researching SERs is subject to substantial between- and within-patient variability in amplitude [42], which complicates researching SERs in individual patients. This was evident for the case studies in this thesis: differences between SER amplitudes were occasionally exceptionally large in these individual patients (Figure 3.11). In the data used for this thesis, it was not feasible to create larger groups of responders and non-responders. Based on the patients who were responders to one of the paradigms and non-responders to the other paradigm, a subtle trend was observed towards higher SER amplitudes during the paradigm to which they were a responder. Consequently, potential further research on the correlation between the effect of SCS on the SER amplitude and the effect of SCS on chronic pain should focus on patients that are known responders to either tonic or burst SCS and known non-responders to the other paradigm. If such a correlation exists, it could potentially be used to identify patients who are responders to a specific paradigm based on the assessment of non-painful SERs during different SCS paradigms, which is an easier process compared to the current process of multiple trial periods for the different SCS paradigms.

4.4.4. Other Regions of Interest

Cerebellum

The cerebellum is classically considered to be a brain region involved in motor processing, but it has also been linked to chronic pain [117, 118]. It has been suggested that the cerebellum may have a role in nociceptive processing and pain. For instance, it has been suggested that the cerebellum may engage the pain modulating circuitry in the brainstem, which is referred to as the descending pain inhibitory pathway in this thesis [4, 119]. Furthermore, Moens et al. reported that pain relief obtained by short-term SCS negatively correlated with activity in the cerebellum using functional magnetic resonance imaging (fMRI) [120]. However, the role of the cerebellum in the experience of pain is still not well defined.

For SERs elicited by non-painful stimuli, it has been suggested that the somatosensory pathway in SERs travels through the cerebellum and that the SER may consequently be altered by the cerebellum [109]. Additionally, for one of the patients included in this thesis, remarkable activation was visible in the cerebellar area following the non-painful stimulation of the median nerve and the tibial nerve. Consequently, the cerebellum may be an interesting additional structure to research in the context of chronic pain, SCS, and SERs elicited by non-painful stimuli. In Brainstorm, the ASEG volume parcellation is available as atlas and includes the cerebellum as subcortical structure [121, 122]. Using this atlas, the cerebellar activity following non-painful stimulation of the tibial nerve and the median nerve may be assessed for the patients who were included in this thesis.

Periaqueductal gray
The periaqueductal gray (PAG) is a substructure of the brain stem and has been correlated to pain and pain processing as well as emotiononal processing [123, 124]. It has been identified as a key structure of the descending pain modulation system, which is referred to as the descending pain inhibitory pathway in this thesis [4, 125, 126]. In pain research, the PAG has been researched in the context of painful peripheral stimulation and conditioned pain modulation, due to its considered inhibitory function [127]. In this thesis, predominantly the ascending medial and ascending lateral pathways were assessed based on the selected ROIs. The only ROI of the descending pathway that was selected was the pgACC, however, this was part of the encompassing ACC and did not exhibit different results. Consequently, to additionally assess the descending pathway, the PAG may be an interesting structure to include in further research on the SERs elicited by non-painful stimuli that were assessed in this thesis. Similar to the cerebellum, the brain stem is available as structure in the ASEG volume parcellation, which is available in Brainstorm [121, 122].

Additional ROIs
Additional (cortical) ROIs are mentioned in chronic pain research. For instance, the orbitofrontal cortex (OFC) and dorsolateral prefrontal cortex (DLPFC) have been suggested to play a role in the distraction of pain [128, 129], whereas the supplementary motor area (SMA) and primary motor cortex (M1) have been suggested to be correlated with the somatosensory processing of pain [46]. An approach to identify additional potentially interesting ROIs to evaluate the effect of SCS on the SERs that were analyzed in this thesis is to determine and analyze the differences between the source models of various groups. This can be done in Brainstorm by subtracting two source models [130]. This approach is most straightforward for the surface source models, but can also be applied to the volume source models. This approach allows for the observation of possible differences in activity in specific brain regions between groups. This method was also used by Niso et al. to identify the origin of the observed differences in the SERs during burst SCS compared to tonic and sham SCS [46].

4.4.5. Comparison to EEG
In addition to the ROIs described in subsection 2.2.5, the vertex was defined as ROI to facilitate a potential comparison with EEG research. For this study, in addition to the MEG measurement, EEG sensors were used at the vertex (Cz), CP3, and CP4 according to the 10-20 system for EEG, to capture the SERs. These EEG signals can be compared to the MEG signals to examine the similarities and differences between the two imaging modalities in this same dataset. Besides, the EEG signal can potentially be compared to other EEG research in the field; the majority of studies employed EEG measurements from the vertex [54, 59, 60, 62, 67–69, 72–74]. This is primarily relevant for the early components of the SER, considering the location of the EEG sensors situated on the S1.

4.4.6. Time-Frequency Representation
Next to the somatosensory *evoked* responses (SERs), the *induced* response following from non-painful peripheral stimulation can be analyzed using the time-frequency representation (TRF). The TRF provides temporal and spectral information of the induced response [131]. The induced response consists of induced oscillations after stimulation that are not phase locked to the stimulus [132]. These brain oscillations can be described in terms of frequency bands, each associated with a certain brain state [133]. Ploner et al. reported that a painful stimulus globally suppressed spontaneous oscillations in somatosensory, motor and visual areas in healthy individuals [134]. Additionally, Jin et al. applied electrical pain and reported reduced beta power in and around the sensorimotor cortex together with reduced subjective pain ratings in chronic pain patients and healthy controls during conditioned pain modulation [135]. These results suggest that the TFR may be interesting to explore for the SERs elicited by non-painful stimulation in included in this thesis as well.

5

Conclusion

The primary objective of this thesis was to assess how various spinal cord stimulation (SCS) paradigms affect the supraspinal somatosensory evoked response (SER) elicited by a non-painful peripheral stimulus. Supraspinal SERs elicited by non-painful transcutaneous electrical stimulation of the tibial nerve as well as of the median nerve were evaluated in chronic pain patients treated with tonic and burst SCS, utilizing magnetoencephalography (MEG) as a measurement technique.

The results suggested an inhibitory effect of SCS on the SER elicited by tibial nerve stimulation, whereas the amplitude of the SER elicited by median nerve stimulation tended to increase during SCS. The comparison between SERs elicited by tibial nerve stimulation and SERs elicited by median nerve stimulation in patients before and during SCS suggested a spinal effect of SCS on the SER. However, supraspinal mechanisms of action (MOAs) of SCS on the SER and on chronic pain likely play a role as well. For both the SERs elicited by tibial nerve and by median nerve stimulation, the SER amplitudes were predominantly higher during burst SCS compared to tonic SCS. The hypothesis that tonic SCS solely acts on the lateral pain pathway and burst SCS additionally acts on the medial pain pathway (associated with emotional/attentional processing) could not be confirmed with our results. Our results do not suggest decreased emotional/attentional processing of the SER during burst SCS compared to tonic SCS. Furthermore, no evidence was found to support a correlation between the effect of SCS on the SER and the effect of SCS on the chronic pain condition, underscoring the complexity of the relationship between the somatosensory processing and the experience of chronic pain in the context of spinal cord stimulation.

References

[1] S. N. Raja *et al.*, "The revised international association for the study of pain definition of pain: Concepts, challenges, and compromises," *Pain*, vol. 161, no. 9, pp. 1976–1982, Sep. 1, 2020. DOI: 10.1097/j.pain.0000000000001939.

[2] V. Santiago, "Painful truth: The need to re-center chronic pain on the functional role of pain," *Journal of Pain Research*, vol. 15, pp. 497–512, Feb. 16, 2022. DOI: 10.2147/JPR.S347780.

[3] R.-D. Treede *et al.*, "Chronic pain as a symptom or a disease: The IASP classification of chronic pain for the international classification of diseases (ICD-11)," *Pain*, vol. 160, no. 1, pp. 19–27, Jan. 2019. DOI: 10.1097/j.pain.0000000000001384.

[4] D. De Ridder, S. Vanneste, M. Smith, and D. Adhia, "Pain and the triple network model," *Frontiers in Neurology*, vol. 13, p. 757 241, 2022. DOI: 10.3389/fneur.2022.757241.

[5] S. P. Cohen, L. Vase, and W. M. Hooten, "Chronic pain: An update on burden, best practices, and new advances," *The Lancet*, vol. 397, no. 10289, pp. 2082–2097, May 29, 2021. DOI: 10.1016/S0140-6736(21)00393-7.

[6] A. Berger, E. M. Dukes, and G. Oster, "Clinical characteristics and economic costs of patients with painful neuropathic disorders," *The Journal of Pain*, vol. 5, no. 3, pp. 143–149, Apr. 1, 2004. DOI: 10.1016/j.jpain.2003.12.004.

[7] D. S. Goldberg and S. J. McGee, "Pain as a global public health priority," *BMC public health*, vol. 11, p. 770, Oct. 6, 2011. DOI: 10.1186/1471-2458-11-770.

[8] M. L. Ferreira *et al.*, "Global, regional, and national burden of low back pain, 1990–2020, its attributable risk factors, and projections to 2050: A systematic analysis of the global burden of disease study 2021," *The Lancet Rheumatology*, vol. 5, no. 6, e316–e329, Jun. 1, 2023. DOI: 10.1016/S2665-9913(23)00098-X.

[9] J. Hartvigsen *et al.*, "What low back pain is and why we need to pay attention," *Lancet (London, England)*, vol. 391, no. 10137, pp. 2356–2367, Jun. 9, 2018. DOI: 10.1016/S0140-6736(18)30480-X.

[10] S. E. E. Mills, K. P. Nicolson, and B. H. Smith, "Chronic pain: A review of its epidemiology and associated factors in population-based studies," *BJA: British Journal of Anaesthesia*, vol. 123, no. 2, e273, Aug. 2019. DOI: 10.1016/j.bja.2019.03.023.

[11] B. Kulkarni *et al.*, "Attention to pain localization and unpleasantness discriminates the functions of the medial and lateral pain systems," *European Journal of Neuroscience*, vol. 21, no. 11, pp. 3133–3142, 2005. DOI: 10.1111/j.1460-9568.2005.04098.x.

[12] D. De Ridder and S. Vanneste, "Burst and tonic spinal cord stimulation: Different and common brain mechanisms," *Neuromodulation: Technology at the Neural Interface*, vol. 19, no. 1, pp. 47–59, Jan. 1, 2016. DOI: 10.1111/ner.12368.

[13] D. De Ridder, D. Adhia, and S. Vanneste, "The anatomy of pain and suffering in the brain and its clinical implications," *Neuroscience & Biobehavioral Reviews*, vol. 130, pp. 125–146, Nov. 1, 2021. DOI: 10.1016/j.neubiorev.2021.08.013.

[14] S. Vanneste and D. De Ridder, "Chronic pain as a brain imbalance between pain input and pain suppression," *Brain Communications*, vol. 3, no. 1, fcab014, 2021. DOI: 10.1093/braincomms/fcab014.

[15] L. Kapural, "Spinal cord stimulation for intractable chronic pain," *Current Pain and Headache Reports*, vol. 18, no. 4, p. 406, Apr. 2014. DOI: 10.1007/s11916-014-0406-7.

[16] T. Cameron, "Safety and efficacy of spinal cord stimulation for the treatment of chronic pain: A 20-year literature review," *J Neurosurg*, vol. 100, no. 3, pp. 254–67, Mar. 2004. DOI: 10.3171/spi.2004.100.3.0254.

[17] K. Kumar, G. Hunter, and D. Demeria, “Spinal cord stimulation in treatment of chronic benign pain: Challenges in treatment planning and present status, a 22-year experience,” *Neurosurgery*, vol. 58, no. 3, 481–96, discussion 481–96, Mar. 2006. DOI: 10.1227/01.NEU.0000192162.99567.96.

[18] K. J. Burchiel *et al.*, “Prospective, multicenter study of spinal cord stimulation for relief of chronic back and extremity pain,” *Spine*, vol. 21, no. 23, pp. 2786–94, Dec. 1996. DOI: 10.1097/00007632-199612010-00015.

[19] O. Viswanath, I. Urits, E. Bouley, J. M. Peck, W. Thompson, and A. D. Kaye, “Evolving spinal cord stimulation technologies and clinical implications in chronic pain management,” *Curr Pain Headache Rep*, vol. 23, no. 6, p. 39, May 2019. DOI: 10.1007/s11916-019-0778-9.

[20] K. V. Slavin, R. B. North, T. R. Deer, P. Staats, K. Davis, and R. Diaz, “Tonic and burst spinal cord stimulation waveforms for the treatment of chronic, intractable pain: Study protocol for a randomized controlled trial,” *Trials*, vol. 17, p. 569, Dec. 1, 2016. DOI: 10.1186/s13063-016-1706-5.

[21] S. M. Sherman, “Tonic and burst firing: Dual modes of thalamocortical relay,” *Trends in Neurosciences*, vol. 24, no. 2, pp. 122–126, Feb. 1, 2001. DOI: 10.1016/S0166-2236(00)01714-8.

[22] T. Kirketeig, C. Schultheis, X. Zuidema, C. W. Hunter, and T. Deer, “Burst spinal cord stimulation: A clinical review,” *Pain Medicine*, vol. 20, S31–+, Jun. 2019. DOI: 10.1093/pm/pnz003.

[23] H. A. Swadlow and A. G. Gusev, “The impact of ’bursting’ thalamic impulses at a neocortical synapse,” *Nature Neuroscience*, vol. 4, no. 4, pp. 402–408, Apr. 2001. DOI: 10.1038/86054.

[24] R. Melzack and P. D. Wall, “Pain mechanisms: A new theory,” *Science*, vol. 150, no. 3699, pp. 971–9, Nov. 19, 1965. DOI: 10.1126/science.150.3699.971.

[25] A. D. Sdrulla, Y. Guan, and S. N. Raja, “Spinal cord stimulation: Clinical efficacy and potential mechanisms,” *Pain Practice*, vol. 18, no. 8, pp. 1048–1067, Nov. 2018. DOI: 10.1111/papr.12692.

[26] L. Heijmans and E. A. Joosten, “Mechanisms and mode of action of spinal cord stimulation in chronic neuropathic pain,” *Postgraduate Medicine*, vol. 132, pp. 17–21, Nov. 16, 2020. DOI: 10.1080/00325481.2020.1769393.

[27] J. C. Oakley and J. P. Prager, “Spinal cord stimulation - mechanisms of action,” *Spine*, vol. 27, no. 22, pp. 2574–2583, Nov. 15, 2002. DOI: 10.1097/00007632-200211150-00034.

[28] E. Sivanesan, D. P. Maher, S. N. Raja, B. Linderoth, and Y. Guan, “Supraspinal mechanisms of spinal cord stimulation for modulation of pain five decades of research and prospects for the future,” *Anesthesiology*, vol. 130, no. 4, pp. 651–665, Apr. 2019. DOI: 10.1097/Aln.0000000000002353.

[29] K. Chakravarthy, R. Malayil, T. Kirketeig, and T. Deer, “Burst spinal cord stimulation: A systematic review and pooled analysis of real-world evidence and outcomes data,” *Pain Medicine*, vol. 20, S47–+, Jun. 2019. DOI: 10.1093/pm/pnz046.

[30] D. De Ridder *et al.*, “A 2-center comparative study on tonic versus burst spinal cord stimulation: Amount of responders and amount of pain suppression,” *The Clinical Journal of Pain*, vol. 31, no. 5, pp. 433–437, May 2015. DOI: 10.1097/AJP.0000000000000129.

[31] J.-B. Peeters and C. Raftopoulos, “Tonic, burst, high-density, and 10-kHz high-frequency spinal cord stimulation: Efficiency and patients’ preferences in a failed back surgery syndrome predominant population. review of literature,” *World Neurosurgery*, vol. 144, e331–e340, Dec. 1, 2020. DOI: 10.1016/j.wneu.2020.08.128.

[32] C. C. de Vos, M. J. Bom, S. Vanneste, M. W. P. M. Lenders, and D. de Ridder, “Burst spinal cord stimulation evaluated in patients with failed back surgery syndrome and painful diabetic neuropathy,” *Neuromodulation: Technology at the Neural Interface*, vol. 17, no. 2, pp. 152–159, Feb. 1, 2014. DOI: 10.1111/ner.12116.

[33] P. Courtney *et al.*, “Improved pain relief with burst spinal cord stimulation for two weeks in patients using tonic stimulation: Results from a small clinical study,” *Neuromodulation: Technology at the Neural Interface*, vol. 18, no. 5, pp. 361–366, 2015. DOI: 10.1111/ner.12294.

[34] T. Deer *et al.*, “Success using neuromodulation with BURST (SUNBURST) study: Results from a prospective, randomized controlled trial using a novel burst waveform,” *Neuromodulation: Technology at the Neural Interface*, vol. 21, no. 1, pp. 56–66, Jan. 1, 2018. DOI: 10.1111/ner.12698.

[35] K. Garcia, J. K. Wray, and S. Kumar, “Spinal cord stimulation,” in *StatPearls*, Treasure Island (FL): StatPearls Publishing, 2023.

[36] C.-T. Yen and P.-L. Lu, “Thalamus and pain,” *Acta Anaesthesiologica Taiwanica*, vol. 51, no. 2, pp. 73–80, Jun. 1, 2013. DOI: 10.1016/j.aat.2013.06.011.

[37] Y. Tu *et al.*, “Distinct thalamocortical network dynamics are associated with the pathophysiology of chronic low back pain,” *Nature Communications*, vol. 11, no. 1, p. 3948, Aug. 7, 2020. DOI: 10.1038/s41467-020-17788-z.

[38] K. D. Davis, C. L. Kwan, A. P. Crawley, and D. J. Mikulis, “Functional MRI study of thalamic and cortical activations evoked by cutaneous heat, cold, and tactile stimuli,” *Journal of Neurophysiology*, vol. 80, no. 3, pp. 1533–1546, Sep. 1, 1998. DOI: 10.1152/jn.1998.80.3.1533.

[39] Y. Jin *et al.*, “The medial thalamus plays an important role in the cognitive and emotional modulation of orofacial pain: A functional magnetic resonance imaging-based study,” *Frontiers in Neurology*, vol. 11, 2021. DOI: 10.3389/fneur.2020.589125.

[40] K. P. Meuwissen, A. van der Toorn, J. W. Gu, T. C. Zhang, R. M. Dijkhuizen, and E. A. Joosten, “Active recharge burst and tonic spinal cord stimulation engage different supraspinal mechanisms: A functional magnetic resonance imaging study in peripherally injured chronic neuropathic rats,” *Pain Practice*, vol. 20, no. 5, pp. 510–521, 2020. DOI: 10.1111/papr.12879.

[41] T. Maudrich, S. Haehner, R. Kenville, and P. Ragert, “Somatosensory-evoked potentials as a marker of functional neuroplasticity in athletes: A systematic review,” *Frontiers in Physiology*, vol. 12, Jan. 17, 2022. DOI: 10.3389/fphys.2021.821605.

[42] G. Cruccu *et al.*, “Recommendations for the clinical use of somatosensory-evoked potentials,” *Clinical Neurophysiology*, vol. 119, no. 8, pp. 1705–1719, Aug. 1, 2008. DOI: 10.1016/j.clinph.2008.03.016.

[43] A. C. Schouten, “TM12005: Advanced signal processing - lecture 6: Input signals,” 2020.

[44] R. Kakigi, S. Koyama, M. Hoshiyama, M. Shimojo, Y. Kitamura, and S. Watanabe, “Topography of somatosensory-evoked magnetic-fields following posterior tibial nerve-stimulation,” *Electroencephalography and Clinical Neurophysiology*, vol. 95, no. 2, pp. 127–134, Aug. 1995. DOI: 10.1016/0013-4694(95)00053-2.

[45] H. Poláček, J. Kozak, I. Vrba, J. Vrana, and A. Stancak, “Effects of spinal cord stimulation on the cortical somatosensory evoked potentials in failed back surgery syndrome patients,” *Clin Neurophysiol*, vol. 118, no. 6, pp. 1291–1302, Jun. 2007. DOI: 10.1016/j.clinph.2007.02.029.

[46] G. Niso, M. C. Tjepkema-Cloostermans, M. Lenders, and C. C. de Vos, “Modulation of the somatosensory evoked potential by attention and spinal cord stimulation,” *Front Neurol*, vol. 12, p. 694 310, 2021. DOI: 10.3389/fneur.2021.694310.

[47] C. Kany and R. D. Treede, “Median and tibial nerve somatosensory evoked potentials: Middle-latency components from the vicinity of the secondary somatosensory cortex in humans,” *Electroencephalography and Clinical Neurophysiology*, vol. 104, no. 5, pp. 402–410, Sep. 1997. DOI: 10.1016/s0168-5597(97)00045-2.

[48] P. L. Gildenberg and K. S. Murthy, “Influence of dorsal column stimulation upon human thalamic somatosensory-evoked potentials,” *Appl Neurophysiol*, vol. 43, no. 1, pp. 8–17, 1980. DOI: 10.1159/000102228.

[49] L. E. Augustinsson, C. A. Carlsson, and P. Leissner, “Effect of dorsal column stimulation on pain-induced intracerebral impulse patterns,” *Appl Neurophysiol*, vol. 42, no. 4, pp. 212–216, 1979. DOI: 10.1159/000102372.

[50] H. Bastuji, M. Frot, S. Mazza, C. Perchet, M. Magnin, and L. Garcia-Larrea, “Thalamic responses to nociceptive-specific input in humans: Functional dichotomies and thalamo-cortical connectivity,” *Cerebral Cortex*, vol. 26, no. 6, pp. 2663–2676, Jun. 1, 2016. DOI: 10.1093/cercor/bhv106.

[51] I. M. Colrain and K. B. Campbell, “The use of evoked potentials in sleep research,” *Sleep Medicine Reviews*, vol. 11, no. 4, pp. 277–293, Aug. 2007. DOI: 10.1016/j.smrv.2007.05.001.

[52] S. H. Patel and P. N. Azzam, “Characterization of n200 and p300: Selected studies of the event-related potential,” *Int J Med Sci*, vol. 2, no. 4, pp. 147–54, 2005. DOI: 10.7150/ijms.2.147.

[53] R. Kakigi, “Somatosensory-evoked magnetic-fields following median nerve-stimulation,” *Neuroscience Research*, vol. 20, no. 2, pp. 165–174, Aug. 1994. DOI: 10.1016/0168-0102(94)90034-5.

[54] D. Floridia *et al.*, “Treatment of pain post-brachial plexus injury using high-frequency spinal cord stimulation,” *J Pain Res*, vol. 11, pp. 2997–3002, 2018. DOI: 10.2147/jpr.S168031.

[55] T. Morioka, F. Shima, M. Kato, and M. Fukui, “Origin and distribution of thalamic somatosensory evoked potentials in humans,” *Electroencephalography and Clinical Neurophysiology/Evoked Potentials Section*, vol. 74, no. 3, pp. 186–193, May 1, 1989. DOI: 10.1016/0013-4694(89)90004-7.

[56] A. Nowacki *et al.*, “Directional recordings of somatosensory evoked potentials from the sensory thalamus in chronic poststroke pain patients,” *Clinical Neurophysiology*, vol. 151, pp. 50–58, Jul. 1, 2023. DOI: 10.1016/j.clinph.2023.03.359.

[57] E. S. d. S. Pinheiro *et al.*, “Electroencephalographic patterns in chronic pain: A systematic review of the literature,” *PLoS ONE*, vol. 11, no. 2, e0149085, Feb. 25, 2016. DOI: 10.1371/journal.pone.0149085.

[58] N. Hylands-White, R. V. Duarte, P. Beeson, S. D. Mayhew, and J. H. Raphael, “Electroencephalographic evoked pain response is suppressed by spinal cord stimulation in complex regional pain syndrome: A case report,” *J Clin Monit Comput*, vol. 30, no. 6, pp. 845–848, Dec. 2016. DOI: 10.1007/s10877-015-9781-9.

[59] R. P. Iacono, A. N. Guthkelch, and M. V. Boswell, “Dorsal root entry zone stimulation for deafferentation pain,” *Stereotact Funct Neurosurg*, vol. 59, no. 1, pp. 56–61, 1992. DOI: 10.1159/000098918.

[60] T. Kumpulainen, H. Ronty, and J. Koivukangas, “Management of patients with pain,” *Ann Clin Res*, vol. 18 Suppl 47, pp. 97–101, 1986, ISSN: 0003-4762.

[61] S. J. Larson, A. Sances Jr., D. H. Riegel, G. A. Meyer, D. E. Dallmann, and T. Swiontek, “Neurophysiological effects of dorsal column stimulation in man and monkey,” *J Neurosurg*, vol. 41, no. 2, pp. 217–23, Aug. 1974. DOI: 10.3171/jns.1974.41.2.0217.

[62] P. Mazzone, R. Pisani, N. Pizio, A. Arrigo, and F. Nobili, “Cerebral blood flow and somatosensory evoked response changes induced by spinal cord stimulation: Preliminary follow-up observations,” *Stereotact Funct Neurosurg*, vol. 62, no. 1, pp. 179–85, 1994. DOI: 10.1159/000098615.

[63] P. A. Pahapill and W. Zhang, “Restoration of altered somatosensory cortical representation with spinal cord stimulation therapy in a patient with complex regional pain syndrome: A magnetoencephalography case study,” *Neuromodulation*, vol. 17, no. 1, pp. 22–27, 2014. DOI: 10.1111/ner.12033.

[64] W. A. Pluijms, R. Slangen, M. van Kleef, E. A. Joosten, and J. P. Reulen, “Increased contact heat evoked potential stimulation latencies in responders to spinal cord stimulation for painful diabetic polyneuropathy,” *Neuromodulation*, vol. 18, no. 2, 126–132, discussion 132, Feb. 2015. DOI: 10.1111/ner.12188.

[65] A. Sestito *et al.*, “Spinal cord stimulation normalizes abnormal cortical pain processing in patients with cardiac syndrome x,” *Pain*, vol. 139, no. 1, pp. 82–89, Sep. 30, 2008. DOI: 10.1016/j.pain.2008.03.015.

[66] R. D. Blair, R. G. Lee, and G. Vanderlinden, “Dorsal column stimulation. its effect on the somatosensory evoked response,” *Arch Neurol*, vol. 32, no. 12, pp. 826–829, Dec. 1975. DOI: 10.1001/archneur.1975.00490540070009.

[67] E. Urasaki, M. Tsuda, S. Nakane, K. Toyoda, T. Umeno, and Y. Yamakawa, “Spinal cord stimulation for intractable pain evaluated by a collision study using somatosensory evoked potentials: A preliminary report,” *Neuromodulation*, vol. 17, no. 8, 746–752, discussion 752, Dec. 2014. DOI: 10.1111/ner.12205.

[68] E. Urasaki, Y. Miyagi, S. Muramatsu, and Y. Ezaki, “Comparison of the interference effects on somatosensory evoked potential from tonic, burst, and high-dose spinal cord stimulations,” *Neurol Med Chir (Tokyo)*, vol. 62, no. 7, pp. 313–321, Jul. 15, 2022. DOI: 10.2176/jns-nmc.2021-0298.

[69] T. Wolter, K. Kieselbach, R. Sircar, and M. Gierthmuehlen, “Spinal cord stimulation inhibits cortical somatosensory evoked potentials significantly stronger than transcutaneous electrical nerve stimulation,” *Pain physician*, vol. 16, no. 4, pp. 405–414, Jul. 2013, ISSN: 2150-1149.

[70] L. D. Bentley, R. V. Duarte, P. L. Furlong, R. L. Ashford, and J. H. Raphael, “Brain activity modifications following spinal cord stimulation for chronic neuropathic pain: A systematic review,” *European Journal of Pain (London, England)*, vol. 20, no. 4, pp. 499–511, Apr. 2016. DOI: 10.1002/ejp.782.

[71] T. Bocci *et al.*, “Neurophysiological comparison among tonic, high frequency, and burst spinal cord stimulation: Novel insights into spinal and brain mechanisms of action,” *Neuromodulation*, vol. 21, no. 5, pp. 480–488, Jul. 2018. DOI: 10.1111/ner.12747.

[72] M. Buonocore, A. Bodini, L. Demartini, and C. Bonezzi, “Inhibition of somatosensory evoked potentials during spinal cord stimulation and its possible role in the comprehension of antalgic mechanisms of neurostimulation for neuropathic pain,” *Minerva Anestesiol*, vol. 78, no. 3, pp. 297–302, Mar. 2012, ISSN: 1827-1596.

[73] M. Buonocore and L. Demartini, “Inhibition of somatosensory evoked potentials during different modalities of spinal cord stimulation: A case report,” *Neuromodulation*, vol. 19, no. 8, pp. 882–884, Dec. 2016. DOI: 10.1111/ner.12380.

[74] D. C. de Andrade, B. Bendib, M. Hattou, Y. Keravel, J. P. Nguyen, and J. P. Lefaucheur, “Neurophysiological assessment of spinal cord stimulation in failed back surgery syndrome,” *Pain*, vol. 150, no. 3, pp. 485–491, Sep. 2010. DOI: 10.1016/j.pain.2010.06.001.

[75] M. Doerr, J. U. Krainick, and U. Thoden, “Pain perception in man after long term spinal cord stimulation,” *J Neurol*, vol. 217, no. 4, pp. 261–270, Mar. 1978. DOI: 10.1007/BF00312987.

[76] S. P. Singh, “Magnetoencephalography: Basic principles,” *Annals of Indian Academy of Neurology*, vol. 17, S107–S112, Suppl 1 Mar. 2014. DOI: 10.4103/0972-2327.128676.

[77] P. Volegov, A. N. Matlachov, M. A. Espy, J. S. George, and R. H. Kraus Jr., “Simultaneous magnetoencephalography and SQUID detected nuclear MR in microtesla magnetic fields,” *Magnetic Resonance in Medicine*, vol. 52, no. 3, pp. 467–470, 2004. DOI: 10.1002/mrm.20193.

[78] M. Ploner and E. S. May, “Electroencephalography and magnetoencephalography in pain research—current state and future perspectives,” *PAIN*, vol. 159, no. 2, p. 206, Feb. 2018. DOI: 10.1097/j.pain.0000000000001087.

[79] R. Hari *et al.*, “IFCN-endorsed practical guidelines for clinical magnetoencephalography (MEG),” *Clinical Neurophysiology*, vol. 129, no. 8, pp. 1720–1747, Aug. 1, 2018. DOI: 10.1016/j.clinph.2018.03.042.

[80] B. J. Baars and N. M. Gage, “Chapter 4 - the tools: Imaging the living brain,” in *Cognition, Brain, and Consciousness (Second Edition)*, B. J. Baars and N. M. Gage, Eds., London: Academic Press, Jan. 1, 2010, pp. 94–125. DOI: 10.1016/B978-0-12-375070-9.00004-8.

[81] S. Baillet, “Magnetoencephalography for brain electrophysiology and imaging,” *Nature Neuroscience*, vol. 20, no. 3, pp. 327–339, Mar. 2017. DOI: 10.1038/nn.4504.

[82] F. Tadel and J. C. Mosher. “Warping the anatomy templates.” (Mar. 22, 2023), [Online]. Available: https://neuroimage.usc.edu/brainstorm/Tutorials/TutWarping.

[83] E. Bock. “Digitize EEG sensor locations and head shape.” (Apr. 6, 2023), [Online]. Available: https://neuroimage.usc.edu/brainstorm/Tutorials/TutDigitize.

[84] F. Tadel, S. Baillet, J. C. Mosher, D. Pantazis, and R. M. Leahy, “Brainstorm: A user-friendly application for MEG/EEG analysis,” *Computational Intelligence and Neuroscience*, vol. 2011, e879716, Apr. 13, 2011. DOI: 10.1155/2011/879716.

[85] F. Tadel, E. Bock, and S. Baillet. “Tutorial 2: Import the subject anatomy - MNI normalization.” (Jan. 24, 2023), [Online]. Available: https://neuroimage.usc.edu/brainstorm/Tutorials/ImportAnatomy#MNI_normalization.

[86] F. Tadel, E. Bock, and S. Baillet. “Tutorial 4: Channel file / MEG-MRI coregistration.” (Mar. 16, 2023), [Online]. Available: https://neuroimage.usc.edu/brainstorm/Tutorials/ChannelFile.

[87] F. Tadel, E. Bock, and S. Baillet. “Tutorial 14: Additional bad segments.” (Jul. 3, 2019), [Online]. Available: https://neuroimage.usc.edu/brainstorm/Tutorials/BadSegments.

[88] M. Lalancette. “Tutorial - head motion.” (Jun. 30, 2022), [Online]. Available: https://neuroimage.usc.edu/brainstorm/Tutorials/HeadMotion.

[89] F. Tadel, E. Bock, and S. Baillet. “Tutorial 11: Bad channels.” (Mar. 7, 2019), [Online]. Available: https://neuroimage.usc.edu/brainstorm/Tutorials/BadChannels.

[90] A. de Cheveigné and I. Nelken, “Filters: When, why, and how (not) to use them,” *Neuron*, vol. 102, no. 2, pp. 280–293, Apr. 17, 2019. DOI: 10.1016/j.neuron.2019.02.039.

[91] H. Shahabi, F. Tadel, E. Bock, J. C. Mosher, R. Leahy, and S. Baillet. “Tutorial 10: Power spectrum and frequency filters.” (Mar. 19, 2021), [Online]. Available: https://neuroimage.usc.edu/brainstorm/Tutorials/ArtifactsFilter.

[92] F. Tadel, E. Bock, and S. Baillet. “Tutorial 15: Import epochs.” (Apr. 25, 2022), [Online]. Available: https://neuroimage.usc.edu/brainstorm/Tutorials/Epoching.

[93] F. Tadel, E. Bock, and J. C. Mosher. “Tutorial 7: Event markers.” (Sep. 8, 2020), [Online]. Available: https://neuroimage.usc.edu/brainstorm/Tutorials/EventMarkers.

[94] F. Tadel and E. Bock. “Tutorial 8: Stimulation delays.” (May 25, 2022), [Online]. Available: https://neuroimage.usc.edu/brainstorm/Tutorials/StimDelays.

[95] F. Tadel, E. Bock, R. R. Ramirez, J. C. Mosher, and R. Leahy. “Tutorial 22: Source estimation.” (May 29, 2023), [Online]. Available: https://neuroimage.usc.edu/brainstorm/Tutorials/SourceEstimation.

[96] F. Tadel, E. Bock, D. Pantazis, J. C. Mosher, R. Leahy, and S. Baillet. “Tutorial 27: Workflows.” (Jun. 5, 2023), [Online]. Available: https://neuroimage.usc.edu/brainstorm/Tutorials/Workflows.

[97] F. Tadel, E. Bock, J. C. Mosher, R. Leahy, and S. Baillet. “Tutorial 20: Head modeling.” (Nov. 1, 2022), [Online]. Available: https://neuroimage.usc.edu/brainstorm/Tutorials/HeadModel.

[98] J.-E. Le Douget, F. Tadel, and D. Schwartz. “DBA tutorial: Compute sources in deep cerebral structures.” (May 16, 2023), [Online]. Available: https://neuroimage.usc.edu/brainstorm/Tutorials/DeepAtlas.

[99] F. Tadel, E. Bock, J. C. Mosher, and S. Baillet. “Tutorial 23: Scouts.” (May 29, 2023), [Online]. Available: https://neuroimage.usc.edu/brainstorm/Tutorials/Scouts.

[100] A. Klein and J. Tourville, “101 labeled brain images and a consistent human cortical labeling protocol,” *Frontiers in Neuroscience*, vol. 6, 2012. DOI: 10.3389/fnins.2012.00171.

[101] A. Rolls, “Immunoception: The insular cortex perspective,” *Cellular & Molecular Immunology*, vol. 20, no. 11, pp. 1270–1276, Nov. 2023. DOI: 10.1038/s41423-023-01051-8.

[102] J. Jones, R. Sharma, and Y. Weerakkody. “Insular cortex,” Radiopaedia. ().

[103] E. T. Rolls, C.-C. Huang, C.-P. Lin, J. Feng, and M. Joliot, “Automated anatomical labelling atlas 3,” *NeuroImage*, vol. 206, p. 116 189, Feb. 1, 2020. DOI: 10.1016/j.neuroimage.2019.116189.

[104] U. Bingel, M. Quante, R. Knab, B. Bromm, C. Weiller, and C. Büchel, “Single trial fMRI reveals significant contralateral bias in responses to laser pain within thalamus and somatosensory cortices,” *NeuroImage*, vol. 18, no. 3, pp. 740–748, Mar. 1, 2003. DOI: 10.1016/S1053-8119(02)00033-2.

[105] J.-S. Tang, C.-L. Qu, and F.-Q. Huo, “The thalamic nucleus submedius and ventrolateral orbital cortex are involved in nociceptive modulation: A novel pain modulation pathway,” *Progress in Neurobiology*, vol. 89, no. 4, pp. 383–389, Dec. 10, 2009. DOI: 10.1016/j.pneurobio.2009.10.002.

[106] J. S. Tang, B. Yuan, Y. Q. Zhang, and S. Zhang, "The roles of thalamic nucleus submedius in nociception and pain modulation," *Sheng Li Ke Xue Jin Zhan [Progress in Physiology]*, vol. 26, no. 4, pp. 312–316, Oct. 1995, ISSN: 0559-7765.

[107] M. Lalancette. "Flattening of orientation-unconstrained source models." (Jun. 5, 2023), [Online]. Available: https://neuroimage.usc.edu/brainstorm/Tutorials/PCA#Unconstrained_source_flattening_with_PCA.

[108] D. Nichols. "Coloring for colorblindness." (), [Online]. Available: http://www.davidmathlogic.com/colorblind/.

[109] S. R. Passmore, B. Murphy, and T. D. Lee, "The origin, and application of somatosensory evoked potentials as a neurophysiological technique to investigate neuroplasticity," *J Can Chiropr Assoc*, vol. 58, no. 2, pp. 170–83, Jun. 2014, ISSN: 0008-3194 (Print) 1715-6181 (Electronic). [Online]. Available: https://www.ncbi.nlm.nih.gov/pubmed/24932021.

[110] M. H. Morgalla, Y. Zhang, M. F. de Barros Filho, G. Lepski, and B. S. Chander, "Laser-evoked potentials recover gradually when using dorsal root ganglion stimulation, and this influences nociceptive pathways in neuropathic pain patients," *Pain Practice*, vol. 22, no. 3, pp. 372–380, 2022. DOI: 10.1111/papr.13094.

[111] M. H. Morgalla, M. F. de Barros Filho, B. S. Chander, S. R. Soekadar, M. Tatagiba, and G. Lepski, "Neurophysiological effects of dorsal root ganglion stimulation (DRGS) in pain processing at the cortical level," *Neuromodulation*, vol. 22, no. 1, pp. 36–43, Jan. 2019. DOI: 10.1111/ner.12900.

[112] R. Vellucci, "Heterogeneity of chronic pain," *Clinical Drug Investigation*, vol. 32, no. 1, pp. 3–10, Feb. 1, 2012. DOI: 10.2165/11630030-000000000-00000.

[113] A. M. Boonstra *et al.*, "Cut-off points for mild, moderate, and severe pain on the numeric rating scale for pain in patients with chronic musculoskeletal pain: Variability and influence of sex and catastrophizing," *Frontiers in Psychology*, vol. 7, p. 1466, Sep. 30, 2016. DOI: 10.3389/fpsyg.2016.01466.

[114] D. De Ridder, "Spinal cord stimulation to treat pain," U.S. Patent 20120283797A1, Nov. 8, 2012.

[115] C. Brooker *et al.*, "ECAP-controlled closed-loop spinal cord stimulation efficacy and opioid reduction over 24-months: Final results of the prospective, multicenter, open-label avalon study," *Pain Practice: The Official Journal of World Institute of Pain*, vol. 21, no. 6, pp. 680–691, Jul. 2021. DOI: 10.1111/papr.13008.

[116] Medtronic. "Inceptiv™ neurostimulator." (), [Online]. Available: https://europe.medtronic.com/xd-en/healthcare-professionals/products/neurological/spinal-cord-stimulation-systems/inceptiv-neurostimulator.html.

[117] E. A. Moulton, J. D. Schmahmann, L. Becerra, and D. Borsook, "The cerebellum and pain: Passive integrator or active participator?" *Brain research reviews*, vol. 65, no. 1, pp. 14–27, Oct. 5, 2010. DOI: 10.1016/j.brainresrev.2010.05.005.

[118] J. Claassen *et al.*, "Cerebellum is more concerned about visceral than somatic pain," *Journal of Neurology, Neurosurgery & Psychiatry*, vol. 91, no. 2, pp. 218–219, Feb. 1, 2020. DOI: 10.1136/jnnp-2019-321025.

[119] C. Y. Saab and W. D. Willis, "Cerebellar stimulation modulates the intensity of a visceral nociceptive reflex in the rat," *Experimental Brain Research*, vol. 146, no. 1, pp. 117–121, Sep. 1, 2002. DOI: 10.1007/s00221-002-1107-8.

[120] M. Moens *et al.*, "Spinal cord stimulation modulates cerebral function: An fMRI study," *Neuroradiology*, vol. 54, no. 12, pp. 1399–1407, Dec. 1, 2012. DOI: 10.1007/s00234-012-1087-8.

[121] F. Tadel, E. Bock, and S. Baillet. "Tutorial 3: Display the anatomy." (Jul. 21, 2022), [Online]. Available: https://neuroimage.usc.edu/brainstorm/Tutorials/ExploreAnatomy.

[122] F. Tadel. "Using freesurfer - subcortical structures: Aseg atlas." (Apr. 6, 2023), [Online]. Available: https://neuroimage.usc.edu/brainstorm/Tutorials/LabelFreeSurfer#Subcortical_structures:_aseg_atlas.

[123] S. Ramaswamy and T. Wodehouse, "Conditioned pain modulation—a comprehensive review," *Neurophysiologie Clinique*, vol. 51, no. 3, pp. 197–208, Jun. 1, 2021. DOI: 10.1016/j.neucli.2020.11.002.

[124] L. Pessoa, “Chapter 29 - the emotional brain,” in *Conn’s Translational Neuroscience*, P. M. Conn, Ed., San Diego: Academic Press, Jan. 1, 2017, pp. 635–656. DOI: 10.1016/B978-0-12-802381-5.00046-4.

[125] K. S. Hemington and M.-A. Coulombe, “The periaqueductal gray and descending pain modulation: Why should we study them and what role do they play in chronic pain?” *Journal of Neurophysiology*, vol. 114, no. 4, pp. 2080–2083, Oct. 2015. DOI: 10.1152/jn.00998.2014.

[126] M. Mokhtar and P. Singh, “Neuroanatomy, periaqueductal gray,” in *StatPearls*, Treasure Island (FL): StatPearls Publishing, 2023.

[127] M. Vila-Pueyo, J. Hoffmann, M. Romero-Reyes, and S. Akerman, “Brain structure and function related to headache: Brainstem structure and function in headache,” *Cephalalgia*, vol. 39, no. 13, pp. 1635–1660, Nov. 1, 2019. DOI: 10.1177/0333102418784698.

[128] R. Moont, Y. Crispel, R. Lev, D. Pud, and D. Yarnitsky, “Temporal changes in cortical activation during conditioned pain modulation (CPM), a LORETA study,” *PAIN®*, vol. 152, no. 7, pp. 1469–1477, Jul. 1, 2011. DOI: 10.1016/j.pain.2011.01.036.

[129] R. Moont, Y. Crispel, R. Lev, D. Pud, and D. Yarnitsky, “Temporal changes in cortical activation during distraction from pain: A comparative LORETA study with conditioned pain modulation,” *Brain Research*, vol. 1435, pp. 105–117, Jan. 30, 2012. DOI: 10.1016/j.brainres.2011.11.056.

[130] F. Tadel, E. Bock, D. Pantazis, R. Leahy, and S. Baillet. “Tutorial 25: Difference.” (Sep. 18, 2019), [Online]. Available: https://neuroimage.usc.edu/brainstorm/Tutorials/Difference.

[131] Y. Hu, K. D. K. Luk, W. W. Lu, and J. C. Y. Leong, “Application of time–frequency analysis to somatosensory evoked potential for intraoperative spinal cord monitoring,” *Journal of Neurology, Neurosurgery & Psychiatry*, vol. 74, no. 1, pp. 82–87, Jan. 1, 2003. DOI: 10.1136/jnnp.74.1.82.

[132] O. David, J. M. Kilner, and K. J. Friston, “Mechanisms of evoked and induced responses in MEG/EEG,” *NeuroImage*, vol. 31, no. 4, pp. 1580–1591, Jul. 15, 2006. DOI: 10.1016/j.neuroimage.2006.02.034.

[133] P. A. Abhang, B. W. Gawali, and S. C. Mehrotra, “Chapter 2 - technological basics of EEG recording and operation of apparatus,” in *Introduction to EEG- and Speech-Based Emotion Recognition*, San Diego, UNITED STATES: Elsevier Science & Technology, 2016, pp. 19–50, ISBN: 978-0-12-804531-2.

[134] M. Ploner, J. Gross, L. Timmermann, B. Pollok, and A. Schnitzler, “Pain suppresses spontaneous brain rhythms,” *Cerebral Cortex*, vol. 16, no. 4, pp. 537–540, Apr. 1, 2006. DOI: 10.1093/cercor/bhj001.

[135] H. Jin, B. Witjes, M. Roy, S. Baillet, and C. C. de Vos, “Neurophysiological oscillatory markers of hypoalgesia in conditioned pain modulation,” *Pain Reports*, vol. 8, no. 6, e1096, Oct. 23, 2023. DOI: 10.1097/PR9.0000000000001096.

[136] N. Vukovic. “Illustration of a piece of cortex showing the cross-section of a gyrus and upper layer of nerve cells,” figshare. (Oct. 27, 2014).

[137] “Magnetoencephalography (MEG) at the BIC real-time, millisecond brain imaging,” McConnell Brain Imaging Centre. (), [Online]. Available: https://www.mcgill.ca/bic/meg-unit.

[138] F. Tadel, E. Bock, J. C. Mosher, and S. Baillet. “Tutorial 13: Artifact cleaning with SSP.” (May 16, 2022), [Online]. Available: https://neuroimage.usc.edu/brainstorm/Tutorials/ArtifactsSsp.

[139] F. Tadel. “Group analysis: Subject coregistration.” (Aug. 9, 2022), [Online]. Available: https://neuroimage.usc.edu/brainstorm/Tutorials/CoregisterSubjects.

[140] F. Tadel and J. C. Mosher. “Volume source estimation.” (May 30, 2023), [Online]. Available: https://neuroimage.usc.edu/brainstorm/Tutorials/TutVolSource (visited on 10/29/2023).

[141] S. Musall. “Stdshade.” (), [Online]. Available: https://nl.mathworks.com/matlabcentral/fileexchange/29534-stdshade.

A

Magnetoencephalography (MEG)

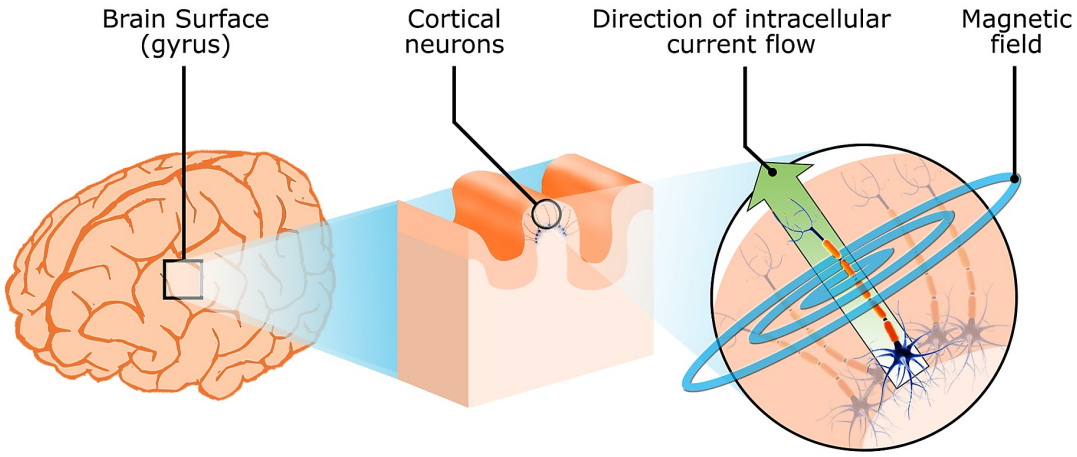

Figure A.1: The magnetic fields produced by neuronal activity that can be detected using magnetoencephalography (MEG). Figure from N. Vukovic [136].

Figure A.2: A patient in a CTF magnetoencephalography (MEG) system with their head in the MEG ”helmet”. Figure from [137].

B

Methods Flowchart

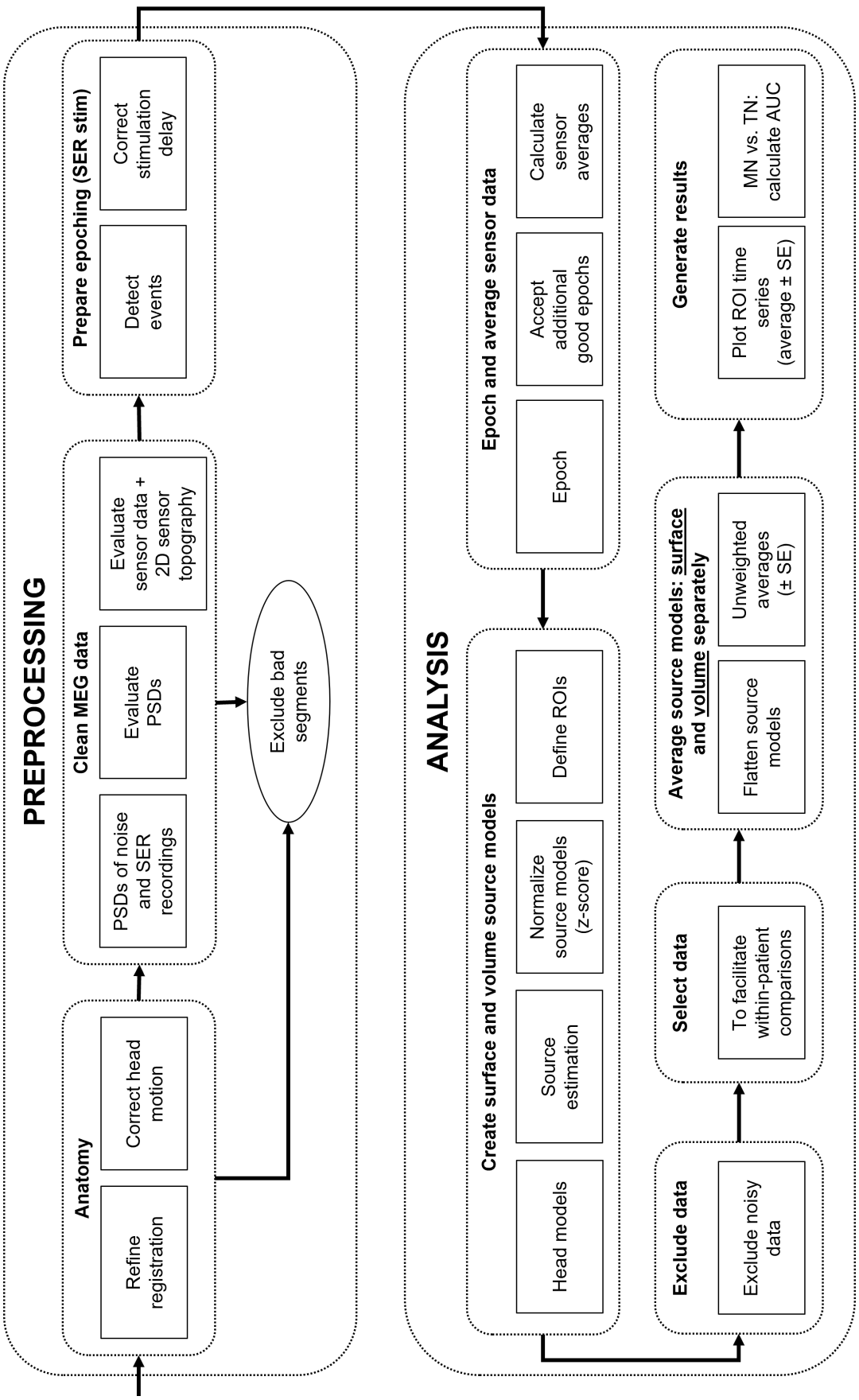

Figure B.1: Flowchart illustrating an overview of the steps described in the Methods section of this thesis. The flowchart starts in the left upper corner. The sequence of the steps is indicated by arrows.

C

Brainstorm Steps and Details

C.1. Preprocessing

C.1.1. Anatomy

1. Warping: CTF channels > MRI registration > Edit, followed by CTF channels > Digitized head points > Warp > Deform default anatomy [82]

2. Improving co-registration: CTF channels > MRI registration > Refine using headpoints, or via the Process1 box using Import > Channel file > Refine registration [86].

3. Change reference position: via the Process1 box, using ”Import > Channel file > Adjust coordinate system”. In the ”Adjust coordinate system” window, the options ”Adjust head position to median location - CTF only” and ”For adjust option, exclude bad segments” were used. The latter is to make sure that the new median head position is defined without using the segments with evident head motion [88].

C.1.2. MEG Data Cleaning

1. Create PSDs: via the Process1 box, using Frequency > Power Spectrum Density (Welch). Default settings: All file, Window Length 4s, overlap 50%, Physical units, MEG [91]. (Before you can do this, the recordings should be converted to continuous via the Process1 box: Import > Import recordings > Convert to continuous (CTF). Process options: Continuous.)

2. Rationale to omit filtering:

- **Powerline and SCS:** In general, we decided to apply minimal filtering as the removal of artifacts inevitably results in the loss of valuable information alongside noise [90]. Frequency filtering of powerline and spinal cord stimulator noise was omitted because this should only be done if certain frequencies are expected to cause a problem in the analysis, which was not the case [91]. Both the powerline and spinal cord stimulator operate on a constant frequency, whereas the SER stimulation frequency varied randomly. Consequently, the noise introduced by the powerline and the spinal cord stimulator is not time-locked to the stimulus and can be effectively attenuated with the averaging of multiple trials [91]. This is shown in Figure C.1.

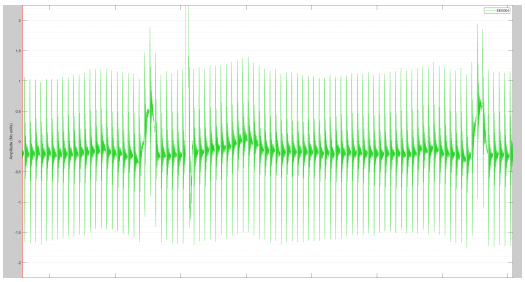

(a) Spinal cord stimulation artifact captured with the sensor applied on the patient’s back, in the raw signal

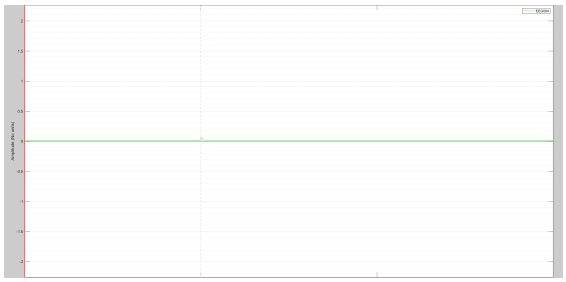

(b) Spinal cord stimulation artifact captured with the sensor applied on the patient’s back after averaging of epochs. The artifact has been effectively attenuated with the averaging of multiple trials.

Figure C.1: Brainstorm images of the spinal cord stimulation artifact, showing the effect of averaging multiple trials.

- **Physiological noise:**
  Respiration: The noise introduced by respiration was minimal and, in addition, slow and constant in nature. Due to its slow nature, this type of noise primarily introduces a baseline shift when looking at the individual trials. This baseline shift will be eliminated during epoching, as was described in subsection 2.2.2. Hence, this type of noise was effectively removed with epoching and averaging trials.

  Heartbeats: For the removal of noise caused by ocular movements and heartbeats, Brainstorm offers cleaning using signal-space-projection (SSP) as these artifacts occur frequently in the same shape and at the same location [138]. However, as heartbeats occur with a relatively constant frequency, the resulting noise could be effectively eliminated through the averaging of trials, by the same reasoning as the SCS and powerline noise.
  Ocular artifacts: Ocular movement artifacts mainly consisted of eye blinks. In theory, eye blink artifacts can be approximately time-locked to the peripheral nerve stimulation if a patient is startled by the stimulation. This possibility was assessed by inspecting the measurements and was not observed. As a result, the eye blink artifacts were not further removed, and it was assumed that this noise would be eliminated by averaging trials. Moreover, eye blinks that were visible in the MEG signal were marked as bad segments, which preserved more data than removing all eye blink-related noise using SSP.
- **SER stimulation:** Following the reasoning for SSP cleaning, this method could in theory be suitable for the stimulation artifact caused by SER stimulation as well, as it occurred roughly in the same shape and at the same location within each recording. This option was explored in a subset of patients with small, intermediate, and large SER stimulation artifacts. The SSP cleaning method was not effective in removing the stimulation artifact. In fact, using this method would remove other valuable information from the signal, such as the early latency component of the SER. For this reason, the decision was made to not apply this method to the SER stimulation artifact. Furthermore, the stimulation artifact is quite brief, often brief enough to not interfere with the early component of the SER. This exploration led to the decision to not clean out the stimulation artifact using filtering methods. However, in extreme cases, the SER stimulation could cause channels to malfunction and become erratic. These channels were removed in the deleting bad channels process. In less extreme cases, it occurred that channels exhibited an occasional baseline shift due to the SER stimulation. In these cases, the stimulation segment with the baseline shift was marked as ”bad”, while the channel was retained. An example of this is shown in Figure C.2. The elevated baseline is no longer a concern after epoching the data, as the direct current (DC) component will be removed in that process.

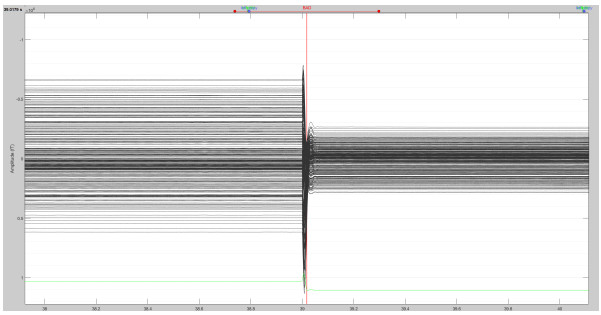

Figure C.2: Brainstorm image showing the baseline shift caused by SER stimulation. The segment of the shift itself was marked as ”bad”. The remaining change in direct current (DC) offset will be removed during epoching.

C.2. Epoching and Averaging

1. Detect events: via the Process1 box: ”Events > Detect events above threshold”, using a minimum duration between two events of 20 ms and a maximum threshold of 0.1 standard deviations. Done for the Stim(D) UPPT001 signal.
2. Convert events to simple: Events > Convert to simple events > Keep the start of the events.
3. Remove hardware delay: via the Process1 box: ”Events > Add time offset”. Use 2.5 milliseconds for the Montreal recordings and 1.7 milliseconds for Nijmegen recordings.

4. Epoching: Right-click on raw file > Import in database. Select the events to be used and select ”Remove DC offset” using the preferred time range. Epoching can also be done using a Matlab-script, which can be generated via Process1: Import > Import recordings > Import MEG/EEG: Events > Generate .m script.
5. Accept (selected) bad epochs as good: right-click on epoch > Accept trial.
6. Average: via the Process1 box: ”Average > Average files > By trial group (folder average)”

C.3. Head Models and Source Estimation

1. Calculate the noise covariance using an empty-room recording: Right-click on link to raw file > Noise covariance > Compute noise from recordings. Settings: Baseline entire file. Remove DC offset: block by block. MEG signals (not EEG!).
2. Surface head models: via the Process1 box, Sources > Compute head model. Cortex surface. MEG method: Overlapping sphers. All other sensors: None.
3. Surface source estimation: use the sensor averages in the Process1 box (Filter: Search names, Select files, ’avg’), Sources > Compute sources [2018]. Kernel only: one per file. MN: MEG, Minimum norm imaging, Current density map, Unconstrained, MEG.
4. For the volume models, first create a source grid. Create a ”Group analysis” entry and generate a template grid in the group analysis folder [139].
5. Volume head models: via the Process1 box, Sources > Compute head model. MRI volume. MRI volume grid: Use template grid for group analysis. MEG method: Overlapping spheres. All other sensors: None.
6. Volume source estimation: use the sensor averages in the Process1 box (Filter: Search names, Select files, ’avg’), Sources > Compute sources [2018]. Kernel only: one per file. Comment: MN: MEG Volume, Minimum norm imaging, Current density map, Unconstrained, MEG.
7. Make sure that the correct head model is selected (green in the graphical user interface) before performing source estimation! Following these steps in the correct order makes sure that the correct head model is used for source estimation.

Background information:
For MEG recordings, the channel files and sensor locations with respect to the subject’s head can differ between recordings. This prevents averaging at the sensor level across patients or recordings, as one sensor does not necessarily correspond to the same brain region [95, 96]. For further analysis of brain activity, a model is needed that explains how the neural electric currents, called the ”source space”, produce magnetic fields at external sensors, called the ”sensor space”, taking into account the different tissues between the brain and the MEG helmet [97]. The process that models how data values can be obtained outside of the head with MEG sensors, from electrical current dipoles in the brain, is called forward modeling or solving a forward problem. The outcome of this modeling step is called a ”head model” in Brainstorm, describing an approximation of the head geometry based on the subject’s anatomy and the locations of the MEG sensors. The subsequent process estimates the brain activity at potentially thousands of brain locations, which are determined by the forward head model, from much fewer sensor locations [95]. This process is an ill-posed inverse problem and is called ”source estimation” in Brainstorm. In theory, an infinite number of source activity patterns may explain equivalently well the data recorded at the sensors; this is inherent to the analysis.

Surface models: When the anatomy is imported, the subject’s cortex surface is downsampled to approximately 15,000 vertices. This number of vertices balances the adequate geometrical sampling of cortical folds with the volume of data to be analyzed [97]. By solving the forward problem for the cortical surface, the head geometry is simplified based on the subject’s anatomy and the locations of the MEG sensors, which relates the activity of the 15,000 brain sources to the sensor data collected during the experiment. This head model is used in the following step, known as ”source modeling”, or solving the inverse problem; the brain activity at the 15,000 vertices is estimated from much fewer sensor locations. For the forward problem, the recommended model for MEG is the ”Overlapping spheres” model, which simplifies the head geometry as multiple overlapping spheres, one for each MEG sensor. Each sphere is a local estimation of the shape of the inner skull immediately below the sensor. As magnetic fields are less sensitive to the heterogeneity of tissue in the brain, skull, and scalp, the overlapping spheres method is found to achieve reasonable accuracy relative to more complex methods [97].

For source estimation, the Minimum Norm (MN) imaging approach is chosen. MN imaging estimates the amplitude of brain sources distributed across the brain or constrained to the cortex, by fitting the sensor data with minimal overall amplitude of brain activity. This method is recommended by Brainstorm, as it is a simple and robust approach that is less sensitive to approximations of the head model compared to other methods [95]. MN imaging requires a noise covariance matrix to specify the noise statistics, which is provided through the empty-room recordings. The empty-room recordings were used to calculate a noise covariance matrix for every subject, for every visit. To compensate for the inhomogeneous sensitivity of MEG with depth and orientation of the current flow, it is recommended to use standardized maps. Standardization of MN imaging can be done either with respect to the noise covariance, which is done with the dSPM approach, or with respect to a time segment of no interest, which is done by using the current density map approach and standardizing this using a z-score transformation. For an analysis of evoked activity, it is more appropriate to employ normalization relative to a time segment without evoked activity rather than noise covariance [95]. For this normalization, the time segment was the same as the baseline window used to remove the DC offset with epoching, which was 200 ms to 5 ms before SER stimulation.

As described above, the inverse problem estimates brain activity at approximately 15,000 vertices determined by the surface head model. The current at each vertex is modeled by the orientation of an equivalent current dipole. For cortical surface source estimation, the orientation of these dipoles can be set to be normal to the cortex (”Constrained”) or can consist of three orthogonal dipoles along the Cartesian directions of the coordinate system for each vertex (”Unconstrained”). The constrained option is beneficial for computational efficiency, however, the unconstrained option is recommended when using the template anatomy instead of individual MRI scans, as this may account for some of the model uncertainties [95]. Therefore, unconstrained current density maps standardized using a z-score transformation with respect to a time segment of no interest were used.

Volume models: If subcortical structures are regions of interest, Brainstorm offers the possibility to use the whole brain volume as source space, in which the vertices are used to sample the entire brain volume instead of the cortical surface [97]. Because the thalamus is a region of interest in this thesis, volume head models and volume source estimation are employed as well. To enable the averaging of volume source models, a Group Analysis entry and a Volume Source Grid are created [139]. Next, the ”head model” is created using ”Overlapping spheres”, similar to the surface model [97]. The ”Source space” is set to ”MRI volume”, and ”Use template grid for group analysis” is used as ”Volume source grid”. Source estimation was done based on this volume head model, using ”Minimum norm imaging” as ”Method”, ”Current density map” as ”Measure”, and Unconstrained dipole orientations [140]. For volume source estimation, only the Unconstrained dipole orientation is available; for a random grid point, it is not possible to choose one particular orientation for the dipoles. Three orthogonal dipoles will be defined at each grid point. The volume source maps were standardized using z-score transformation with respect to the same time segment of no interest.

C.4. Regions of Interest

1. Grow ROIs based on activity: growing the S1 scouts was done based on the averaged source map of all included recordings, separately for the SERs elicited by tibial nerve stimulation and by median nerve stimulation. To grow a ROI based on activity, a ”seed”can be placed in the focus of activity and grown based on this activity using the ’Constrained’ setting [99].
2. Surface ROIs based on atlas: multiple atlases are available in the scout tab. An atlas can be copied using Atlas > New atlas > Copy current atlas. ROIs can be adjusted using the tool to grow scouts (click to add vertex, SHIFT-click to remove vertex).
3. Add volume atlases: in Anatomy view > Right-click on subject (the default anatomy, in the case of a group analysis) > add MNI parcellation > AAL2. Repeat for AAL3. Go back to Functional view, open the source map and go to the scouts tab > Atlas > From subject anatomy > AAL2. Repeat for AAL3. ROIs can be merged by selecting the ROIs and go to Scout > Merge.

C.5. Source Map Averaging

1. Flatten the source map: via the Process1 box, Sources > Unconstrained to flat map. Norm.
2. Project volume models on template anatomy: via the Process1 box, Sources > Project on default anatomy. MRI volume.

3. Average per comparison group: via the Process1 box, select only the source maps to average. Average > Average files. Everything. Arithmetic average + Standard error.

Before averaging, the unconstrained source maps for the surface models as well as the volume models were flattened using the norm of the three orientations, as was advised by Brainstorm for group analysis [96]. After this, averaging of the surface source maps could be done directly because warped brain anatomies were used, meaning that the vertex locations align between patients and do not need to be projected on the default anatomy before averaging. Before volume source map averaging, the source maps were projected on the template anatomy using ”Sources > Project on default anatomy > MRI volume” from the Process1 box [139]. For all averages, unweighted averages were used because all patients should have the same weight in the group average, independent of the amount of stimulation pulses.

Time Series

1. Extract scouts time series: via the Process1 box, Extract > Scout time series. Select the atlas and ROIs for which the time series are needed.

2. Load into Matlab and create graphs. The graphs with shading for the standard error were made using a modified version of the Matlab function **stdshade.m** [141].

D

Regions of Interest

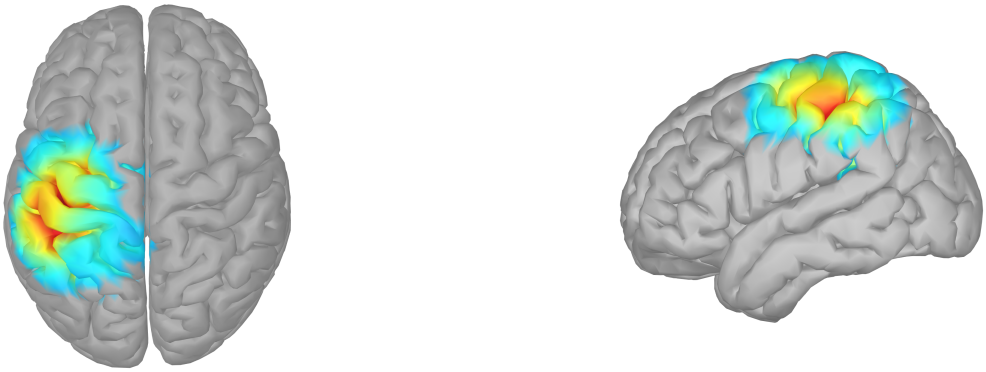

(a) View from above.

(b) View from left side.

Figure D.1: The average of the surface source models of all included recordings after approximately 20 to 40 milliseconds after median nerve stimulation. The activation focus is visible in the hand area of the primary somatosensory cortex (S1).

(a) View from above.

(b) View from midline.

Figure D.2: The average of the surface source models of all included recordings after approximately 40 to 60 milliseconds after tibial nerve stimulation. The activation focus is visible in the foot area of the primary somatosensory cortex (S1).

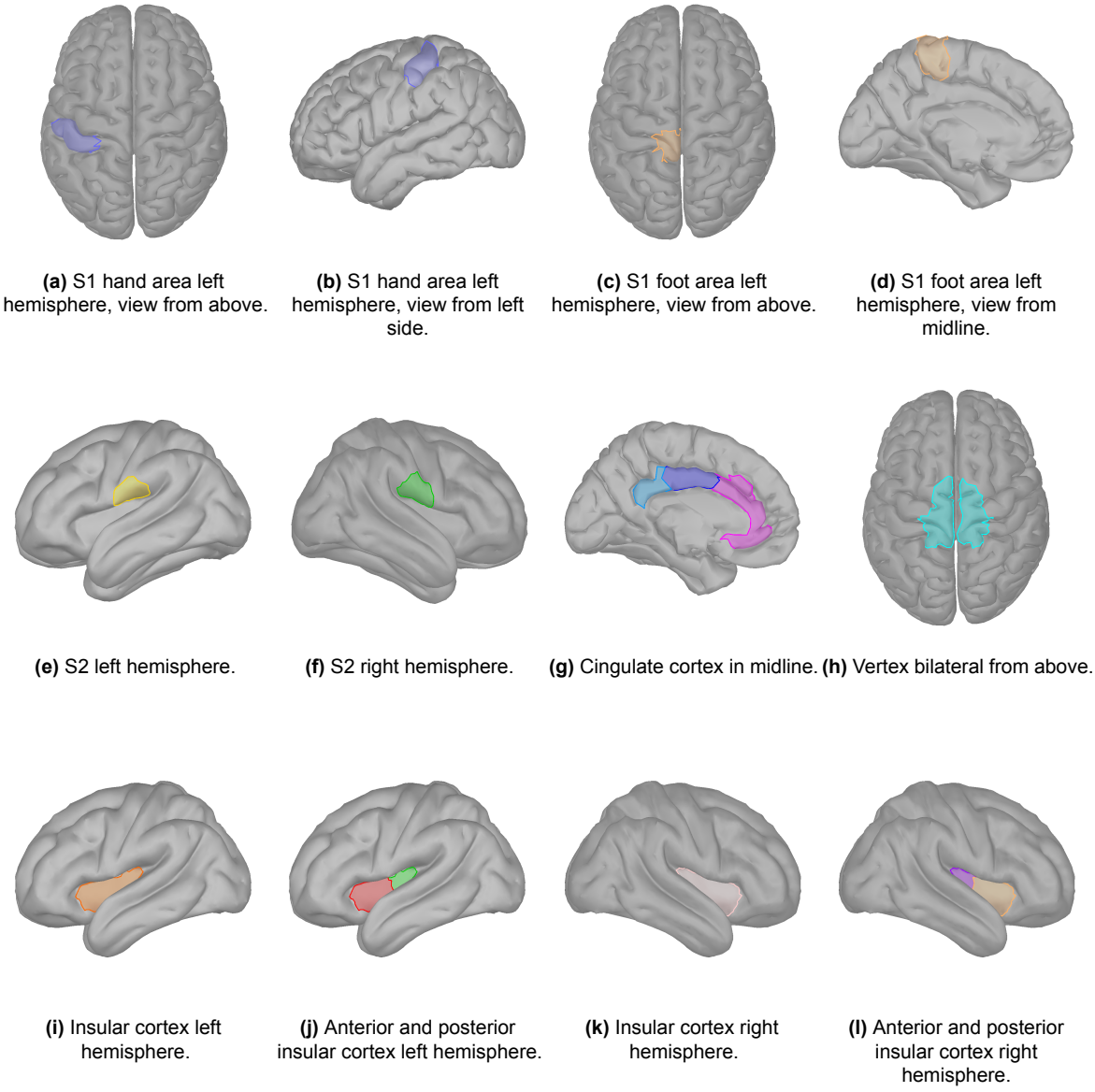

(a) S1 hand area left hemisphere, view from above.

(b) S1 hand area left hemisphere, view from left side.

(c) S1 foot area left hemisphere, view from above.

(d) S1 foot area left hemisphere, view from midline.

(e) S2 left hemisphere.

(f) S2 right hemisphere.

(g) Cingulate cortex in midline.

(h) Vertex bilateral from above.

(i) Insular cortex left hemisphere.

(j) Anterior and posterior insular cortex left hemisphere.

(k) Insular cortex right hemisphere.

(l) Anterior and posterior insular cortex right hemisphere.

Figure D.3: Overview of regions of interest defined on the cortical surface. S1, primary somatosensory cortex; S2, secondary somatosensory cortex.

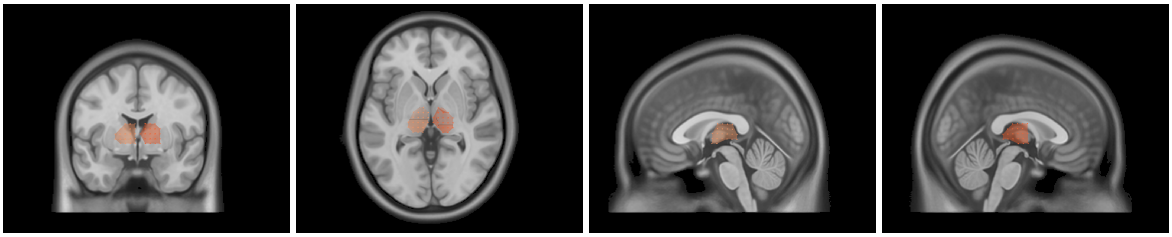

(a) Thalamus, view from back. **(b)** Thalamus, view from above. **(c)** Thalamus, view from left. **(d)** Thalamus, view from right.

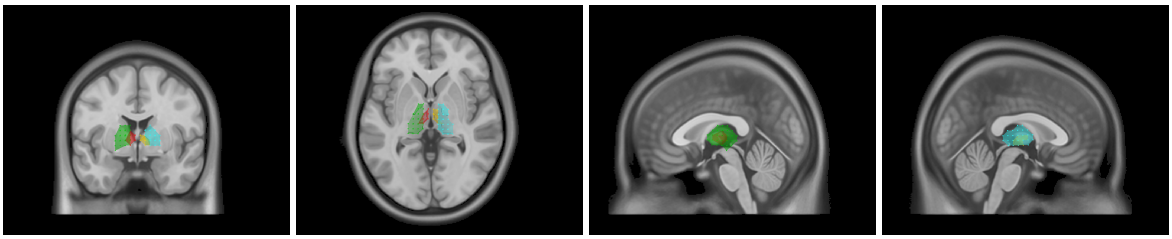

(e) Medial and lateral thalamus, view from back. **(f)** Medial and lateral thalamus, view from above. **(g)** Medial and lateral thalamus, view from left. **(h)** Medial and lateral thalamus, view from right.

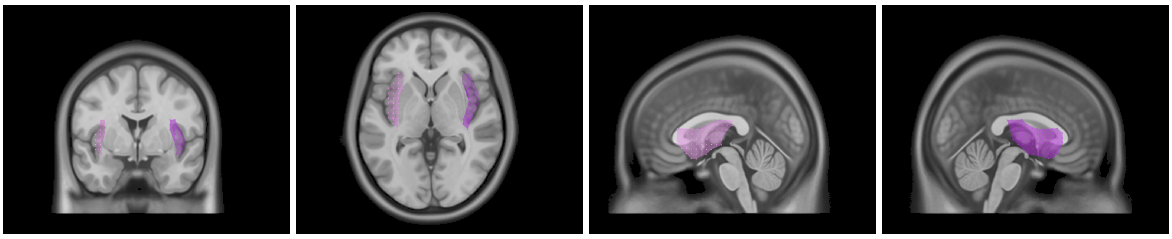

(i) Insula, view from back. **(j)** Insula, view from above. **(k)** Insula, view from left. **(l)** Insula, view from right.

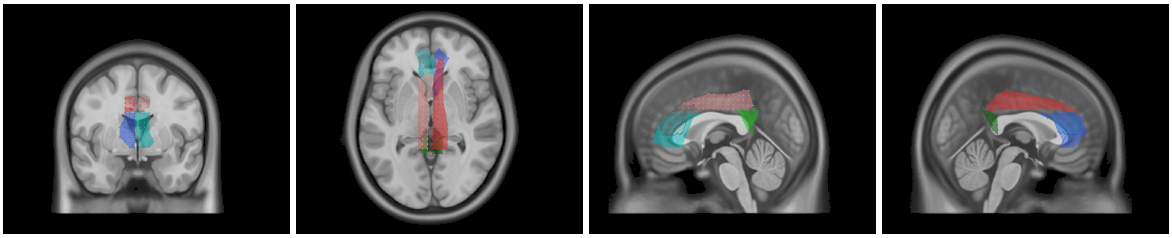

(m) Cingulate cortex, view from front. **(n)** Cingulate cortex, view from above. **(o)** Cingulate cortex, view from left. **(p)** Cingulate cortex, view from right.

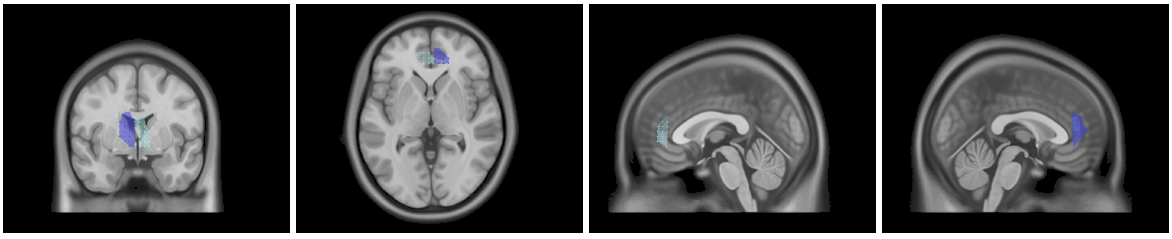

(q) pgACC, view from front. **(r)** pgACC, view from above. **(s)** pgACC, view from left. **(t)** pgACC, view from right.

Figure D.4: Overview of regions of interest defined in the brain volume. pgACC, pregenual anterior cingulate cortex.

E

Subdivision of Thalamic Nuclei

The areas marked green in both the table and figure belong to the medial thalamic subarea, the areas marked yellow belong to the lateral thalamic subarea. Based on the article 'Thalamus and pain' by Yen et al. [36], the majority of the structures defined in the AAL3 atlas could be grouped, as is shown in Table E.1. Of the remaining structures, Thal_AV is added to the medial group and Thal_LP, Thal_VA and Thal_VL are added to the lateral group for the following reasons:

- Thal_AV is added to the medial group due to its anatomical position lying in between the intralaminar nuclei, as shown in Figure E.1. Since the source estimation process is not accurate to the millimeter, activity of the intralaminar nuclei might also be seen in this part of the thalamus.
- Thal_LP is added to the lateral group, also due to its anatomical position (located in between the PO and VP nuclei) and in addition because the lateral thalamus is considered to be an important pain structure [38, 104].
- Thal_VA is added to the lateral subdivision due to its anatomical position and to make sure that all structures are used.
- Thal_VL is added to the lateral group as this structure is considered to be an important pain area together with Thal_VPL by Tu et al. [37], while Thal_VPL already belongs to the lateral subdivision based on the 'Thalamus and pain' article by Yen et al. [36].

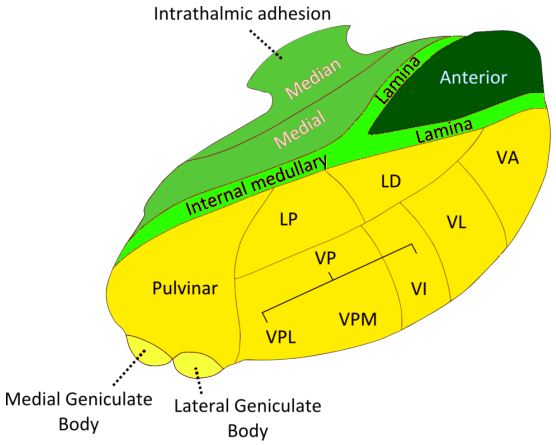

Figure E.1: Thalamus anatomy, marked with green and yellow representing the two subdivisions detailed in Table E.1.

Table E.1: Table with thalamus parts of the AAL3 atlas, regrouped into a medial and lateral subarea. All parts marked green belong to the medial thalamic subarea and all parts marked yellow belong to the lateral thalamic subarea.

AAL3 Subarea	AAL3 Abbrevation	Nucleus	Volume (mm3)	Reason
Anterior	Thal_AV	Anteroventral	154	*
Lateral	Thal_LP	Lateral posterior	198	†
Ventral	Thal_VA	Ventral anterior	610	‡
	Thal_VL	Ventral lateral	2096	§
	Thal_VPL	Ventral posterolateral	1276.5	Yen et al. [36]
Intralaminar	Thal_IL	Intralaminar	428.5	Yen et al. [36]
Medial	Thal_RE	Reuniens	8	Yen et al. [36]
	Thal_MDm	Mediodorsal medial magnocellular	907	Yen et al. [36]
	Thal_MDl	Mediodorsal lateral parvocellular	278.5	Yen et al. [36]
Posterior	Thal_LGN	Lateral geniculate	234	Yen et al. [36]
	Thal_MGN	Medial geniculate	174.5	Yen et al. [36]
	Thal_PuA	Pulvinar anterior	211	Yen et al. [36]
	Thal_PuM	Pulvinal medial	1311.5	Yen et al. [36]
	Thal_PuL	Pulvinal lateral	257	Yen et al. [36]
	Thal_PuI	Pulvinar inferior	205	Yen et al. [36]

* Added as this structure lies in between the laminar nuclei
† Added as this structure lies in between the PO and VP nuclei from Yen et al. and is commonly considered an important pain area
‡ Added as this structure would otherwise remain unused
§ Added as this structure is mentioned alongside the Thal_VPL nuclei by Tu et al. [37]

F

Patient Characteristics

F.1. Patient Characteristics

Table F.1: Patient characteristics of all patients that underwent the magnetoencephalography (MEG) measurements for this thesis.

Patient	Age	Sex	PD (yrs)	Pain condition	Pain location	NRS Tonic	NRS Burst	NRS Sham
PT01	53	m	32	FBSS	Back and left leg	0	0	1
PT02	74	f	50	FBSS	Back	6	7	6
PT03‡	42	f	20	FBSS	Right hip and buttock	4	2	5
PT04	59	m	6	FBSS	Back, left leg and foot	7	5	5
PT05‡	52	m	5	FBSS	Right hip, buttock, leg and foot	6	7	6
PT06	45	f	16	FBSS	Back	1	2	3
PT07	58	m	31	FBSS	Back and left leg	3	2	3
PT08‡	42	f	19	FBSS	Back, left hip, buttock, and leg	4	2	2
PT09	62	f	12	FBSS	Back, neck, right buttock and leg	6	9	4
PT10	70	m	15	DNP	Both feet	6	4	6
PT11	62	f	20	FBSS	Back, right buttock and leg	6	6	5
PTN01	60	m	-	FBSS	Right leg	8	8	9
PTN02	55	m	18	FBSS	Back and right leg	3	4	3
PTN03	52	m	4	FBSS	Right leg and foot	-	-	6
PTN04	43	f	23	FBSS	Back, left leg and foot	4	3	3
PTN05	64	m	9	FBSS	Back	6	2	6
PTN06	70	m	21	FBSS, DNP	Right leg, buttock and foot	1	1	1
PTN07	56	f	3	CRPS	Back and left foot	7	7	-*
PTN08	40	f	5	FBSS	Right leg and foot	2	5	6
PTN09	56	f	35	FBSS	Back and right leg	3	2	5
PTN10	49	f	13	FBSS	Left leg, buttock and foot	5	5	6
PTN11‡	63	m	15	DNP	Back and left leg	2	7	2
PTN12	38	m	7	NP	Left leg, knee, and foot	-	-	-
PTN13	53	m	15	FBSS	Back and left leg	4	-**	7
PTN14	68	m	29	FBSS	Right back and buttock	2	3	3
PTN15	60	m	40	FBSS	Left back, buttock and leg	7	6	2

PD, pain duration; yrs, years; NRS, numerical rating scale; FBSS, failed back surgery syndrome; DNP, diabetic neuropathy; CRPS, complex regional pain syndrome; NP, neuropathy.
* For this patient, the sham recording was missing
** For this patient, it was not possible to program burst stimulation
‡ This patient was also included before SCS treatment

F.2. Included Patients per Comparison

Table F.2: Overview of included patients per comparison

Patient	BS-SCS		TN-MN				TO-BU		Case	TO-BU-SH	
	TN	MN	BS	TO	BU	SH	TN	MN	TN	TN	MN
PT01	No	No	No	Yes	Yes	Yes	Yes	Yes	No	Yes	Yes
PT02	No	No	No	Yes	Yes	Yes	Yes	Yes	No	Yes	Yes
PT03	Yes	Yes	Yes	Yes	Yes	Yes	Yes	Yes	No	Yes	Yes
PT04	No	No	No	Yes	Yes	Yes	Yes	Yes	Yes	Yes	Yes
PT05	Yes	Yes	Yes	Yes	Yes	Yes	Yes	Yes	Yes	Yes	Yes
PT06	No	No	No	Yes	Yes	Yes	Yes	Yes	No	Yes	Yes
PT07	No	No	No	Yes	Yes	Yes	Yes	Yes	No	Yes	Yes
PT08	Yes	Yes	Yes	Yes	Yes	Yes	Yes	Yes	No	Yes	Yes
PT09	No	No	No	Yes	Yes	Yes	Yes	Yes	No	Yes	Yes
PT10	No	No	No	Yes	Yes	Yes	Yes	Yes	No	Yes	Yes
PT11	No	No	No	Yes	Yes	Yes	Yes	Yes	No	Yes	Yes
PTN01	No	No	No	No	No	No	Yes	Yes	No	Yes	No
PTN02	No	No	No	Yes	Yes	Yes	Yes	Yes	No	Yes	Yes
PTN03	No	No	No	Yes	Yes	Yes	Yes	Yes	No	Yes	Yes
PTN04	No	No	No	Yes	Yes	Yes	Yes	Yes	No	Yes	Yes
PTN05	No	No	No	Yes	Yes	Yes	Yes	Yes	Yes	Yes	Yes
PTN06	No	No	No	No	No	No	No	Yes	No	No	No
PTN07	No	No	No	No	No	No	Yes	Yes	No	No	No
PTN08	No	No	No	Yes	Yes	Yes	Yes	Yes	Yes	Yes	Yes
PTN09	No	No	No	Yes	Yes	Yes	Yes	Yes	No	Yes	Yes
PTN10	No	No	No	Yes	Yes	Yes	Yes	Yes	No	Yes	Yes
PTN11	Yes	Yes	Yes	Yes	Yes	Yes	Yes	Yes	No	Yes	Yes
PTN12	No	No	No	No	No	No	No	No	No	No	No
PTN13	No	No	No	No	No	No	No	No	No	No	No
PTN14	No	No	No	No	No	No	No	No	No	No	No
PTN15	No	No	No	No	No	No	No	No	No	No	No
Total	4	4	4	19	19	19	21	22	4	20	19

BS-SCS, Before SCS and During SCS; TN-MN, Tibial Nerve and Median Nerve; TO-BU, Tonic SCS and Burst SCS; Case, Case Studies; TO-BU-SH, Tonic, Burst, and Sham SCS.
SCS, spinal cord stimulation;
TN, tibial nerve; MN, median nerve;
BS, before SCS; TO, tonic SCS; BU, burst SCS; SH, sham SCS.

F.3. Overview of Excluded Recordings

Table F.3: Overview of excluded recordings.

Patient	Recording SCS	SER	Reason
PTN01	sham	median nerve	Bad channel in S1 hand area
PTN06	all	tibial nerve	Stimulation not perceptible
	sham	median nerve	Bad channel in S1 hand area
PTN07	other	all	Not tonic, burst, or sham SCS
PTN12	all	all	Completed only first session
PTN13	tonic	all	Missing TTL pulse
	other	all	Not tonic, burst, or sham SCS
	sham	all	Not usable in comparisons
PTN14	all	all	Dental works
PTN15	all	all	Dental works

SCS, spinal cord stimulation; SER, somatosensory evoked response; S1, primary somatosensory cortex; TTL, transistor-transistor logic.

F.4. Patient Characteristics per Comparison

Table F.4: Characteristics of all included patients.

Characteristics	
Number of patients	22
Age [yrs $\pm$ std]	56 $\pm$ 10
Sex [Male/Female]	11/11
Years lived with chronic pain [yrs $\pm$ std]	18 $\pm$ 12
Pain location	
Back	14/22
Left buttock/hip/leg/foot	9/22
Right buttock/hip/leg/foot	12/22
Pain condition	
FBSS	19/22
DNP	3/22
CRPS	1/22

yrs, years; std, standard deviation; FBSS, failed back surgery syndrome; DNP, diabetic neuropathy; CRPS, complex regional pain syndrome.

Table F.5: Characteristics of the patients who also participated in the study before spinal cord stimulation treatment.

Characteristics	
Number of patients	4
Age [yrs ± std]	50 ± 10
Sex [Male/Female]	2/2
Years lived with chronic pain [yrs ± std]	15 ± 7
Pain location	
Back	2/4
Left buttock/hip/leg/foot	2/4
Right buttock/hip/leg/foot	2/4
Pain condition	
FBSS	3/4
DNP	1/4
CRPS	0/4

yrs, years; std, standard deviation; FBSS, failed back surgery syndrome; DNP, diabetic neuropathy; CRPS, complex regional pain syndrome.

Table F.6: Characteristics of the patients treated with spinal cord stimulation who were included in the comparison between the somatosensory evoked responses elicited by tibial nerve and median nerve stimulation.

Characteristics	
Number of patients	19
Age [yrs ± std]	55 ± 10
Sex [Male/Female]	9/10
Years lived with chronic pain [yrs ± std]	18 ± 12
Pain location	
Back	13/19
Left buttock/hip/leg/foot	8/19
Right buttock/hip/leg/foot	9/19
Pain condition	
FBSS	17/19
DNP	2/19
CRPS	0/19

yrs, years; std, standard deviation; FBSS, failed back surgery syndrome; DNP, diabetic neuropathy; CRPS, complex regional pain syndrome.

Table F.7: Characteristics of the patients who were included in the comparison of the somatosensory evoked responses elicited by tibial nerve stimulation during tonic spinal cord stimulation and burst spinal cord stimulation.

Characteristics	
Number of patients	21
Age [yrs ± std]	55± 9
Sex [Male/Female]	10/11
Years lived with chronic pain [yrs ± std]	18 ± 12
Pain location	
Back	14/21
Left buttock/hip/leg/foot	9/21
Right buttock/hip/leg/foot	10/21
Pain condition	
FBSS	18/21
DNP	2/21
CRPS	1/21

yrs, years; std, standard deviation; FBSS, failed back surgery syndrome; DNP, diabetic neuropathy; CRPS, complex regional pain syndrome.

Table F.8: Characteristics of the patients who were included in the comparison of the somatosensory evoked responses elicited by median nerve stimulation during tonic spinal cord stimulation and burst spinal cord stimulation.

Characteristics	
Number of patients	22
Age [yrs ± std]	56 ± 10
Sex [Male/Female]	11/11
Years lived with chronic pain [yrs ± std]	18 ± 12
Pain location	
Back	14/22
Left buttock/hip/leg/foot	9/22
Right buttock/hip/leg/foot	11/22
Pain condition	
FBSS	19/22
DNP	3/22
CRPS	1/22

yrs, years; std, standard deviation; FBSS, failed back surgery syndrome; DNP, diabetic neuropathy; CRPS, complex regional pain syndrome.

Table F.9: Characteristics of the patients who were included in the comparison of the somatosensory evoked responses elicited by tibial nerve stimulation during tonic, burst, and sham spinal cord stimulation.

Characteristics	
Number of patients	20
Age [yrs ± std]	55± 10
Sex [Male/Female]	10/10
Years lived with chronic pain [yrs ± std]	18 ± 12
Pain location	
Back	13/20
Left buttock/hip/leg/foot	8/20
Right buttock/hip/leg/foot	10/20
Pain condition	
FBSS	18/20
DNP	2/20
CRPS	0/20

yrs, years; std, standard deviation; FBSS, failed back surgery syndrome; DNP, diabetic neuropathy; CRPS, complex regional pain syndrome.

Table F.10: Characteristics of the patients who were included in the comparison of the somatosensory evoked responses elicited by median nerve stimulation during tonic, burst, and sham spinal cord stimulation.

Characteristics	
Number of patients	19
Age [yrs ± std]	55 ± 10
Sex [Male/Female]	9/10
Years lived with chronic pain [yrs ± std]	18 ± 12
Pain location	
Back	13/19
Left buttock/hip/leg/foot	8/19
Right buttock/hip/leg/foot	9/19
Pain condition	
FBSS	17/19
DNP	2/19
CRPS	0/19

yrs, years; std, standard deviation; FBSS, failed back surgery syndrome; DNP, diabetic neuropathy; CRPS, complex regional pain syndrome.

G

All Results ROIs

G.1. Before SCS and During SCS

G.1.1. Tibial Nerve

Table G.1: Overview of the results comparing the somatosensory evoked responses elicited by tibial nerve stimulation in all regions of interest before spinal cord stimulation (SCS) and during tonic and burst SCS.

TN	Early (M45)	Middle (M120)	Late (M220)	Very late (M550)
S1	BS $\geq$ TO, BU			
S2 left		BU $\geq$ BS, TO		
S2 right		BS $\geq$ TO, BU		
ACC		ND	ND	ND
MCC		BS $\geq$ TO, BU	ND	BS $\geq$ BU
PCC		BS > BU > TO	ND	BS $\geq$ BU
IC left		BU > BS	ND	ND
IC right		BS, BU > TO	ND	ND
Thalamus left		ND	BU > BS	ND
Thalamus right		BS > TO, BU	BU > BS, TO	ND

S1, primary somatosensory cortex; S2, secondary somatosensory cortex; ACC, anterior cingulate cortex; MCC, middle cingulate cortex; PCC, posterior cingulate cortex; IC, insular cortex; BS, before spinal cord stimulation treatment; TO, tonic spinal cord stimulation; BU, burst spinal cord stimulation; ND, no difference.

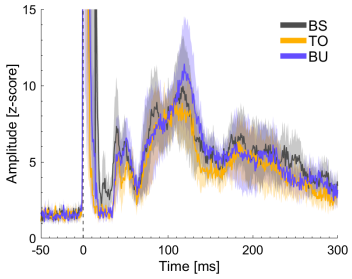

(a) S1 foot area.

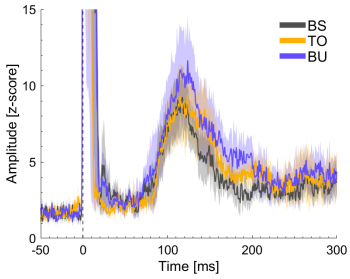

(b) S2 left.

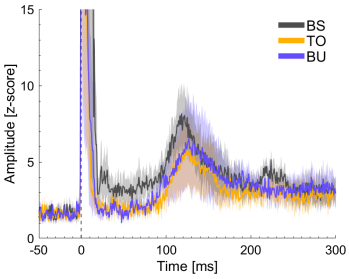

(c) S2 right.

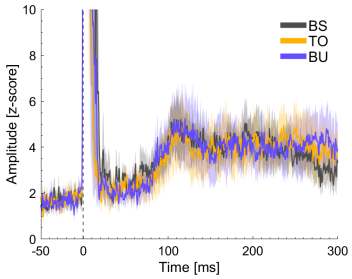

(d) ACC.

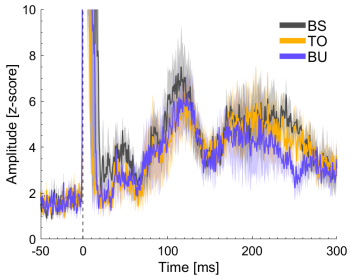

(e) MCC.

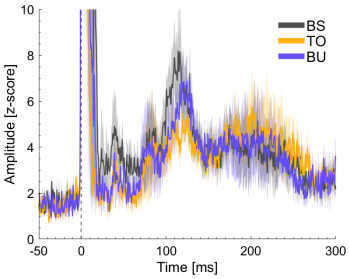

(f) PCC.

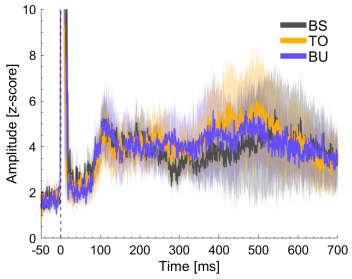

(g) ACC, 700ms.

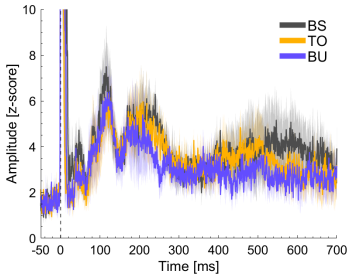

(h) MCC, 700ms.

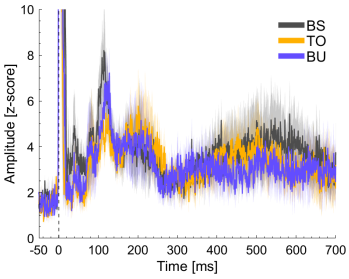

(i) PCC, 700ms.

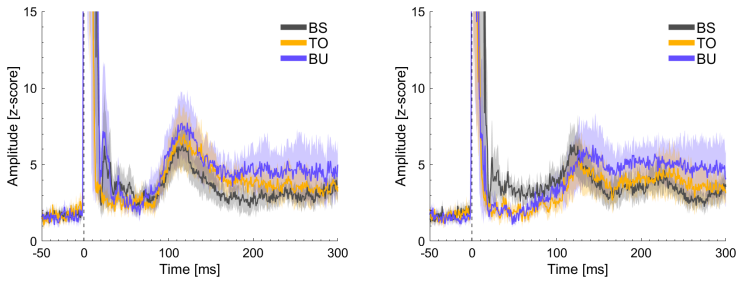

(j) IC left. **(k)** IC right.

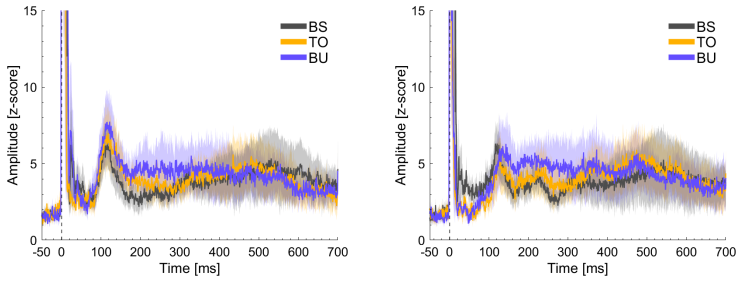

(l) IC left, 700ms. **(m)** IC right, 700ms.

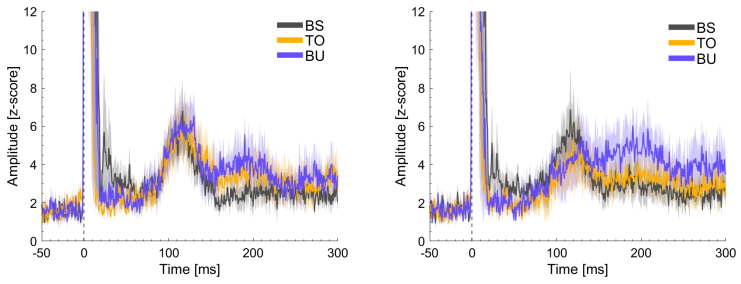

(n) Thalamus left. **(o)** Thalamus right.

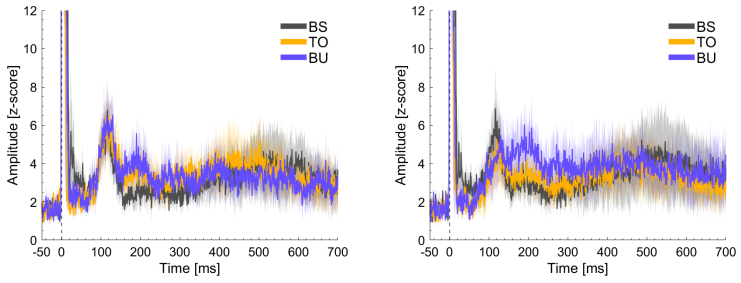

(p) Thalamus left, 700ms. **(q)** Thalamus right, 700ms.

Figure G.1: An overview of the somatosensory evoked responses elicited by tibial nerve stimulation in all regions of interest for the comparison between before spinal cord stimulation treatment and during tonic and burst spinal cord stimulation. Note the two different ranges of the horizontal axis: either -50 to 300 milliseconds or -50 to 700 milliseconds.
S1, primary somatosensory cortex; S2, secondary somatosensory cortex; ACC, anterior cingulate cortex; MCC, middle cingulate cortex; PCC, posterior cingulate cortex; IC, insular cortex; BS, before spinal cord stimulation treatment; TO, tonic spinal cord stimulation; BU, burst spinal cord stimulation.

G.1.2. Median Nerve

Table G.2: Overview of the results comparing the somatosensory evoked responses elicited by median nerve stimulation in all regions of interest before spinal cord stimulation (SCS) and during tonic and burst SCS.

MN	Early (M30)	Middle (M100)	Late (M200)	Very late (M500)
S1	BU > TO > BS			
S2 left		BU > BS, TO		
S2 right		ND		
ACC		BU > BS, TO	ND	BS > TO, BU
MCC		ND	BU $\geq$ BS, TO	BS $\geq$ TO, BU
PCC		ND	ND	BS $\geq$ TO, BU
IC left		BU $\geq$ BS, TO	ND	ND
IC right		ND	ND	ND
Thalamus left		ND	BU $\geq$ BS, TO	BS, BU > TO
Thalamus right		ND	ND	BS, BU > TO

S1, primary somatosensory cortex; S2, secondary somatosensory cortex; ACC, anterior cingulate cortex; MCC, middle cingulate cortex; PCC, posterior cingulate cortex; IC, insular cortex; BS, before spinal cord stimulation treatment; TO, tonic spinal cord stimulation; BU, burst spinal cord stimulation; ND, no difference.

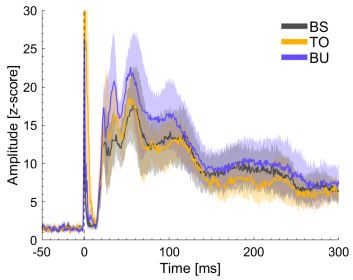

(a) S1 hand area.

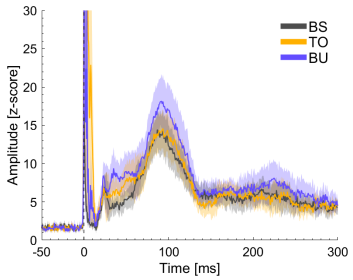

(b) S2 left.

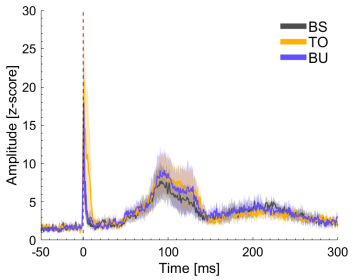

(c) S2 right.

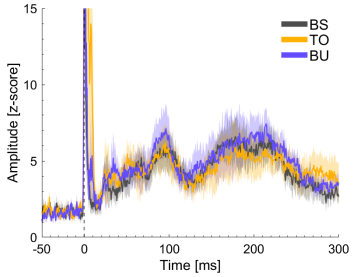

(d) ACC.

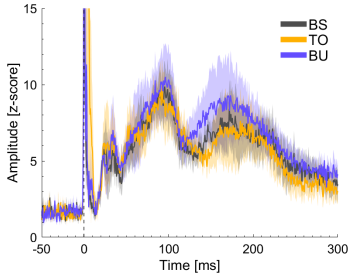

(e) MCC.

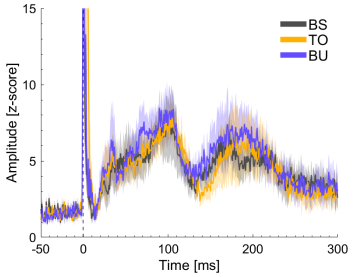

(f) PCC.

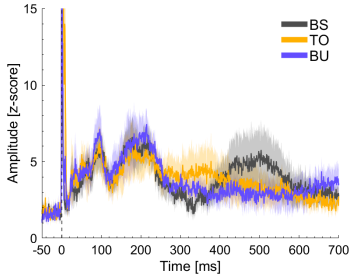

(g) ACC, 700ms.

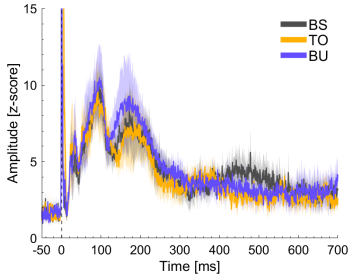

(h) MCC, 700ms.

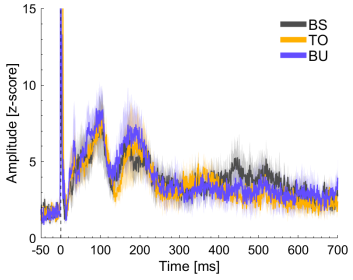

(i) PCC, 700ms.

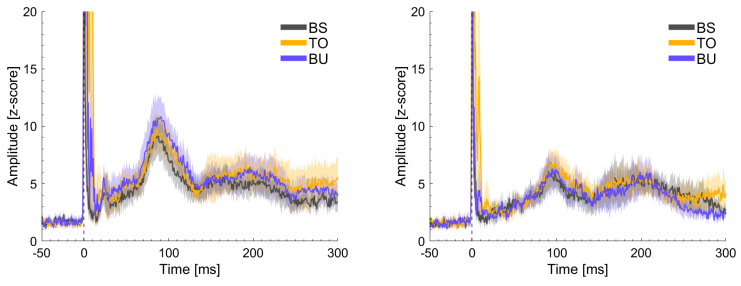

(j) IC left. **(k)** IC right.

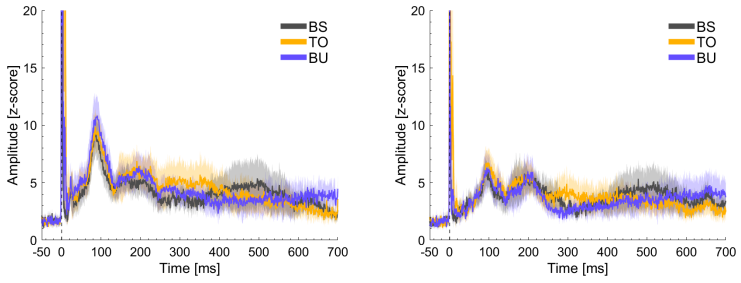

(l) IC left, 700ms. **(m)** IC right, 700ms.

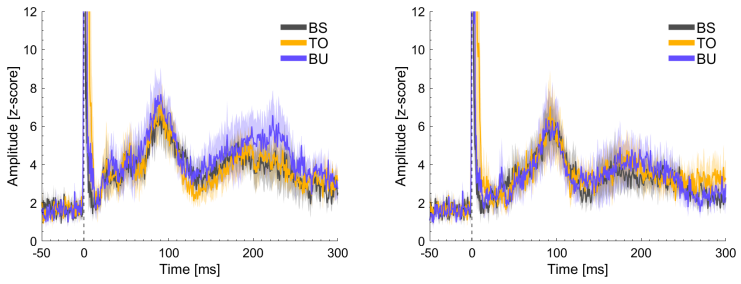

(n) Thalamus left. **(o)** Thalamus right.

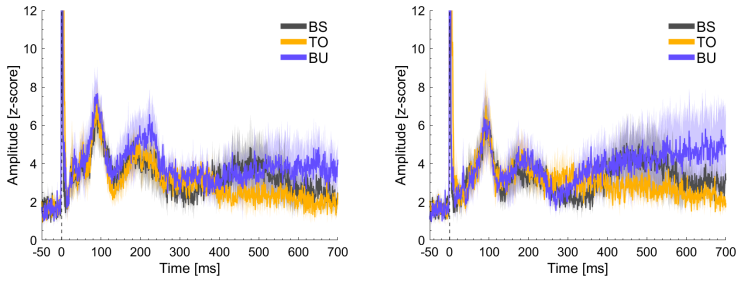

(p) Thalamus left, 700ms. **(q)** Thalamus right, 700ms.

Figure G.2: An overview of the somatosensory evoked responses elicited by median nerve stimulation in all regions of interest for the comparison between before spinal cord stimulation treatment and during tonic and burst spinal cord stimulation. Note the two different ranges of the horizontal axis: either -50 to 300 milliseconds or -50 to 700 milliseconds.
S1, primary somatosensory cortex; S2, secondary somatosensory cortex; ACC, anterior cingulate cortex; MCC, middle cingulate cortex; PCC, posterior cingulate cortex; IC, insular cortex; BS, before spinal cord stimulation treatment; TO, tonic spinal cord stimulation; BU, burst spinal cord stimulation.

G.2. Tibial Nerve and Median Nerve

G.2.1. Before SCS Treatment

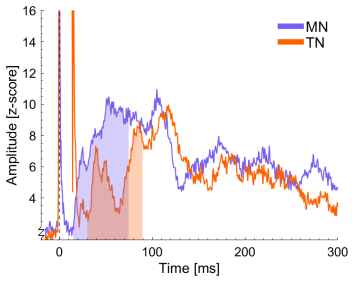

(a) S1 foot area (BS).

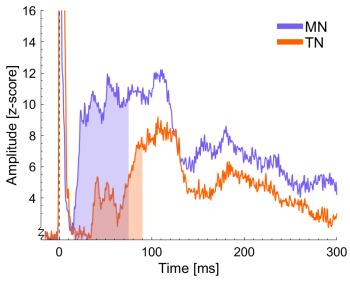

(b) S1 foot area (TO).

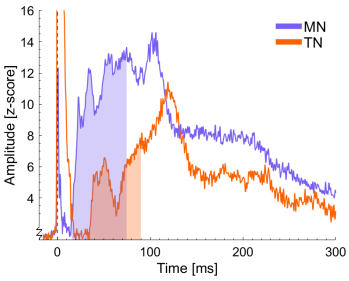

(c) S1 foot area (BU).

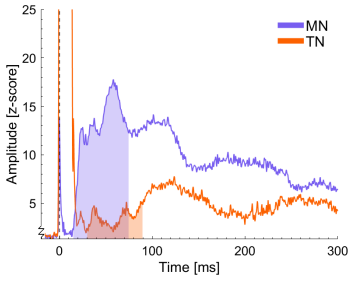

(d) S1 hand area (BS).

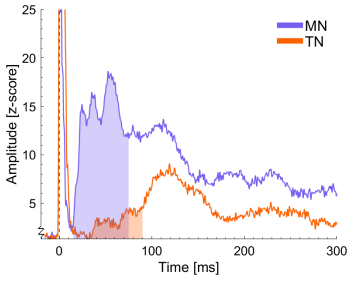

(e) S1 hand area (TO).

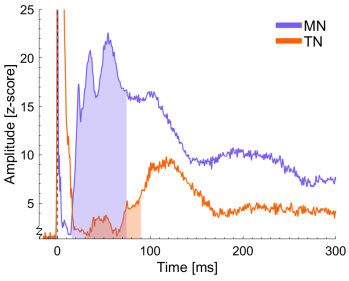

(f) S1 hand area (BU).

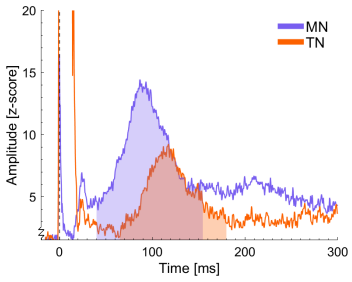

(g) S2 left (BS).

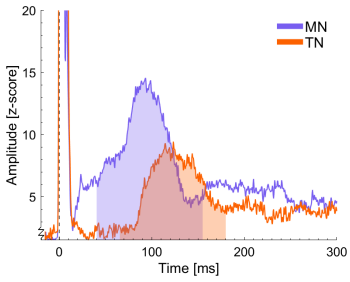

(h) S2 left (TO).

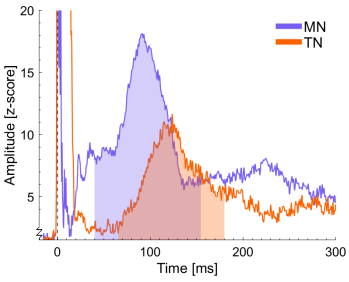

(i) S2 left (BU).

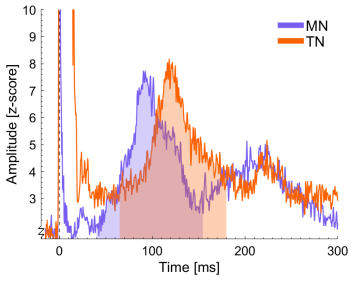

(j) S2 right (BS).

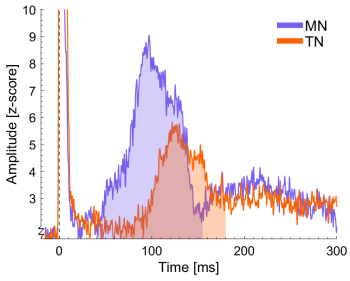

(k) S2 right (TO).

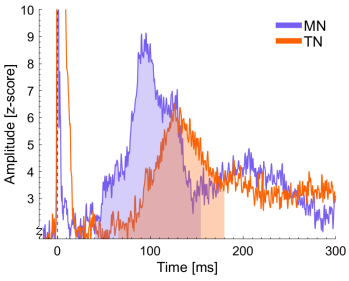

(l) S2 right (BU).

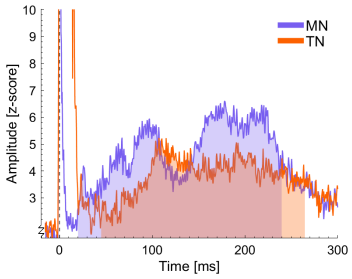

(m) ACC (BS).

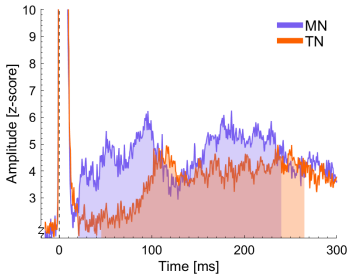

(n) ACC (TO).

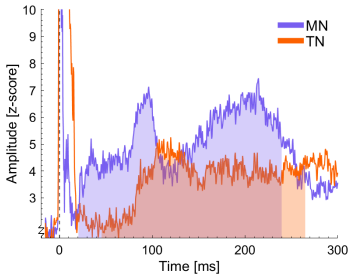

(o) ACC (BU).

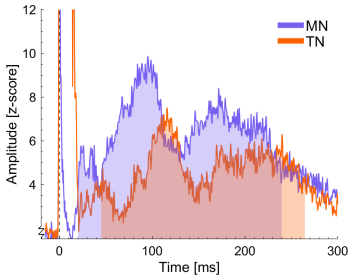

(p) MCC (BS).

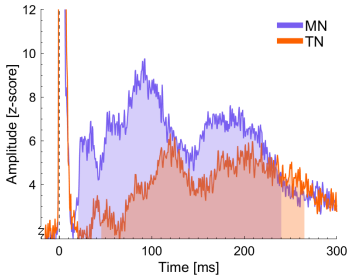

(q) MCC (TO).

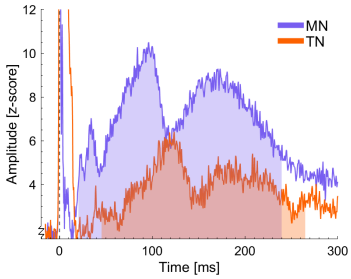

(r) MCC (BU).

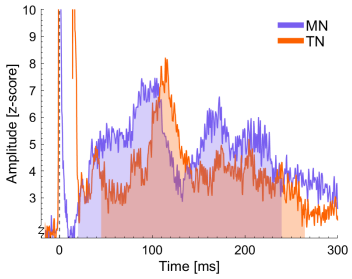

(s) PCC (BS).

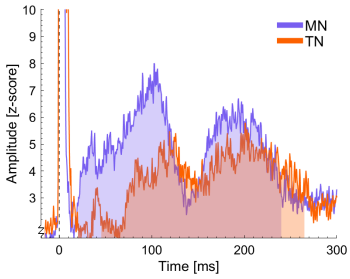

(t) PCC (TO).

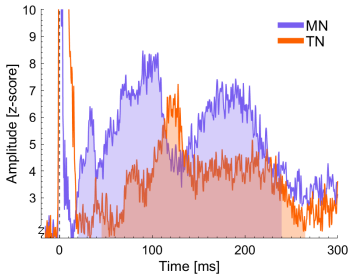

(u) PCC (BU).

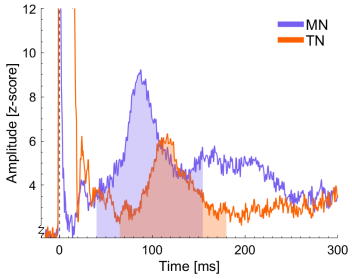

(v) IC left (BS).

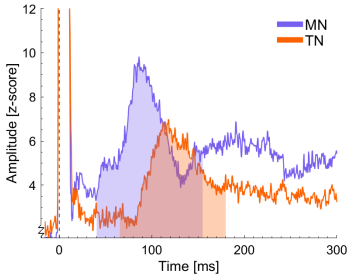

(w) IC left (TO).

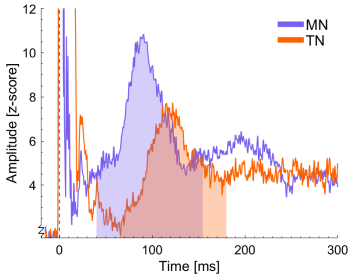

(x) IC left (BU(.

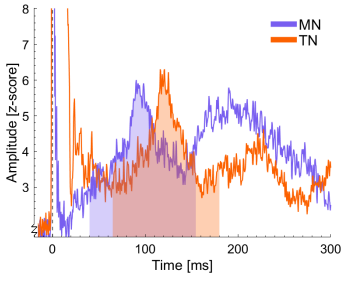

(y) IC right (BS).

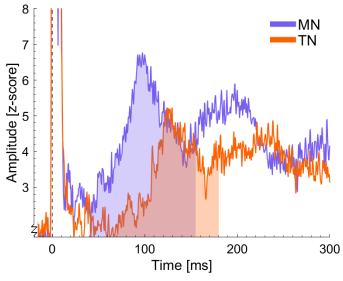

(z) IC right (TO).

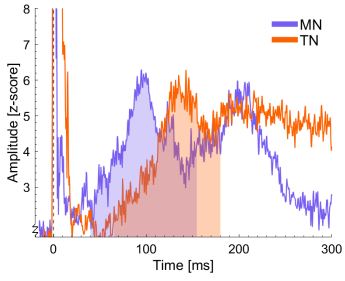

(aa) IC right (BU).

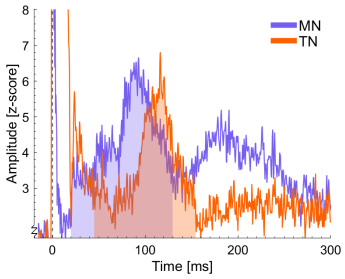

(ab) Thalamus left (BS).

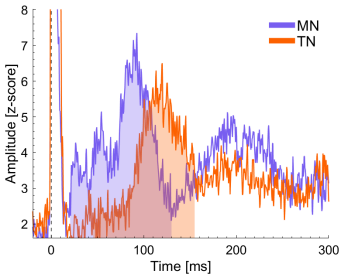

(ac) Thalamus left (TO).

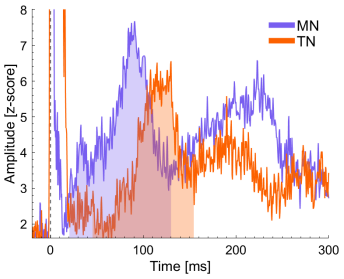

(ad) Thalamus left (BU).

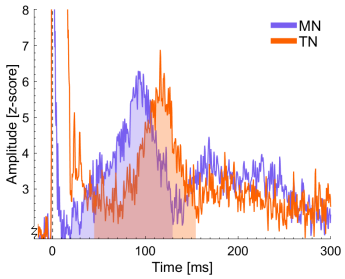

(ae) Thalamus right (BS).

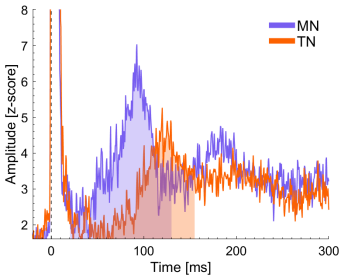

(af) Thalamus right (TO).

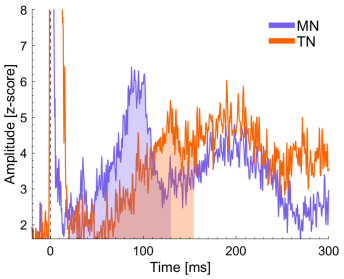

(ag) Thalamus right (BU).

Figure G.3: An overview of the graphs showing the areas under the curves (AUCs) for the somatosensory evoked responses elicited by tibial nerve and median nerve stimulation in all regions of interest, of the patients before spinal cord stimulation treatment (n=4) and of the same patients (n=4) during tonic and burst spinal cord stimulation. The shaded areas represent the AUCs that were used to determine the AUC ratio for each condition, for each region of interest.
S1, primary somatosensory cortex; S2, secondary somatosensory cortex; ACC, anterior cingulate cortex; MCC, middle cingulate cortex; PCC, posterior cingulate cortex; IC, insular cortex; BS, before spinal cord stimulation treatment; TO, tonic spinal cord stimulation; BU, burst spinal cord stimulation; MN, median nerve; TN, tibial nerve.

G.2.2. All Patients

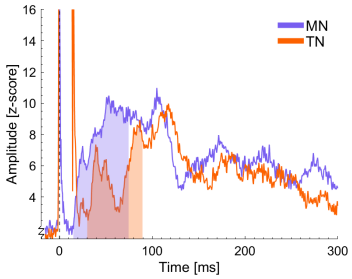

(a) BS S1 foot area.

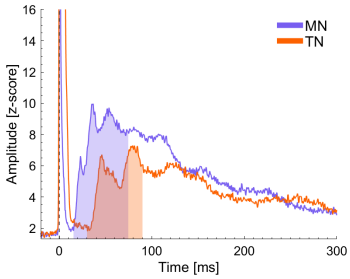

(b) S1 foot area (TO).

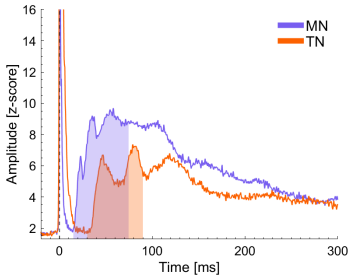

(c) S1 foot area (BU).

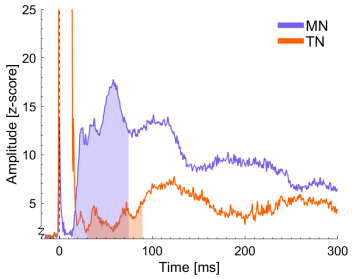

(d) S1 hand area (BS).

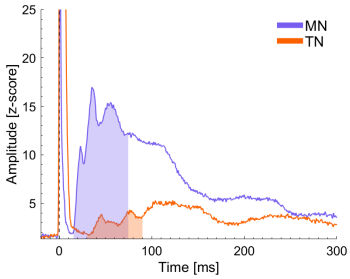

(e) S1 hand area (TO).

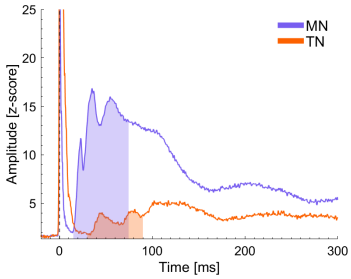

(f) S1 hand area (BU).

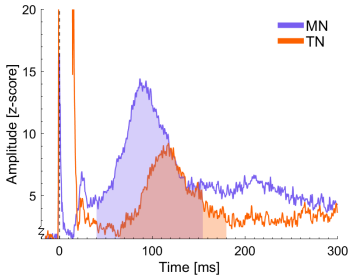

(g) S2 left (BS).

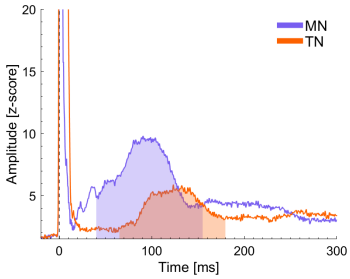

(h) S2 left (TO).

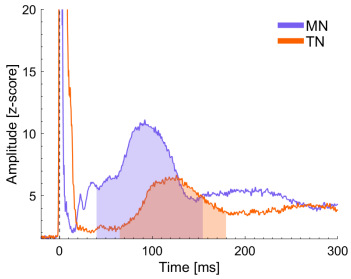

(i) S2 left (BU).

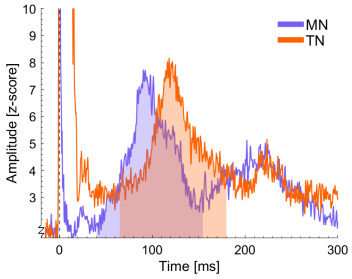

(j) S2 right (BS).

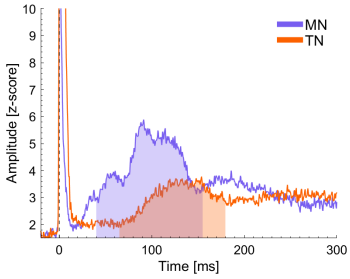

(k) S2 right (TO).

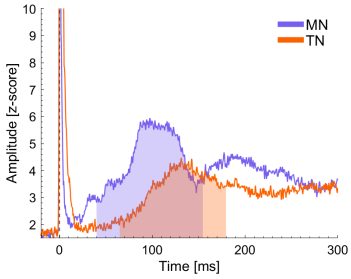

(l) S2 right (BU).

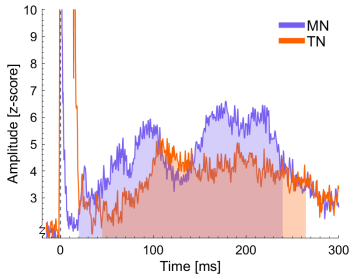

(m) ACC (BS).

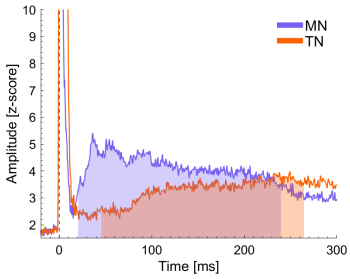

(n) ACC (TO).

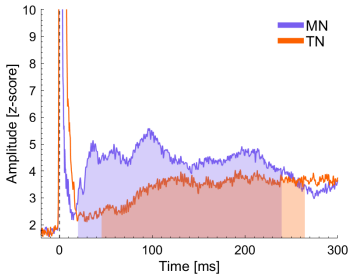

(o) ACC (BU).

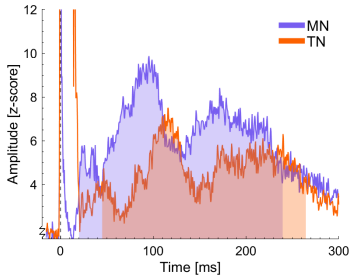

(p) MCC (BS).

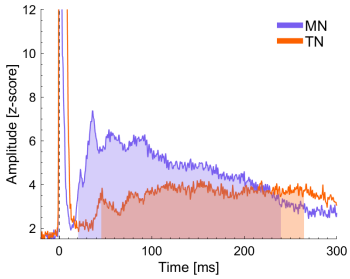

(q) MCC (TO).

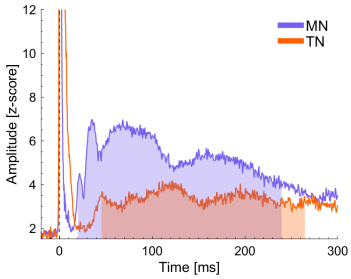

(r) MCC (BU).

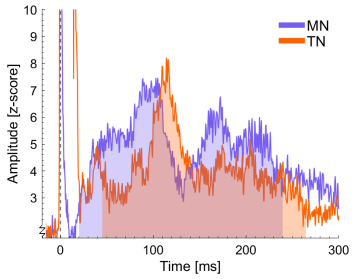

(s) PCC (BS).

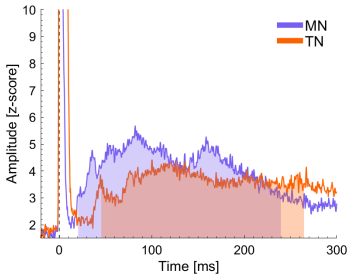

(t) PCC (TO).

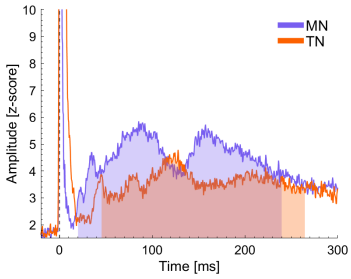

(u) PCC (BU).

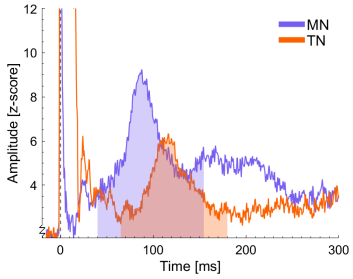

(v) IC left (BS).

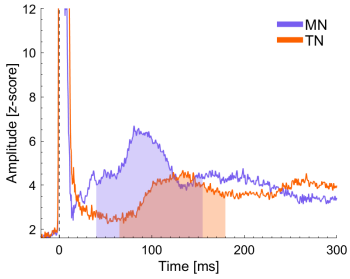

(w) IC left (TO).

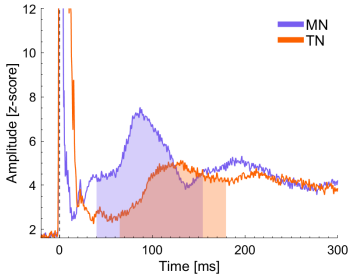

(x) IC left (BU).

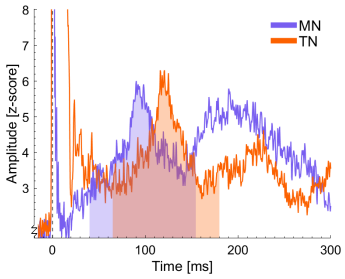

(y) IC right (BS).

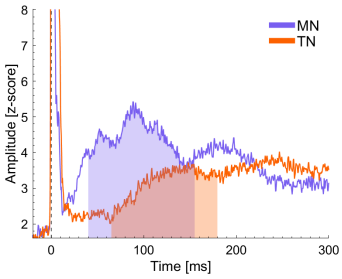

(z) IC right (TO).

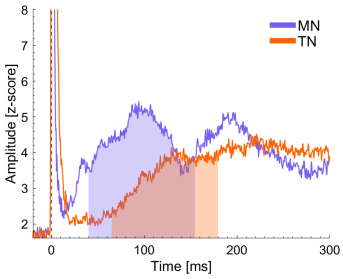

(aa) IC right (BU).

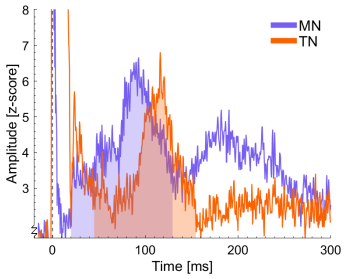

(ab) Thalamus left (BS).

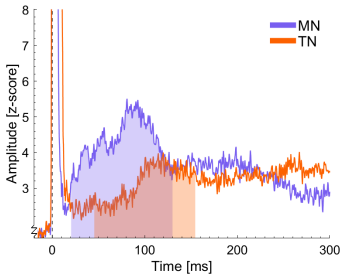

(ac) Thalamus left (TO).

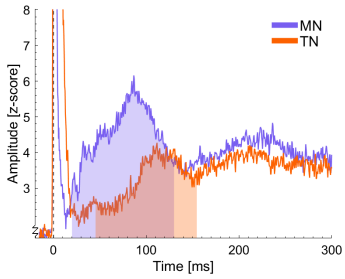

(ad) Thalamus left (BU).

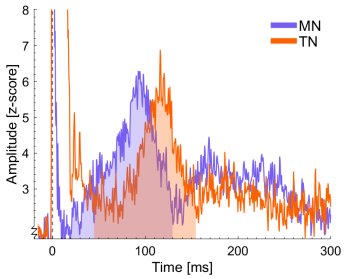

(ae) Thalamus right (BS).

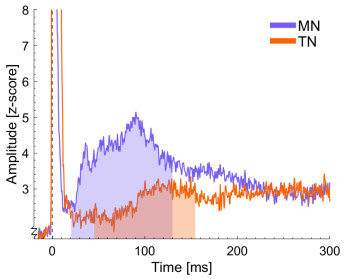

(af) Thalamus right (TO).

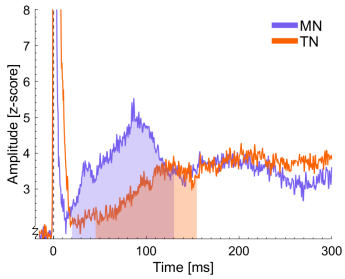

(ag) Thalamus right (BU).

Figure G.4: An overview of the graphs showing the areas under the curves (AUCs) for the somatosensory evoked responses elicited by tibial nerve and median nerve stimulation in all regions of interest, of the patients before spinal cord stimulation treatment (n=4) and of all included patients that were treated with spinal cord stimulation (n=19) during tonic and burst spinal cord stimulation. The shaded areas represent the AUCs that were used to determine the AUC ratio for each condition, for each region of interest.
S1, primary somatosensory cortex; S2, secondary somatosensory cortex; ACC, anterior cingulate cortex; MCC, middle cingulate cortex; PCC, posterior cingulate cortex; IC, insular cortex; BS, before spinal cord stimulation treatment; TO, tonic spinal cord stimulation; BU, burst spinal cord stimulation; MN, median nerve; TN, tibial nerve.

G.3. Tonic SCS and Burst SCS

G.3.1. Tibial Nerve

Table G.3: Overview of the results comparing the somatosensory evoked responses elicited by tibial nerve stimulation in all regions of interest during tonic and burst spinal cord stimulation.

TN	Early (M45)	Middle (M120)	Late (M220)	Very late (M550)
S1	ND			
S2 left		BU > TO		
S2 right		BU > TO		
ACC		ND	ND	BU > TO
MCC		ND	ND	ND
PCC		ND	ND	BU > TO
IC left		BU > TO	BU > TO	BU > TO
IC right		BU $\geq$ TO	BU > TO	BU > TO
Thalamus left		ND	BU > TO	BU > TO
Thalamus right		BU > TO	BU > TO	BU > TO

S1, primary somatosensory cortex; S2, secondary somatosensory cortex; ACC, anterior cingulate cortex; MCC, middle cingulate cortex; PCC, posterior cingulate cortex; IC, insular cortex; BS, before spinal cord stimulation treatment; TO, tonic spinal cord stimulation; BU, burst spinal cord stimulation; ND, no difference.

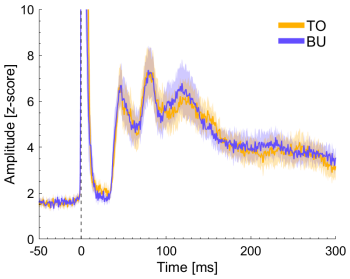

(a) S1 foot area.

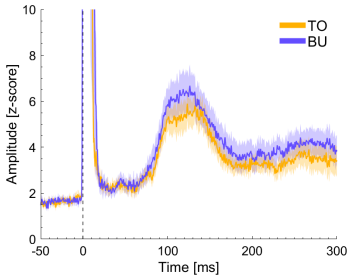

(b) S2 left.

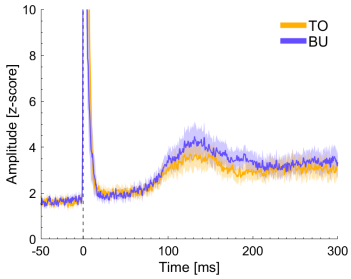

(c) S2 right.

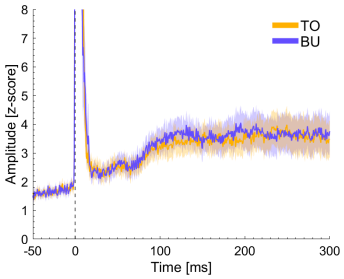

(d) ACC.

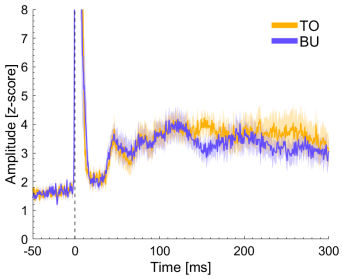

(e) MCC.

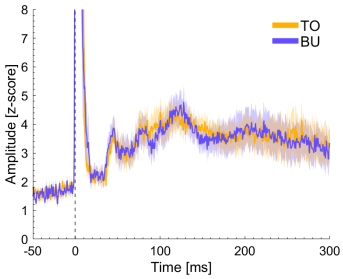

(f) PCC.

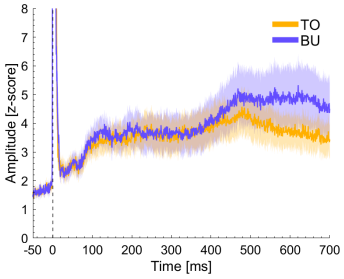

(g) ACC, 700ms.

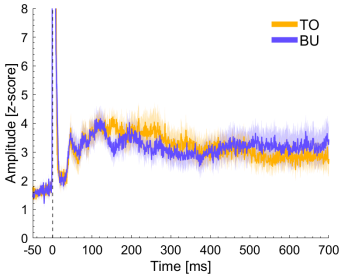

(h) MCC, 700ms.

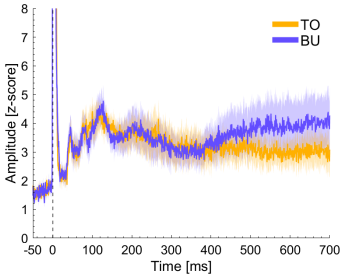

(i) PCC, 700ms.

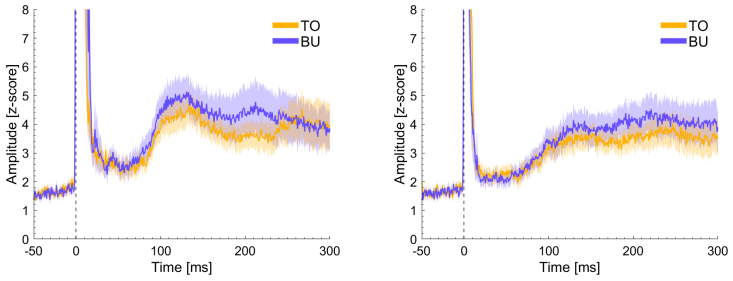

(j) IC left. **(k)** IC right.

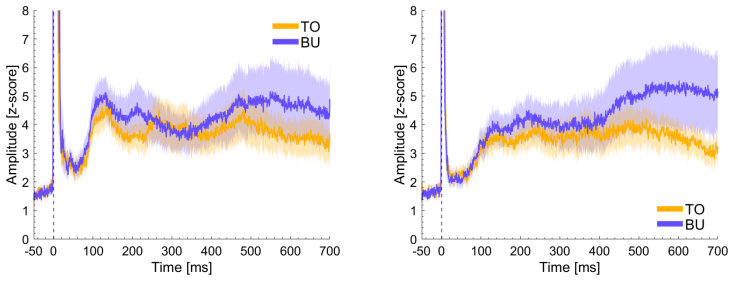

(l) IC left, 700ms. **(m)** IC right, 700ms.

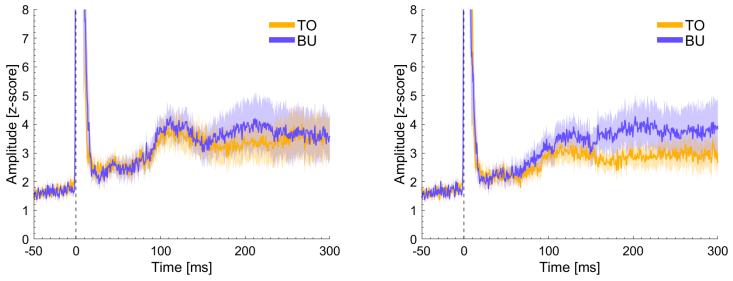

(n) Thalamus left. **(o)** Thalamus right.

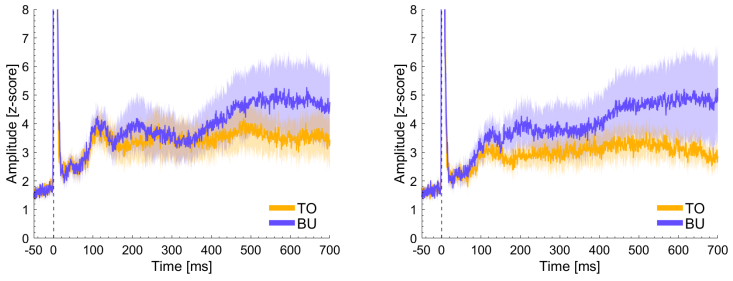

(p) Thalamus left, 700ms. **(q)** Thalamus right, 700ms.

Figure G.5: An overview of the somatosensory evoked responses elicited by tibial nerve stimulation in all regions of interest for the comparison between tonic and burst spinal cord stimulation. Note the two different ranges of the horizontal axis: either -50 to 300 milliseconds or -50 to 700 milliseconds.
S1, primary somatosensory cortex; S2, secondary somatosensory cortex; ACC, anterior cingulate cortex; MCC, middle cingulate cortex; PCC, posterior cingulate cortex; IC, insular cortex; TO, tonic spinal cord stimulation; BU, burst spinal cord stimulation.

G.3.2. Median Nerve

Table G.4: Overview of the results comparing the somatosensory evoked responses elicited by median nerve stimulation in all regions of interest during tonic and burst spinal cord stimulation.

MN	Early (M30)	Middle (M100)	Late (M200)	Very late (M500)
S1	ND			
S2 left		BU > TO		
S2 right		ND		
ACC		BU > TO	BU > TO	BU > TO
MCC		ND	BU $\geq$ TO	BU > TO
PCC		ND	ND	BU > TO
IC left		BU > TO	BU > TO	BU > TO
IC right		ND	BU > TO	BU > TO
Thalamus left		ND	BU > TO	BU > TO
Thalamus right		ND	BU > TO	BU > TO

S1, primary somatosensory cortex; S2, secondary somatosensory cortex; ACC, anterior cingulate cortex; MCC, middle cingulate cortex; PCC, posterior cingulate cortex; IC, insular cortex; BS, before spinal cord stimulation treatment; TO, tonic spinal cord stimulation; BU, burst spinal cord stimulation; ND, no difference.

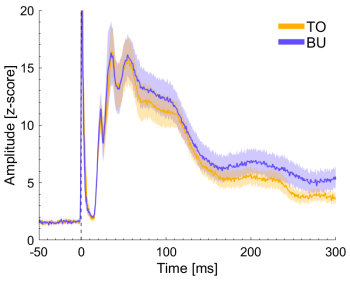

(a) S1 hand area.

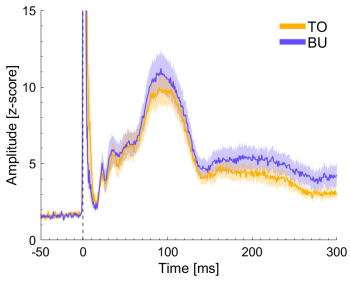

(b) S2 left.

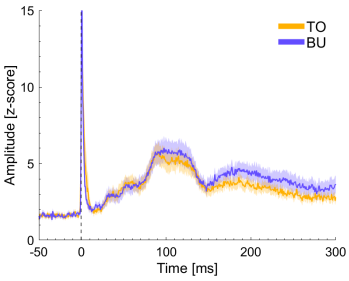

(c) S2 right.

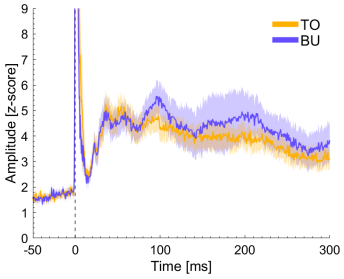

(d) ACC.

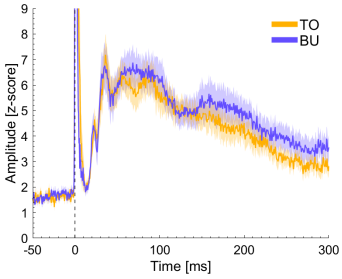

(e) MCC.

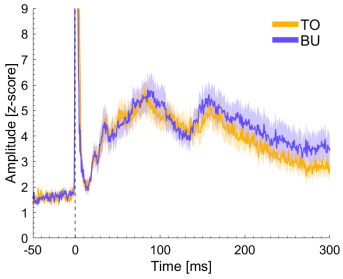

(f) PCC.

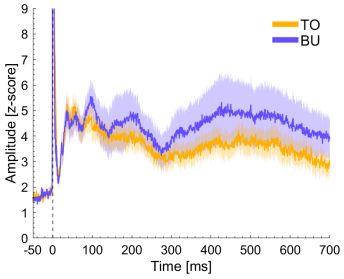

(g) ACC, 700ms.

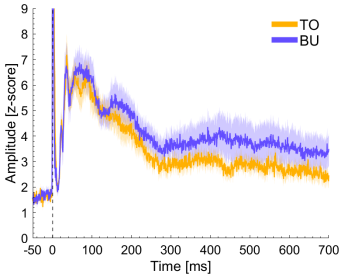

(h) MCC, 700ms.

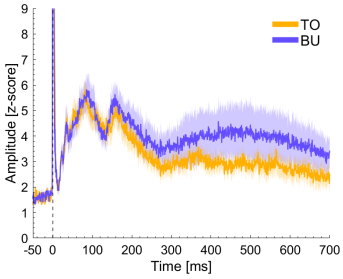

(i) PCC, 700ms.

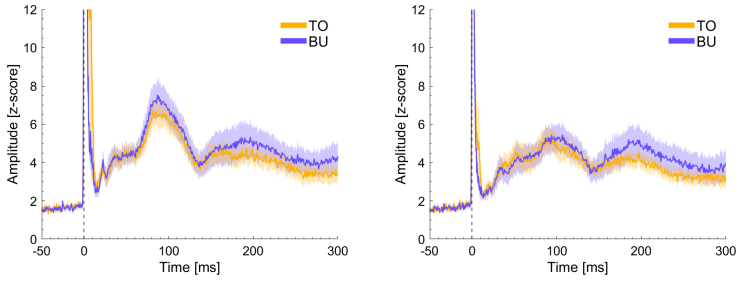

(j) IC left. **(k)** IC right.

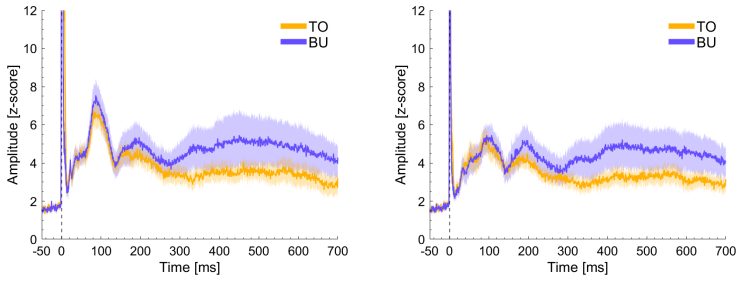

(l) IC left, 700ms. **(m)** IC right, 700ms.

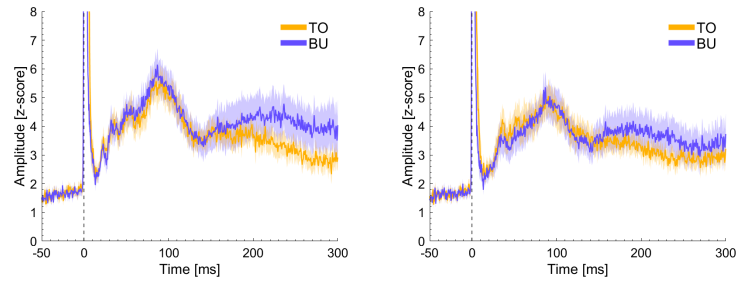

(n) Thalamus left. **(o)** Thalamus right.

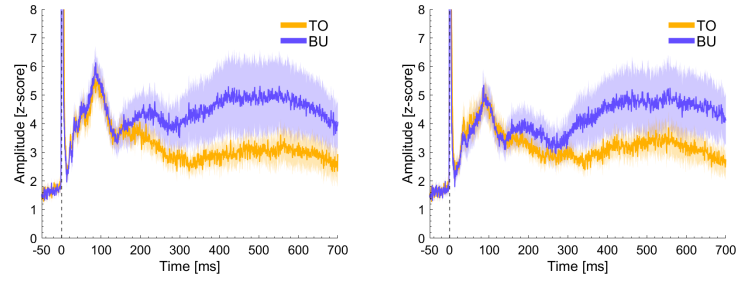

(p) Thalamus left, 700ms. **(q)** Thalamus right, 700ms.

Figure G.6: An overview of the somatosensory evoked responses elicited by median nerve stimulation in all regions of interest for the comparison between tonic and burst spinal cord stimulation. Note the two different ranges of the horizontal axis: either -50 to 300 milliseconds or -50 to 700 milliseconds.
S1, primary somatosensory cortex; S2, secondary somatosensory cortex; ACC, anterior cingulate cortex; MCC, middle cingulate cortex; PCC, posterior cingulate cortex; IC, insular cortex; TO, tonic spinal cord stimulation; BU, burst spinal cord stimulation.

G.4. The Effect of Pain Reduction

G.4.1. Case Study PT05 (Non-Responder): Tibial Nerve

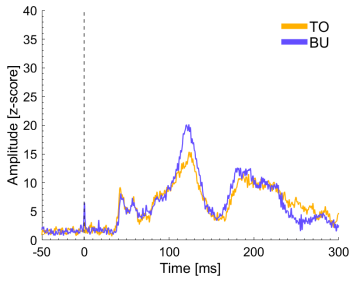

(a) S1 foot area.

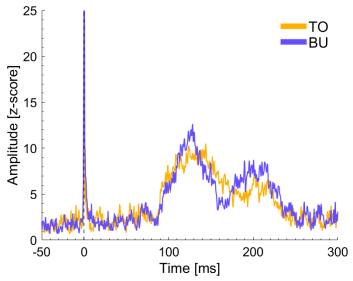

(b) S2 left.

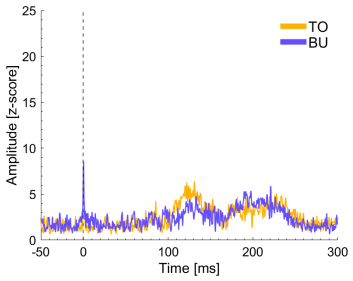

(c) S2 right.

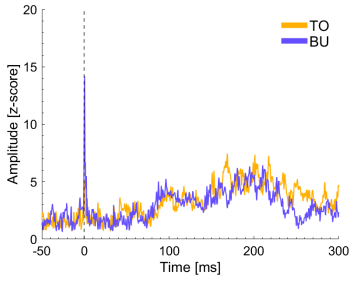

(d) ACC.

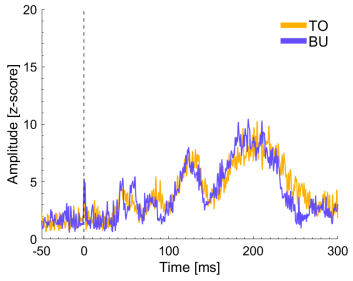

(e) MCC.

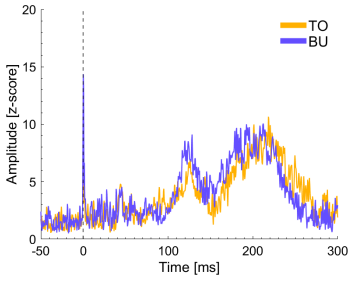

(f) PCC.

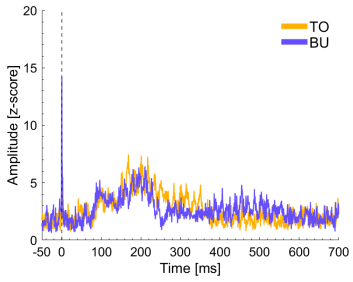

(g) ACC, 700ms.

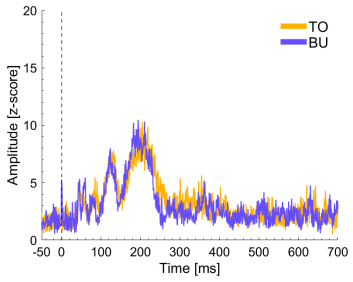

(h) MCC, 700ms.

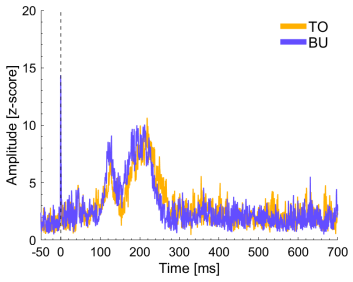

(i) PCC, 700ms.

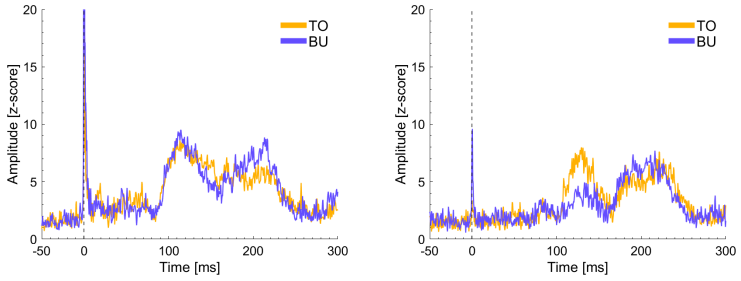

(j) IC left. **(k)** IC right.

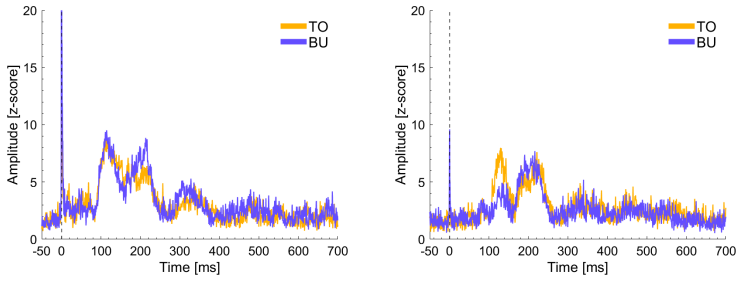

(l) IC left, 700ms. **(m)** IC right, 700ms.

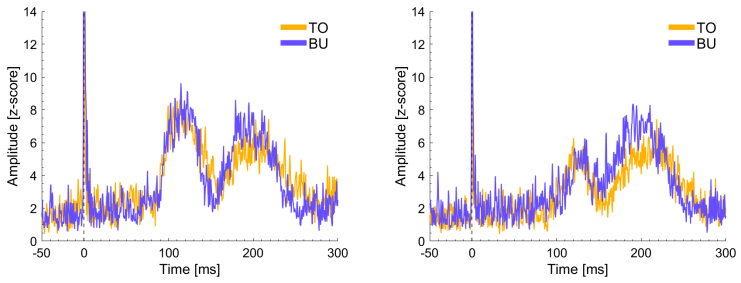

(n) Thalamus left. **(o)** Thalamus right.

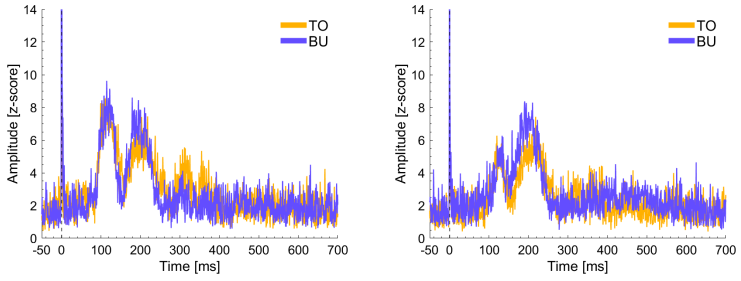

(p) Thalamus left, 700ms. **(q)** Thalamus right, 700ms.

Figure G.7: An overview of the somatosensory evoked responses elicited by tibial nerve stimulation in all regions of interest for the non-responder to both tonic and burst spinal cord stimulation (PT05). Note the two different ranges of the horizontal axis: either -50 to 300 milliseconds or -50 to 700 milliseconds.
S1, primary somatosensory cortex; S2, secondary somatosensory cortex; ACC, anterior cingulate cortex; MCC, middle cingulate cortex; PCC, posterior cingulate cortex; IC, insular cortex; TO, tonic spinal cord stimulation; BU, burst spinal cord stimulation.

G.4.2. Case Study PT05 (Non-Responder): Median Nerve

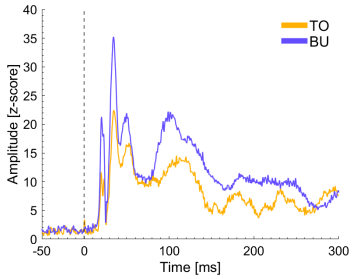

(a) S1 hand area.

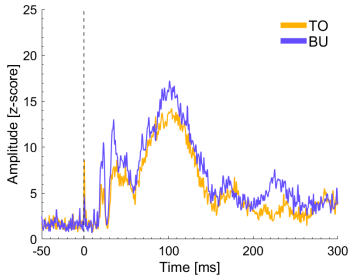

(b) S2 left.

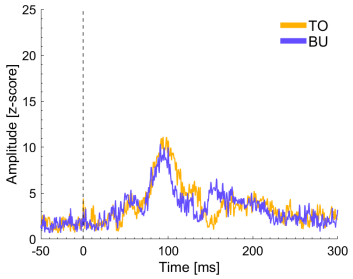

(c) S2 right.

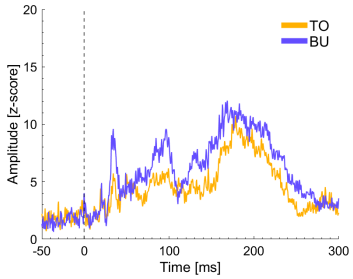

(d) ACC.

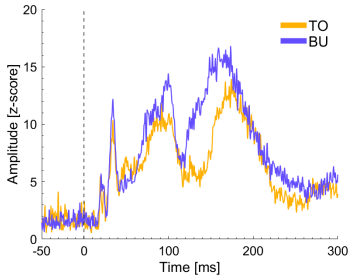

(e) MCC.

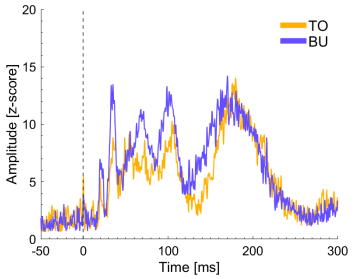

(f) PCC.

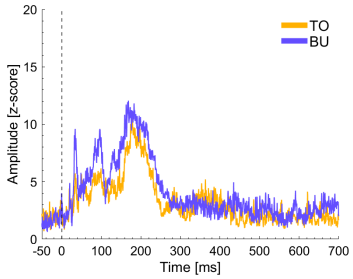

(g) ACC, 700ms.

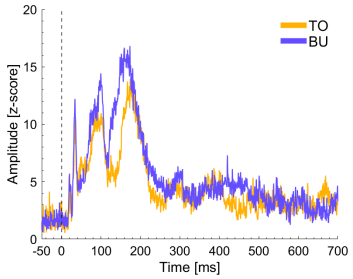

(h) MCC, 700ms.

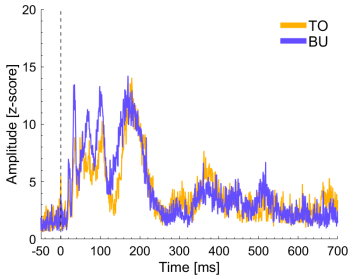

(i) PCC, 700ms.

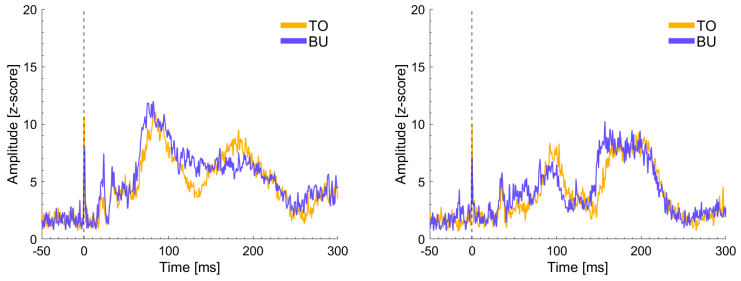

(j) IC left. **(k)** IC right.

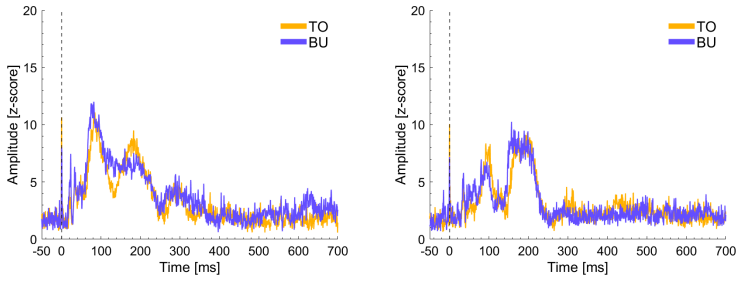

(l) IC left, 700ms. **(m)** IC right, 700ms.

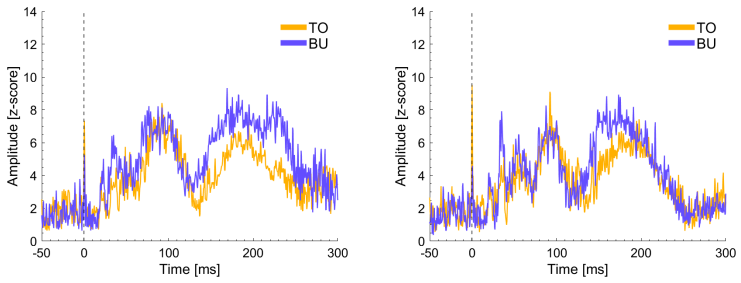

(n) Thalamus left. **(o)** Thalamus right.

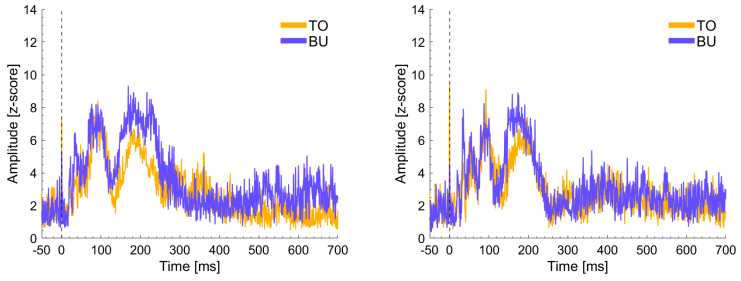

(p) Thalamus left, 700ms. **(q)** Thalamus right, 700ms.

Figure G.8: An overview of the somatosensory evoked responses elicited by median nerve stimulation in all regions of interest for the non-responder to both tonic and burst spinal cord stimulation (PT05). Note the two different ranges of the horizontal axis: either -50 to 300 milliseconds or -50 to 700 milliseconds.
S1, primary somatosensory cortex; S2, secondary somatosensory cortex; ACC, anterior cingulate cortex; MCC, middle cingulate cortex; PCC, posterior cingulate cortex; IC, insular cortex; TO, tonic spinal cord stimulation; BU, burst spinal cord stimulation.

G.4.3. Case Study PT06 (Responder): Tibial Nerve

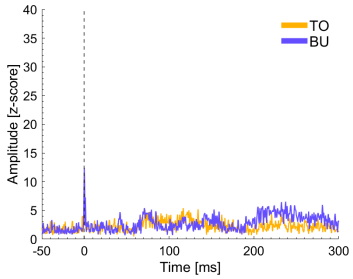

(a) S1 foot area.

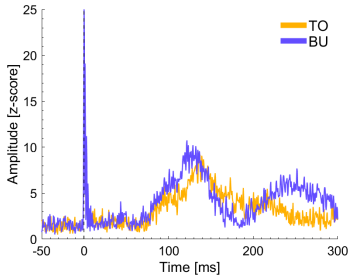

(b) S2 left.

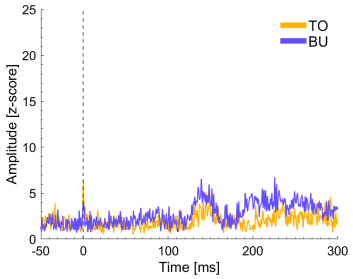

(c) S2 right.

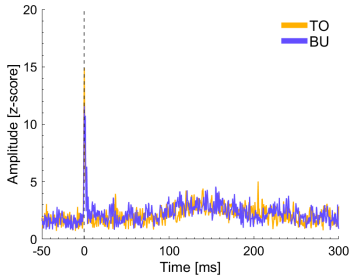

(d) ACC.

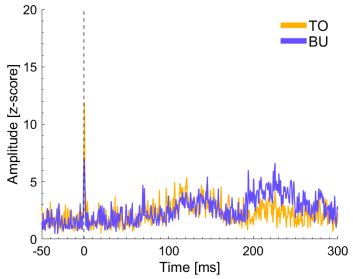

(e) MCC.

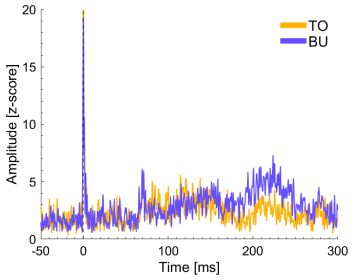

(f) PCC.

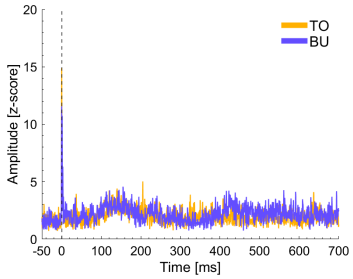

(g) ACC, 700ms.

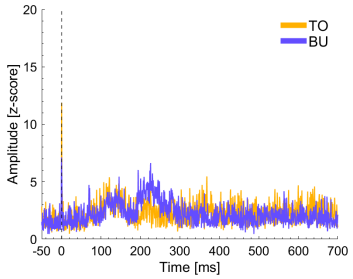

(h) MCC, 700ms.

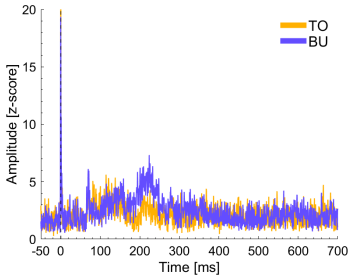

(i) PCC, 700ms.

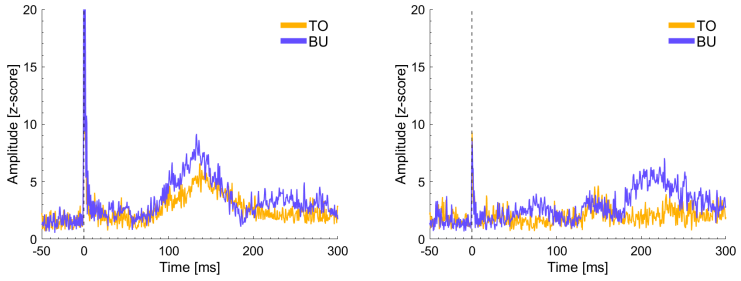

(j) IC left. **(k)** IC right.

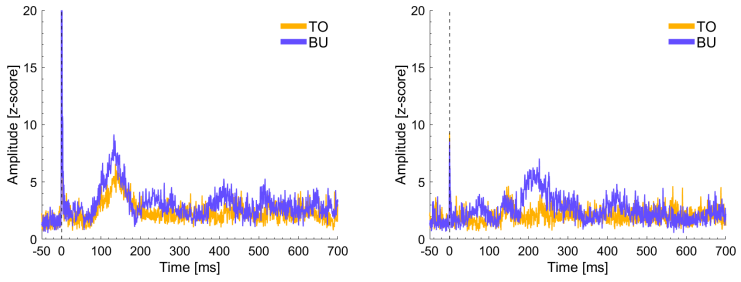

(l) IC left, 700ms. **(m)** IC right, 700ms.

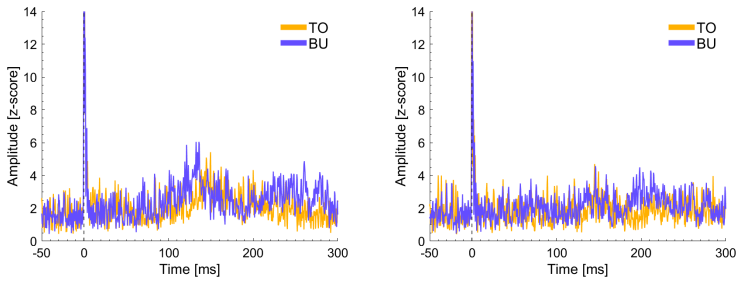

(n) Thalamus left. **(o)** Thalamus right.

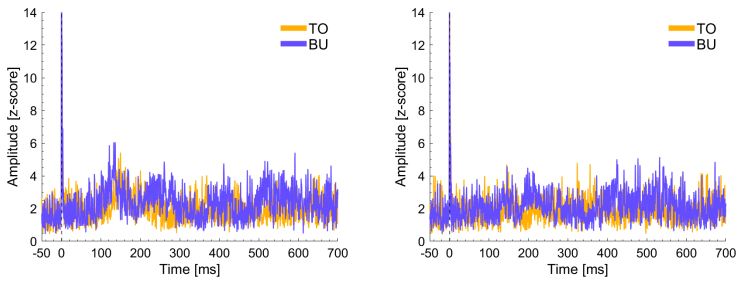

(p) Thalamus left, 700ms. **(q)** Thalamus right, 700ms.

Figure G.9: An overview of the somatosensory evoked responses elicited by tibial nerve stimulation in all regions of interest for the responder to both tonic and burst spinal cord stimulation (PT06). Note the two different ranges of the horizontal axis: either -50 to 300 milliseconds or -50 to 700 milliseconds.
S1, primary somatosensory cortex; S2, secondary somatosensory cortex; ACC, anterior cingulate cortex; MCC, middle cingulate cortex; PCC, posterior cingulate cortex; IC, insular cortex; TO, tonic spinal cord stimulation; BU, burst spinal cord stimulation.

G.4.4. Case Study PT06 (Responder): Median Nerve

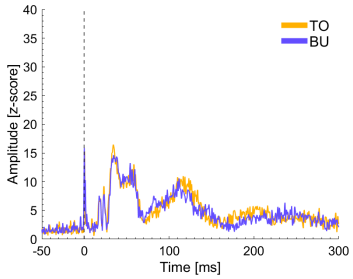

(a) S1 hand area.

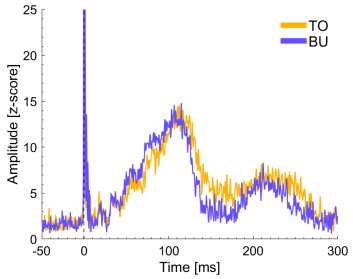

(b) S2 left.

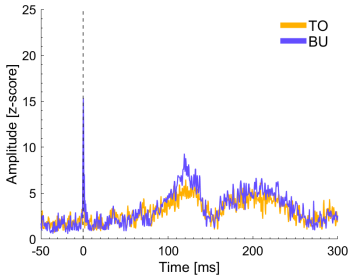

(c) S2 right.

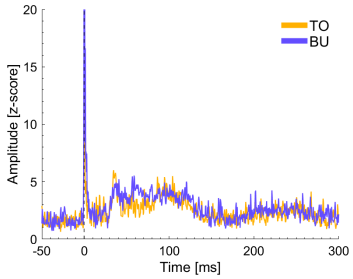

(d) ACC.

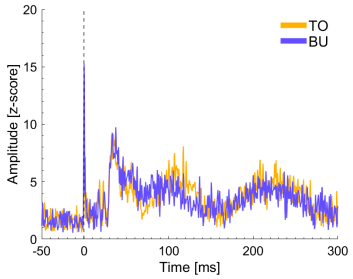

(e) MCC.

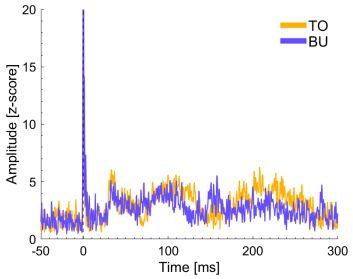

(f) PCC.

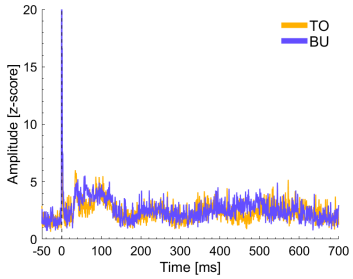

(g) ACC, 700ms.

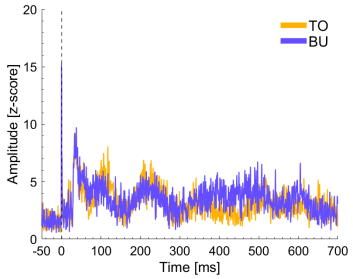

(h) MCC, 700ms.

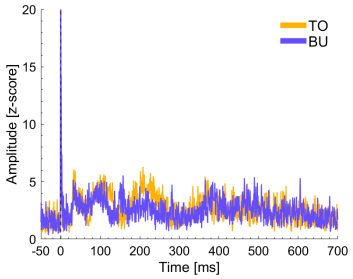

(i) PCC, 700ms.

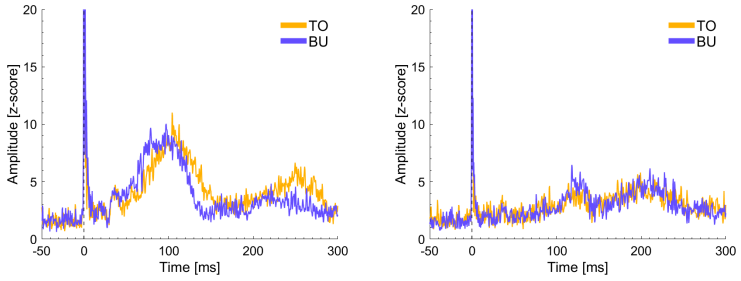

(j) IC left. **(k)** IC right.

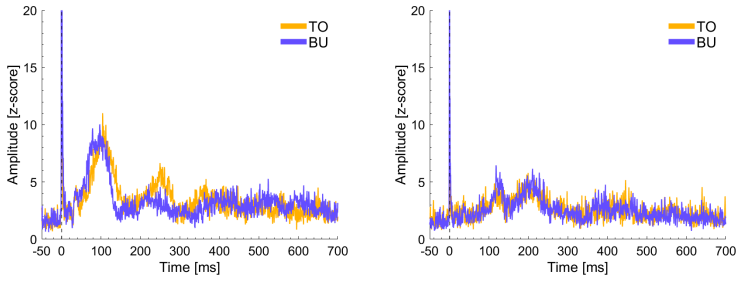

(l) IC left, 700ms. **(m)** IC right, 700ms.

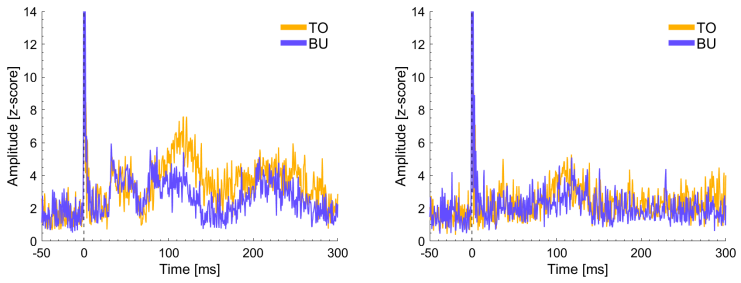

(n) Thalamus left. **(o)** Thalamus right.

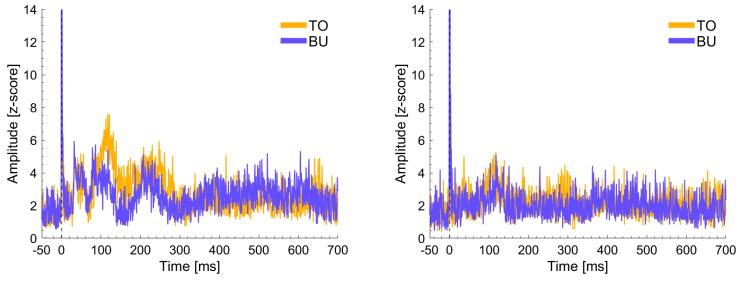

(p) Thalamus left, 700ms. **(q)** Thalamus right, 700ms.

Figure G.10: An overview of the somatosensory evoked responses elicited by median nerve stimulation in all regions of interest for the responder to both tonic and burst spinal cord stimulation (PT06). Note the two different ranges of the horizontal axis: either -50 to 300 milliseconds or -50 to 700 milliseconds.
S1, primary somatosensory cortex; S2, secondary somatosensory cortex; ACC, anterior cingulate cortex; MCC, middle cingulate cortex; PCC, posterior cingulate cortex; IC, insular cortex; TO, tonic spinal cord stimulation; BU, burst spinal cord stimulation.

G.4.5. Case Study PTN05 (Burst-Responder): Tibial Nerve

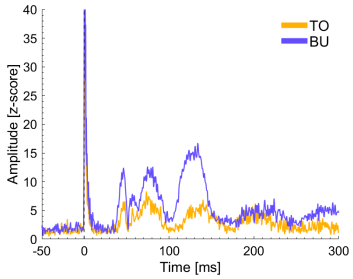

(a) S1 foot area.

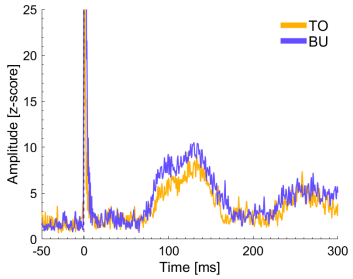

(b) S2 left.

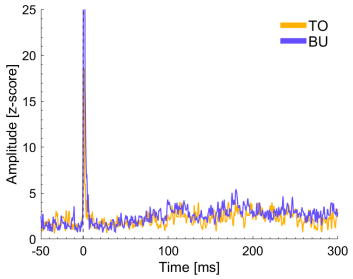

(c) S2 right.

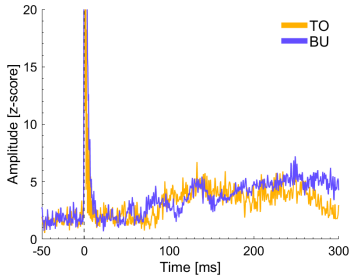

(d) ACC.

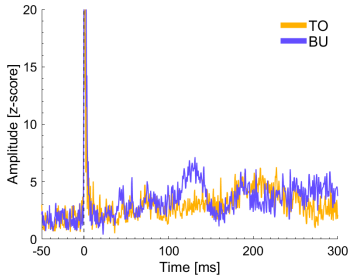

(e) MCC.

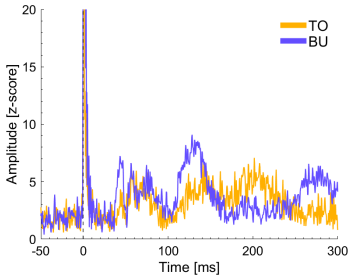

(f) PCC.

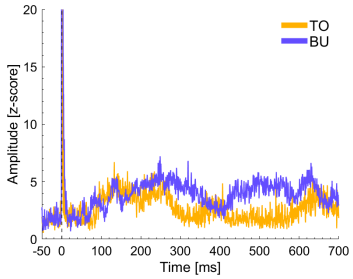

(g) ACC, 700ms.

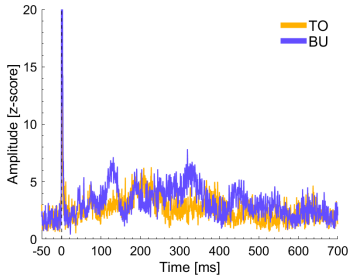

(h) MCC, 700ms.

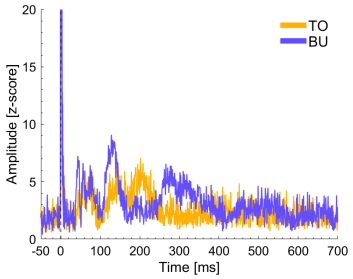

(i) PCC, 700ms.

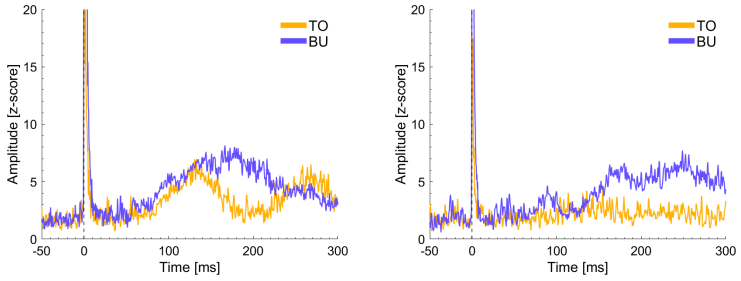

(j) IC left. **(k)** IC right.

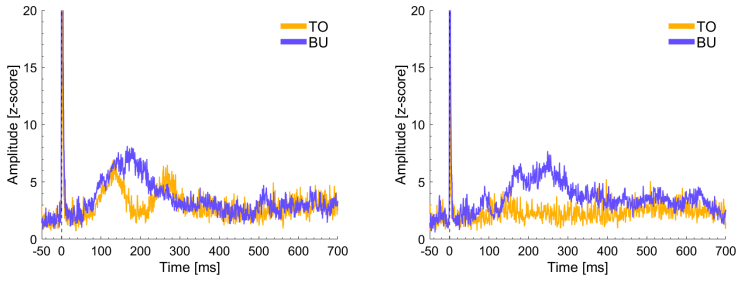

(l) IC left, 700ms. **(m)** IC right, 700ms.

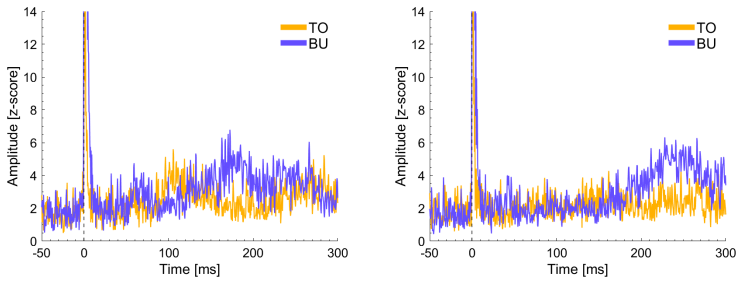

(n) Thalamus left. **(o)** Thalamus right.

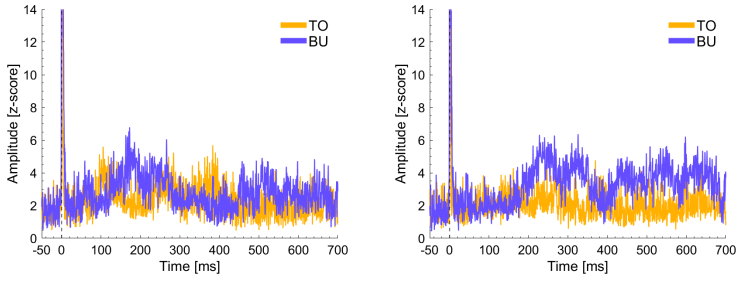

(p) Thalamus left, 700ms. **(q)** Thalamus right, 700ms.

Figure G.11: An overview of the somatosensory evoked responses elicited by tibial nerve stimulation in all regions of interest for the responder to burst spinal cord stimulation (PTN05). Note the two different ranges of the horizontal axis: either -50 to 300 milliseconds or -50 to 700 milliseconds.
S1, primary somatosensory cortex; S2, secondary somatosensory cortex; ACC, anterior cingulate cortex; MCC, middle cingulate cortex; PCC, posterior cingulate cortex; IC, insular cortex; TO, tonic spinal cord stimulation; BU, burst spinal cord stimulation.

G.4.6. Case Study PTN05 (Burst-Responder): Median Nerve

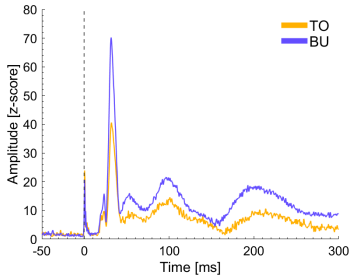

(a) S1 MN, with an exceptionally high amplitude.

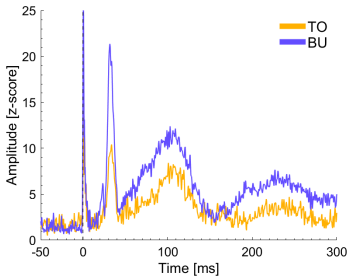

(b) S2 left.

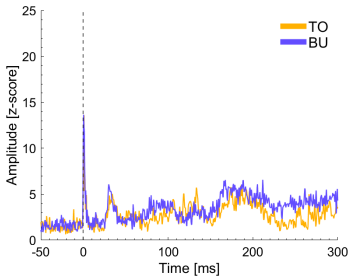

(c) S2 right.

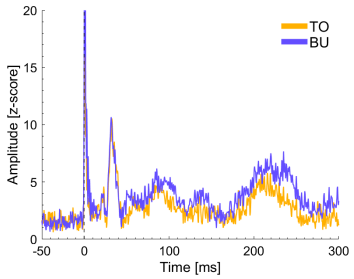

(d) ACC.

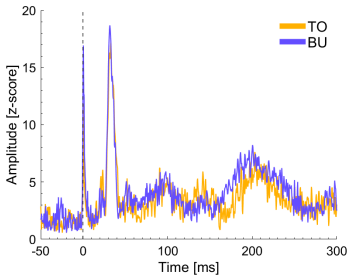

(e) MCC.

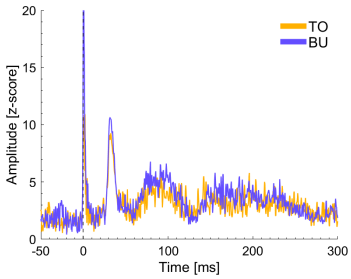

(f) PCC.

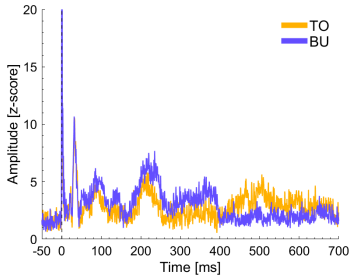

(g) ACC, 700ms.

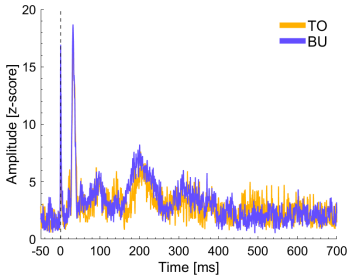

(h) MCC, 700ms.

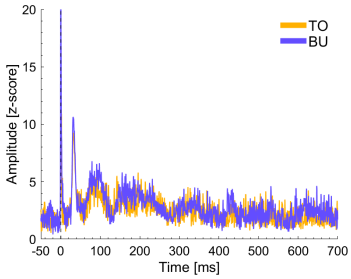

(i) PCC, 700ms.

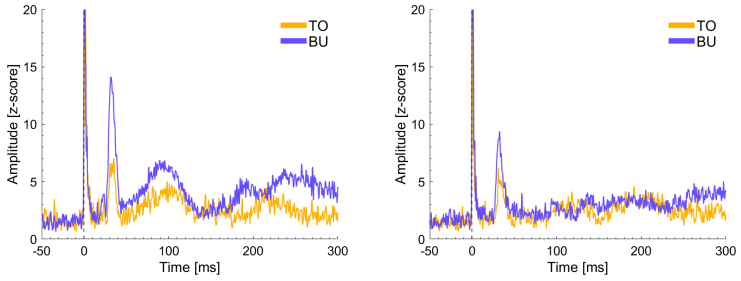

(j) IC left. **(k)** IC right.

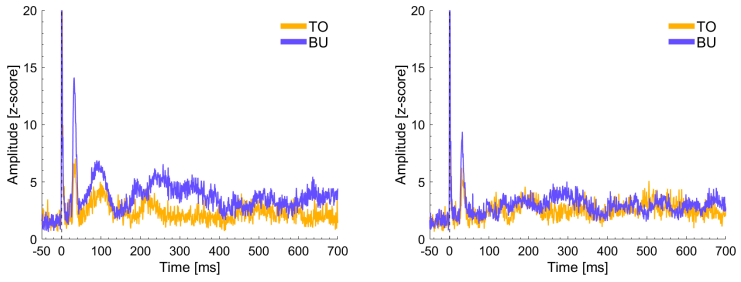

(l) IC left, 700ms. **(m)** IC right, 700ms.

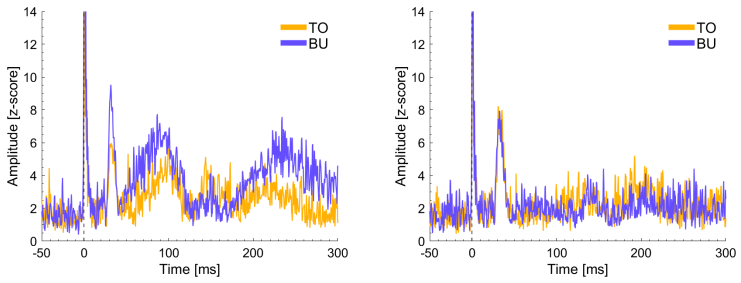

(n) Thalamus left. **(o)** Thalamus right.

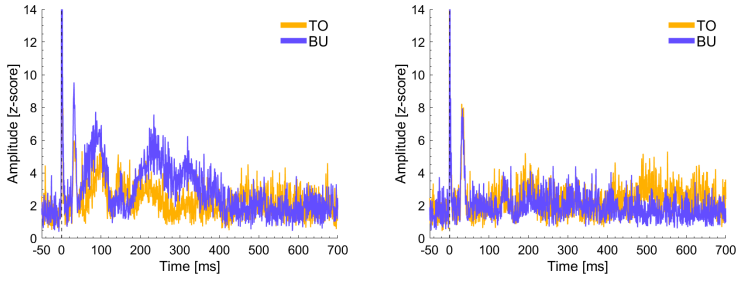

(p) Thalamus left, 700ms. **(q)** Thalamus right, 700ms.

Figure G.12: An overview of the somatosensory evoked responses elicited by median nerve stimulation in all regions of interest for the responder to burst spinal cord stimulation (PTN05). Note the two different ranges of the horizontal axis: either -50 to 300 milliseconds or -50 to 700 milliseconds.
S1, primary somatosensory cortex; S2, secondary somatosensory cortex; ACC, anterior cingulate cortex; MCC, middle cingulate cortex; PCC, posterior cingulate cortex; IC, insular cortex; TO, tonic spinal cord stimulation; BU, burst spinal cord stimulation.

G.4.7. Case Study PTN08 (Tonic-Responder): Tibial Nerve

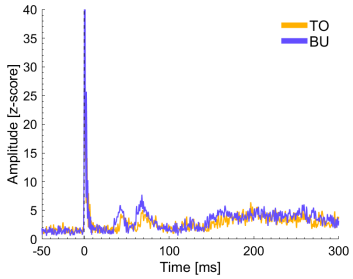

(a) S1 foot area.

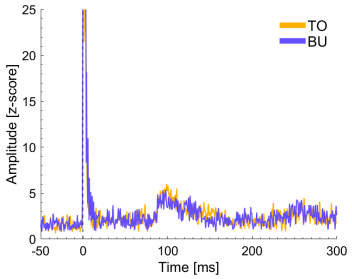

(b) S2 left.

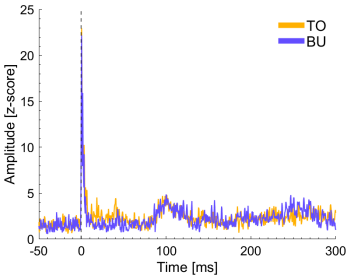

(c) S2 right.

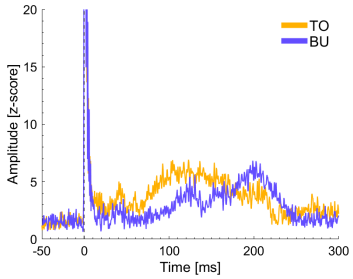

(d) ACC.

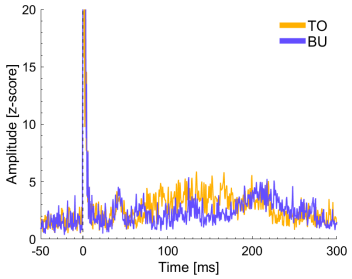

(e) MCC.

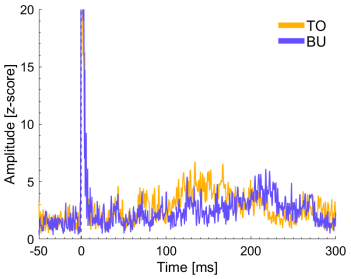

(f) PCC.

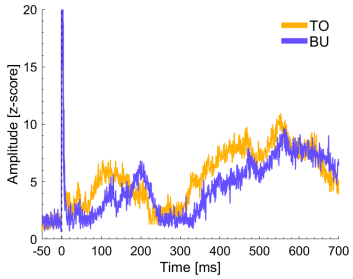

(g) ACC, 700ms.

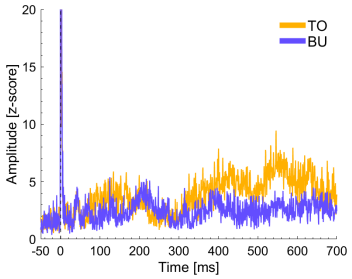

(h) MCC, 700ms.

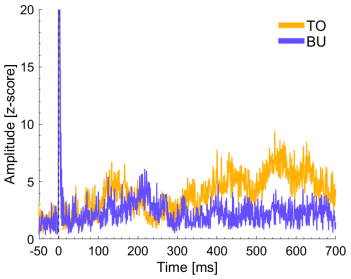

(i) PCC, 700ms.

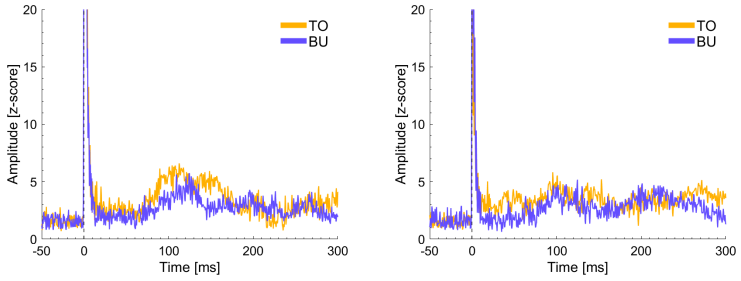

(j) IC left. **(k)** IC right.

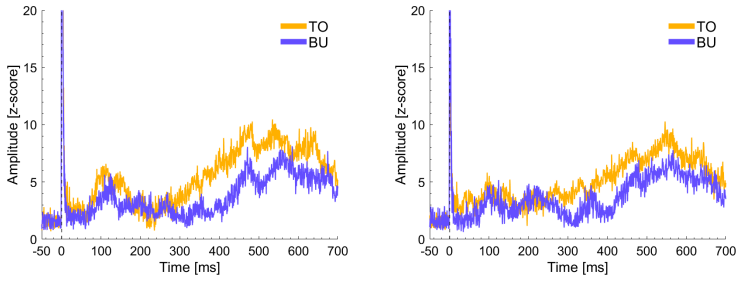

(l) IC left, 700ms. **(m)** IC right, 700ms.

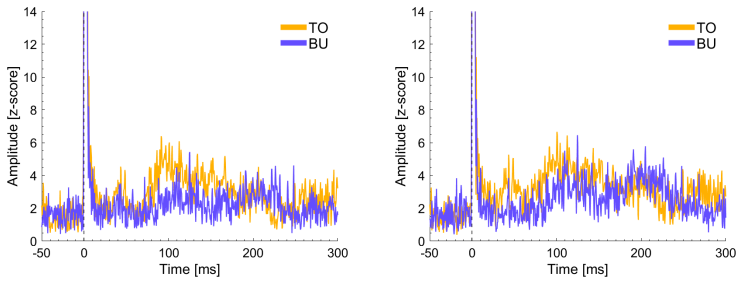

(n) Thalamus left. **(o)** Thalamus right.

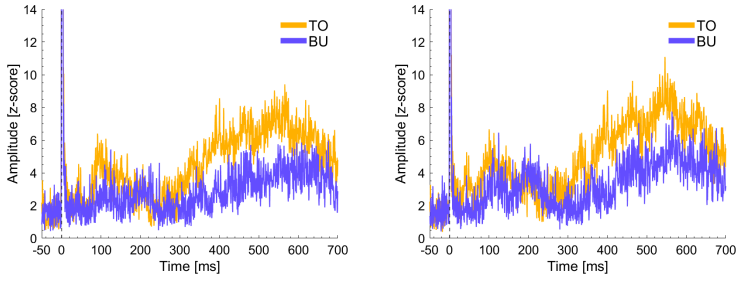

(p) Thalamus left, 700ms. **(q)** Thalamus right, 700ms.

Figure G.13: An overview of the somatosensory evoked responses elicited by tibial nerve stimulation in all regions of interest for the responder to tonic spinal cord stimulation (PTN08). Note the two different ranges of the horizontal axis: either -50 to 300 milliseconds or -50 to 700 milliseconds.
S1, primary somatosensory cortex; S2, secondary somatosensory cortex; ACC, anterior cingulate cortex; MCC, middle cingulate cortex; PCC, posterior cingulate cortex; IC, insular cortex; TO, tonic spinal cord stimulation; BU, burst spinal cord stimulation.

G.4.8. Case Study PTN08 (Tonic-Responder): Median Nerve

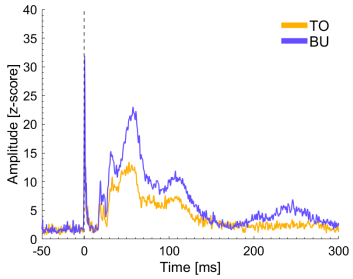

(a) S1 hand area.

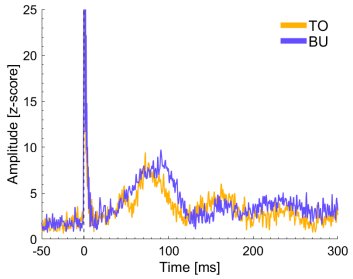

(b) S2 left.

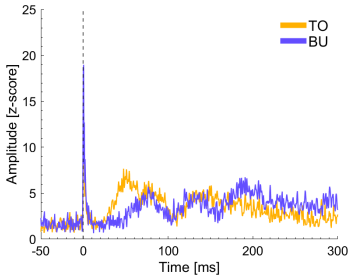

(c) S2 right.

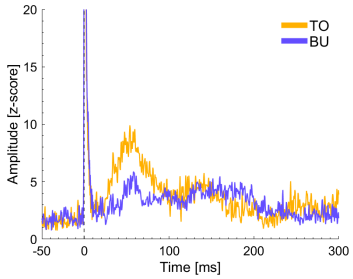

(d) ACC.

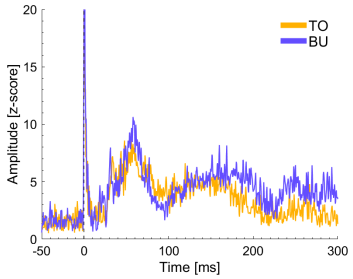

(e) MCC.

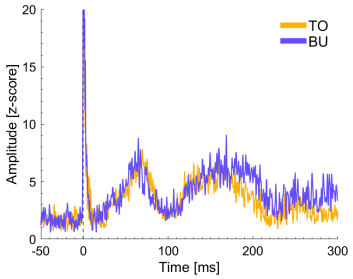

(f) PCC.

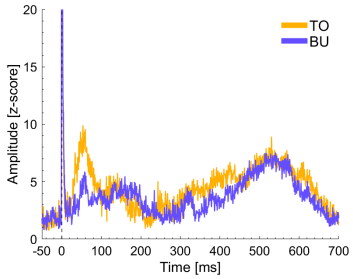

(g) ACC, 700ms.

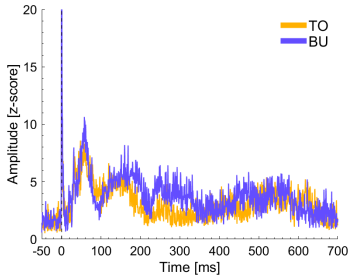

(h) MCC, 700ms.

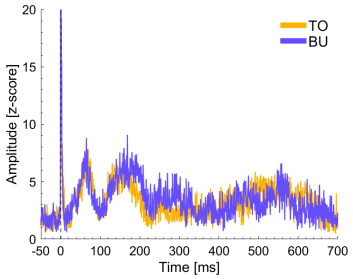

(i) PCC, 700ms.

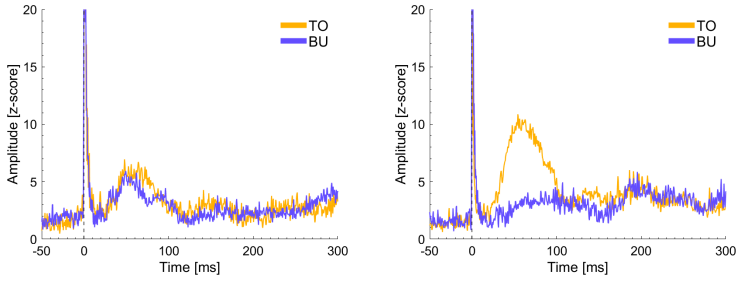

(j) IC left. **(k)** IC right.

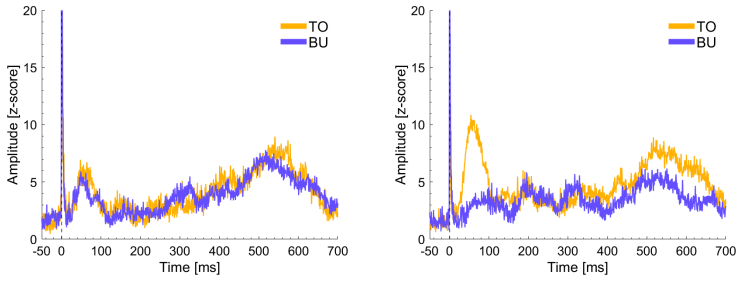

(l) IC left, 700ms. **(m)** IC right, 700ms.

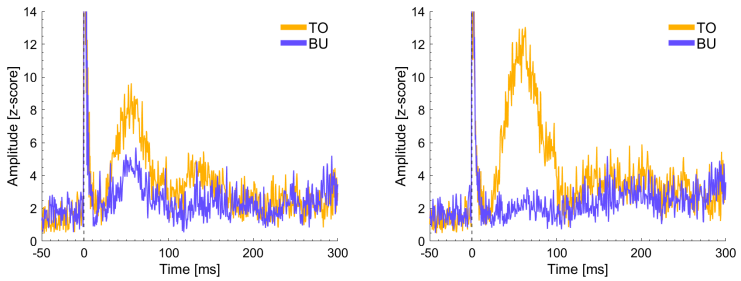

(n) Thalamus left. **(o)** Thalamus right.

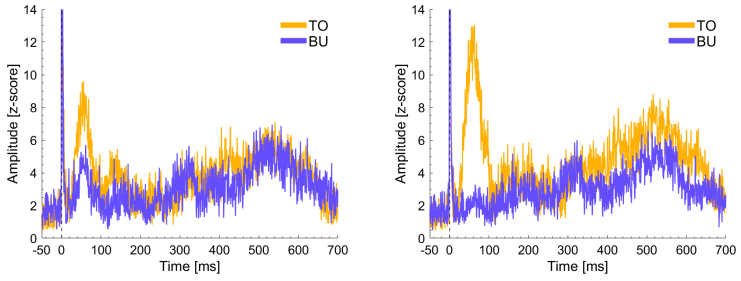

(p) Thalamus left, 700ms. **(q)** Thalamus right, 700ms.

Figure G.14: An overview of the somatosensory evoked responses elicited by medial nerve stimulation in all regions of interest for the responder to tonic spinal cord stimulation (PTN08). Note the two different ranges of the horizontal axis: either -50 to 300 milliseconds or -50 to 700 milliseconds.
S1, primary somatosensory cortex; S2, secondary somatosensory cortex; ACC, anterior cingulate cortex; MCC, middle cingulate cortex; PCC, posterior cingulate cortex; IC, insular cortex; TO, tonic spinal cord stimulation; BU, burst spinal cord stimulation.

H

Sham Spinal Cord Stimulation

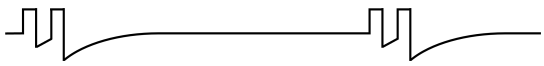

Figure H.1: The sham spinal cord stimulation (SCS) waveform is a modified version of burst SCS and consists of groups of two pulses at the same frequency as burst SCS, at the lowest possible amplitude. It is not clinically used and its therapeutic ability is unknown.

H.1. Hypotheses

H.1.1. Before SCS and During SCS (Aim 1)

In this comparison, the SERs elicited on the tibial nerve as well as on the median nerve in chronic pain patients before SCS treatment will be compared to the SERs in the same individuals when treated with sham SCS.

Tibial Nerve

For sham SCS, no literature is available comparing the SER during ”placebo” SCS to the SER in patients before SCS treatment or an ”SCS off” condition. Based on the study by Niso et al., I anticipate a similar effect of sham SCS to tonic SCS and burst SCS on the early SER component, as Niso et al. did not find a difference between sham, tonic, and burst SCS for the early component of the SER [46]. As the sham SCS setting might have been therapeutic, this could explain an amplitude decrease similar to tonic and burst SCS. For sham SCS, I expect no or less decrease of the late SER amplitude, as is described by Niso et al. [46].

Median Nerve

For the SERs elicited on the median nerve, anticipating the effect of SCS is more challenging due to the research gap for both the location of SER stimulation (entering the spinal cord *above* the SCS) as well as for the sham SCS paradigm. If the mechanism of action (MOA) of SCS on the SER is primarily spinal, this would result in less or no attenuation of the SERs elicited on the median nerve during SCS compared to before SCS. However, particularly for the late latency SER component, supraspinal MOAs of SCS have also been hypothesized, as was described in subsection 1.4.1. Supraspinal MOAs of SCS should, in theory, apply to the SERs elicited on the median nerve similarly to the SERs elicited on the tibial nerve. Consequently, taking into account that the MOA of SCS is most probably a combination of both spinal and supraspinal mechanisms, I anticipate attenuation of the SERs elicited on the median nerve as well, albeit less compared to the SERs elicited on the tibial nerve.

H.1.2. Tibial Nerve and Median Nerve (Aim 2)

In this comparison, the SERs elicited on the tibial nerve will be compared to the SERs elicited on the median nerve in patients before SCS treatment, as well as during sham SCS, to assess whether a spinal MOA possibly contributes to the effect of SCS on the SER. Based on a frequently cited theory for the observed SER amplitude decrease during tonic SCS, called the collision of impulses theory, I expect differences in the decrease of the two distinct SERs during SCS [61, 67–69, 72, 74], similar to the hypotheses stated in subsection 1.7.2.

H.1.3. Various SCS Paradigms (Aim 3)

In this comparison, the SERs elicited on the tibial nerve as well as the SERs elicited on the median nerve will be compared during the tonic, burst, and sham SCS paradigms.

Tibial Nerve

For tibial nerve stimulation, I do not expect differences in the early components of the SER amplitudes between the three SCS paradigms, as has been reported by Niso et al. [46]. Both tonic and burst SCS are considered to act on the lateral pathway, suggesting that both paradigms might affect the early SER component similarly. No theories for the MOA of sham SCS are postulated.

Based on the same study, I expect a greater decrease of the late SER amplitude by burst SCS compared to tonic and sham SCS [46]. Niso et al. reported a decreased amplitude of the late component of the SER elicited on the tibial nerve during burst SCS, compared to tonic and sham SCS, when patients focused on the applied SER stimuli. In alignment with this, during the measurements performed for this thesis, patients focused on the applied stimuli as well; therefore, I anticipate similar results.

The comparison with sham SCS as a control condition is especially complex because the therapeutic ability of sham SCS is unknown, in this research as well as in the study by Niso et al. [46]. However, for completeness, the measurements performed during sham SCS paradigm were analyzed as well.

Median Nerve

For median nerve stimulation, no literature is available comparing various SCS paradigms. No MOAs of sham SCS are hypothesized. However, I hypothesize that for the sham SCS used in this thesis, its effect most closely resembles the effect of burst SCS compared to tonic SCS due to the shape of the waveform (Figure H.1).

H.2. Results

An overview of the included patients for the comparisons including sham SCS is shown in Table F.2.

H.2.1. Before SCS and During SCS

For this comparison, the SERs elicited on the tibial nerve as well as on the median nerve before SCS treatment were compared to the SERs in the same individuals when treated with tonic, burst, and sham SCS. The characteristics of the patients who were included in this comparison are shown in Table F.5.

Tibial Nerve

For the SERs elicited by tibial nerve stimulation, the amplitudes were generally lower or unchanged during tonic and burst SCS compared to before SCS, as was described in subsection 4.2.1. For the sham SCS paradigm, the trend was similar. The amplitude during sham SCS was either similar to burst and tonic SCS or exhibited a greater difference than tonic and burst SCS compared to before SCS. The SERs elicited by tibial nerve stimulation in all ROIs during sham, tonic, and burst SCS and before SCS are shown in subsection I.1.1.

Median Nerve

For the SERs elicited by median nerve stimulation, the amplitudes were generally higher or unchanged during tonic and burst SCS compared to before SCS, as was described in subsection 4.2.1. For the sham SCS paradigm, the trend was similar. The amplitude during sham SCS was either similar to burst and tonic SCS or exhibited a greater difference than tonic and burst SCS compared to before SCS. The SERs in all ROIs elicited by median nerve stimulation during sham, tonic, and burst SCS and before SCS are shown in subsection I.1.2.

H.2.2. Tibial Nerve and Median Nerve

The primary focus of this comparison, comparing the SERs elicited on the tibial nerve to the SERs elicited on the median nerve, was to determine whether the difference between the two distinct SERs is greater during sham SCS compared to before SCS treatment. The characteristics of the patients who were included in this comparison are shown in Table F.5 and Table F.6. The difference between SERs was quantified using the AUC ratio. The comparison between AUC ratios was initially performed in the subpopulation of patients who were also previously included in the study before SCS treatment, comparing the AUC ratios before SCS to the AUC ratios during sham SCS. Subsequently, the AUC

ratios of the patients before SCS treatment were compared to the AUC ratios during and sham SCS in the groups consisting of all included patient recordings.

Before SCS Treatment
The AUC ratios of the patients before SCS treatment (n=4) and the AUC ratios of the same individuals (n=4) during sham SCS are shown in Table H.1. In the S1 hand and foot area, as well as in the right S2, the ACC, the MCC, the right insular cortex, and the left and right thalamus, the AUC ratio was higher during sham SCS compared to before SCS. An overview of the graphs showing the AUCs for the SERs elicited by tibial nerve and median nerve stimulation in all ROIs for the subpopulation (n=4) is provided in subsection I.2.1.

All Patients
The AUC ratios of the patients before SCS treatment (n=4) and the AUC ratios of all included patients during sham SCS are shown in Table H.1. In the S1 hand area, as well as in the left and right S2, the ACC, the MCC, the left and right insular cortex, and the left and right thalamus, the AUC ratio was higher during sham SCS compared to before SCS. An overview of the graphs showing the AUCs for the SERs elicited by tibial nerve and median nerve stimulation in all ROIs for all patients treated with SCS (n=19) is provided in subsection I.2.2.

Table H.1: The area under the curve ratios of the patients before spinal cord stimulation (SCS) treatment (n=4), of the same individuals during sham SCS (n=4), and of all included patients during sham SCS (n=19)

	Before SCS (n=4)	**Sham SCS (n=4)**	**Sham SCS (n=19)**
S1 foot	1.5	**2.1**	1.7
S1 hand	5.9	**8.3**	**7.3**
S2 left	1.9	2.2	**2.3**
S2 right	0.9	**2.7**	**2.7**
ACC	1.4	**2.5**	**2.0**
MCC	1.6	**2.4**	**2.2**
PCC	1.3	1.7	1.6
IC left	1.7	1.9	**2.1**
IC right	1.1	**2.2**	**3.2**
Thalamus left	1.3	**2.5**	**3.0**
Thalamus right	1.1	**3.1**	**3.2**

S1, primary somatosensory cortex; S2, secondary somatosensory cortex; ACC, anterior cingulate cortex; MCC, middle cingulate cortex; PCC, posterior cingulate cortex; IC, insular cortex.

H.2.3. Various SCS Paradigms

In this comparison, the SERs elicited on the tibial nerve as well as the SERs elicited on the median nerve during tonic and burst SCS were compared to the placebo SCS setting (section I.3).

Tibial Nerve
The characteristics of the patients who were included in this comparison are shown in Table F.9. For the SERs elicited by tibial nerve stimulation, the amplitudes for the middle and late latency components during sham SCS were generally similar to during tonic and burst SCS. For the very late latency component, the amplitude during sham SCS was generally lowest and primarily resembled the amplitude during tonic SCS. The SERs elicited by tibial nerve stimulation in all ROIs during sham, tonic, and burst SCS are shown in subsection I.3.1.

Median Nerve
The characteristics of the patients who were included in this comparison are shown in Table F.10. For the SERs elicited by median nerve stimulation, the amplitude of the middle latency component (M100) was generally higher during sham SCS compared to during tonic and burst SCS. This SER component exhibited an exceptionally large standard error during sham SCS, especially in the right insular cortex. The patient who caused this big variability was assessed, and no reasons were found to exclude them

from the comparison other than the exceptionally high SER amplitude in the right insular cortex. For the late and very late latency components, the SER amplitude during sham SCS was lower compared to burst SCS and resembled the SER during tonic SCS. The SERs elicited by median nerve stimulation in all ROIs during sham, tonic, and burst SCS are shown in subsection I.3.2.

H.3. Discussion

As mentioned earlier, the sham SCS paradigm is not clinically used but was developed for this study as a control measure. During this study, the numerical rating scale (NRS) attributed to the chronic pain condition was assessed at each MEG measurement session for the current SCS paradigm. The average NRS scores are presented in Table H.2, illustrating that the therapeutic effect of sham SCS was comparable to the therapeutic effect of tonic and burst SCS. Furthermore, the NRS scores attributed to the SER stimuli during sham SCS did not differ from during tonic and burst SCS.

For sham SCS, no MOAs have been hypothesized like is the case for burst and tonic SCS. Based on the sham SCS waveform, which is a modified version of the burst SCS waveform (Figure H.1) consisting of groups of two pulses instead of five at the same frequency as burst SCS at the lowest possible amplitude, similar results to burst SCS would be expected. In addition to the waveforms that were already quite similar during the MEG measurements, burst SCS is currently applied in the clinic with much lower energy compared to during the measurements for this thesis, implying that the burst SCS paradigm of today gets more similar to the sham SCS paradigm during the study. Nowadays, burst SCS is often applied with the lowest possible amplitude, or with a slightly higher amplitude on a cyclic program (intermittent on/off). This evolving understanding and change in the application of burst SCS may explain why the SCS paradigm demonstrated therapeutic effects in this study.

Table H.2: Average pain intensity on the numerical rating scale (NRS) attributed to the chronic pain condition during tonic, burst, and sham spinal cord stimulation.

	Tonic	**Burst**	**Sham**
NRS [mean ($\pm$ std)]	4 ($\pm$ 2)	4 ($\pm$ 3)	4 ($\pm$ 2)

std, standard deviation.

Table H.3: Average pain intensity on the numerical rating scale (NRS) attributed to the stimuli to elicit the SERs during each paradigm, for the SERs elicited by tibial nerve (TN) stimulation and by median nerve (MN) stimulation.

	Tonic	**Burst**	**Sham**
TN NRS [mean ($\pm$ std)]	3.3 ($\pm$ 1.8)	3.6 ($\pm$ 1.9)	2.9 ($\pm$ 1.9)
MN NRS [mean ($\pm$ std)]	3.2 ($\pm$ 1.6)	2.8 ($\pm$ 1.4)	2.3 ($\pm$ 1.4)

std, standard deviation.

H.3.1. Before SCS and During SCS

The SERs elicited by both tibial nerve and median nerve stimulation during sham SCS resembled the SERs during tonic and burst SCS. This corresponds with the expectations based on Niso et al. for the early component of the SER [46].

H.3.2. Tibial Nerve and Median Nerve

For the comparison of the SERs elicited on the tibial nerve to the SERs elicited on the median nerve before SCS and during SCS, the results during sham SCS were similar to the observed results during tonic and burst SCS.

H.3.3. Various SCS Paradigms

Contrary to expectations, the SERs during sham SCS were either higher compared to tonic and burst SCS or resembled the SER during tonic SCS. This difference could not be attributed to a difference in stimulation intensity, as is shown in Table H.4, similar to the comparison between tonic and burst SCS.

Table H.4: Average stimulation intensity during each spinal cord stimulation paradigm for the somatosensory evoked responses elicited by tibial nerve (TN) and by median nerve (MN) stimulation.

	Tonic	**Burst**	**Sham**
TN stim [mA] [mean (± std)]	27.4 (± 11.4)	28.0 (± 13)	28.2 (± 15.3)
MN stim [mA] [mean (± std)]	17.3 (± 8.2)	16.3 (± 9.0)	17.5 (± 10.7)

std, standard deviation; mA, milliamperes.

I

All Results ROIs (Sham)

I.1. Before SCS and During SCS (Sham)

I.1.1. Tibial Nerve

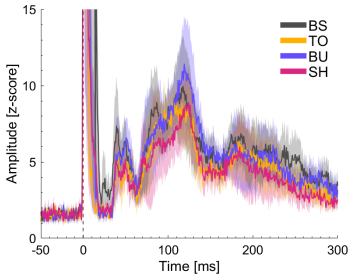

(a) S1 foot area.

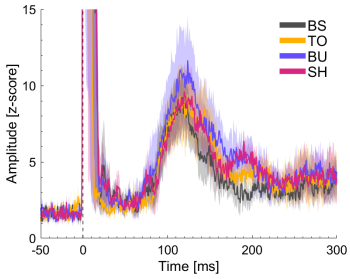

(b) S2 left.

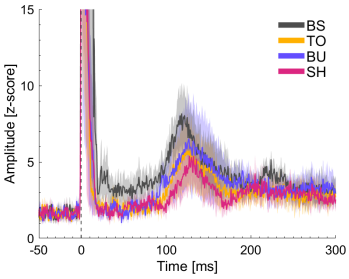

(c) S2 right.

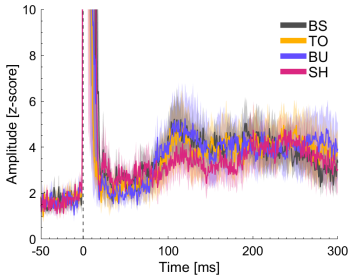

(d) ACC.

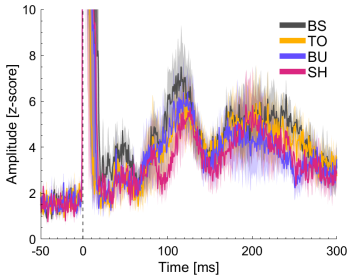

(e) MCC.

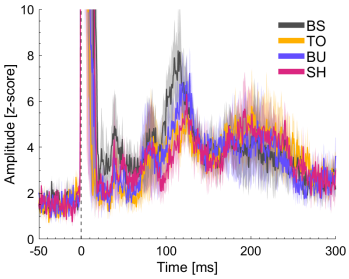

(f) PCC.

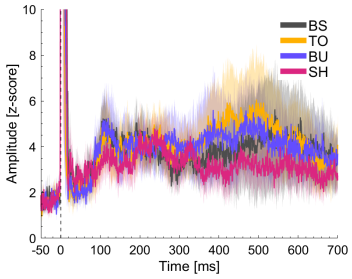

(g) ACC, 700ms.

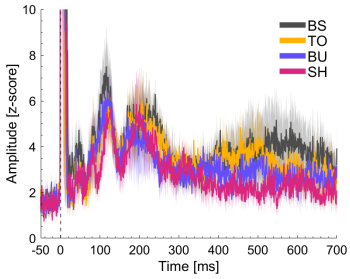

(h) MCC, 700ms.

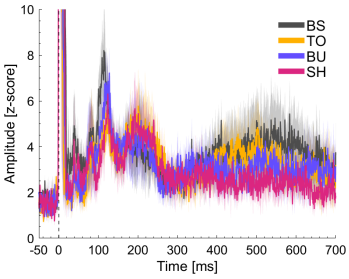

(i) PCC, 700ms.

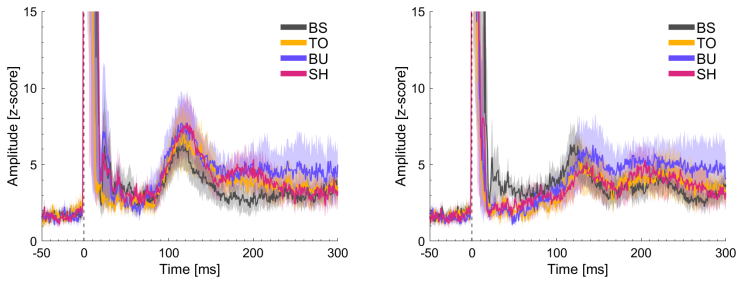

(j) IC left. **(k)** IC right.

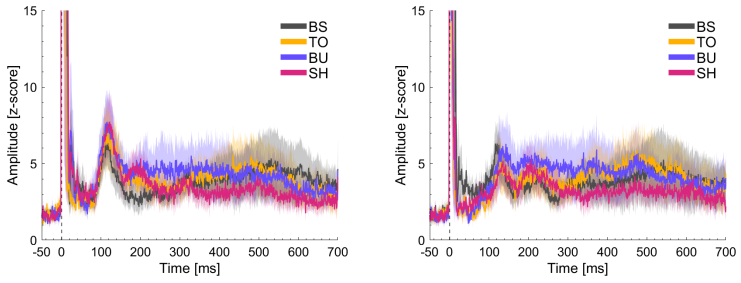

(l) IC left, 700ms. **(m)** IC right, 700ms.

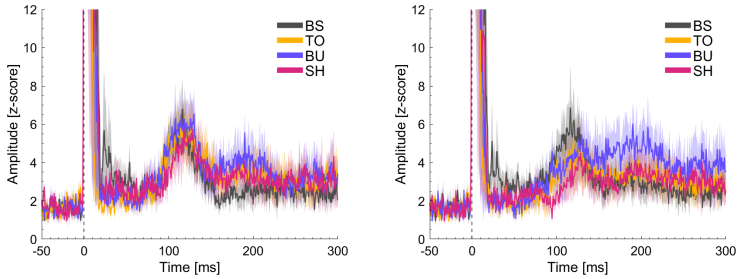

(n) Thalamus left. **(o)** Thalamus right.

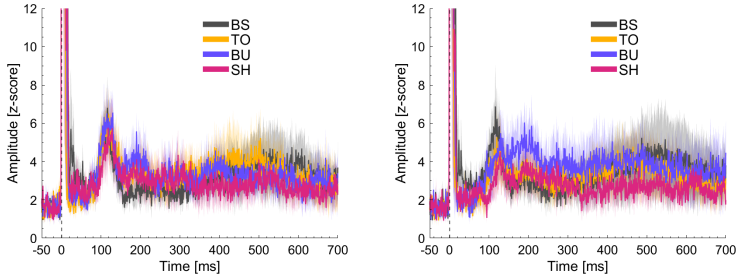

(p) Thalamus left, 700ms. **(q)** Thalamus right, 700ms.

Figure I.1: An overview of the somatosensory evoked responses elicited by tibial nerve stimulation in all regions of interest for the comparison between before spinal cord stimulation treatment and during tonic, burst, and sham spinal cord stimulation. Note the two different ranges of the horizontal axis: either -50 to 300 milliseconds or -50 to 700 milliseconds.
S1, primary somatosensory cortex; S2, secondary somatosensory cortex; ACC, anterior cingulate cortex; MCC, middle cingulate cortex; PCC, posterior cingulate cortex; IC, insular cortex; BS, before spinal cord stimulation treatment; TO, tonic spinal cord stimulation; BU, burst spinal cord stimulation; SH, sham spinal cord stimulation.

I.1.2. Median Nerve

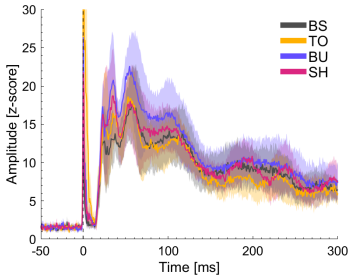

(a) S1 hand area.

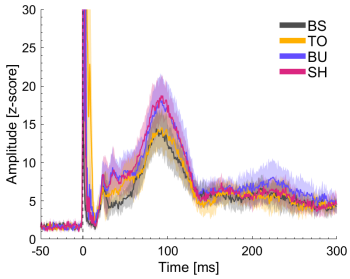

(b) S2 left.

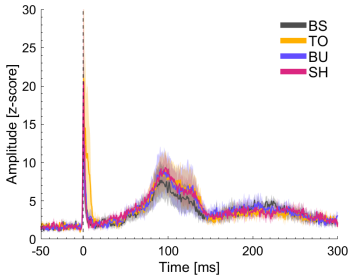

(c) S2 right.

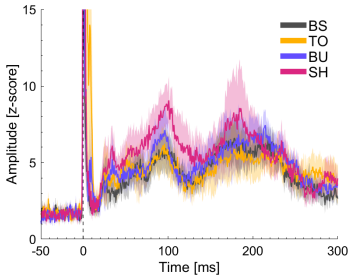

(d) ACC.

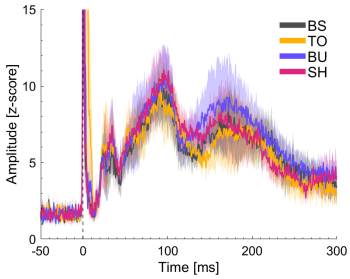

(e) MCC.

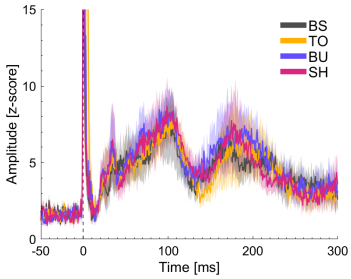

(f) PCC.

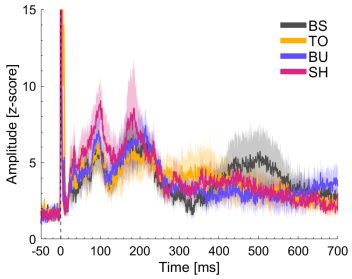

(g) ACC, 700ms.

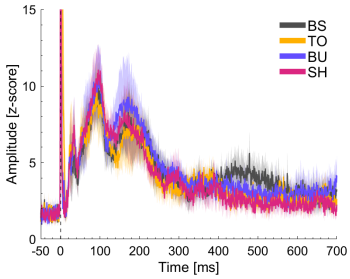

(h) MCC, 700ms.

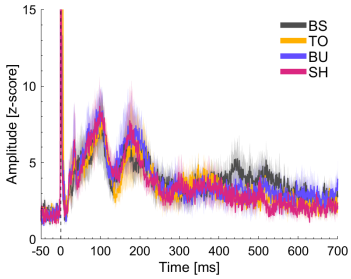

(i) PCC, 700ms.

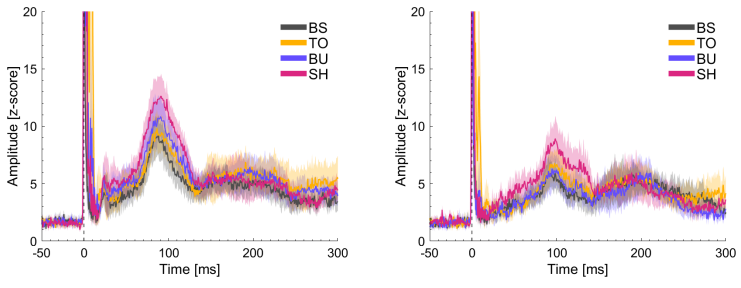

(j) IC left. **(k)** IC right.

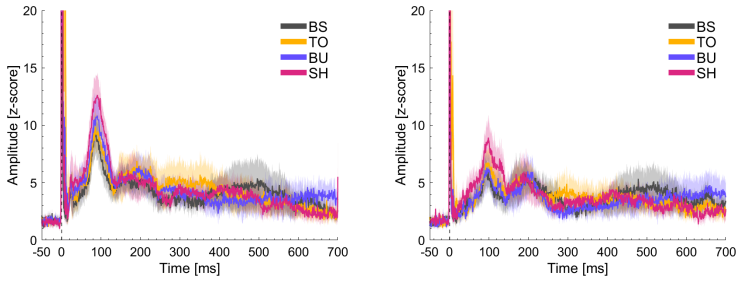

(l) IC left, 700ms. **(m)** IC right, 700ms.

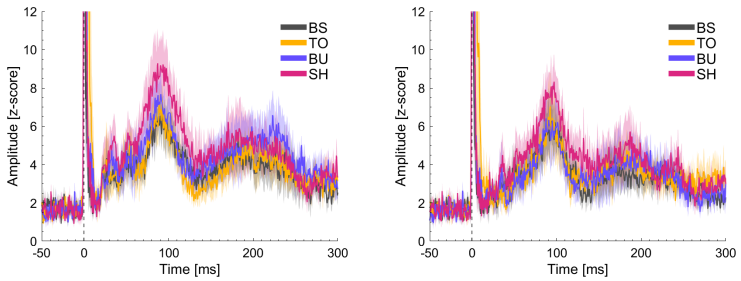

(n) Thalamus left. **(o)** Thalamus right.

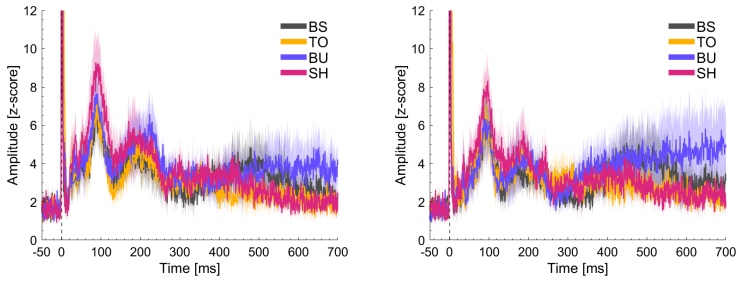

(p) Thalamus left, 700ms. **(q)** Thalamus right, 700ms.

Figure I.2: An overview of the somatosensory evoked responses elicited by median nerve stimulation in all regions of interest for the comparison between before spinal cord stimulation treatment and during tonic, burst, and sham spinal cord stimulation. Note the two different ranges of the horizontal axis: either -50 to 300 milliseconds or -50 to 700 milliseconds.
S1, primary somatosensory cortex; S2, secondary somatosensory cortex; ACC, anterior cingulate cortex; MCC, middle cingulate cortex; PCC, posterior cingulate cortex; IC, insular cortex; BS, before spinal cord stimulation treatment; TO, tonic spinal cord stimulation; BU, burst spinal cord stimulation; SH, sham spinal cord stimulation.

I.2. Tibial Nerve and Median Nerve (Sham)

I.2.1. Before SCS Treatment

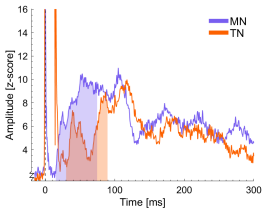

(a) S1 foot area (BS).

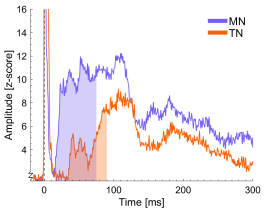

(b) S1 foot area (TO).

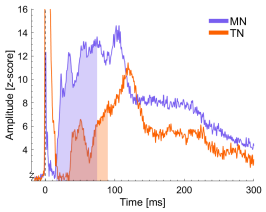

(c) S1 foot area (BU).

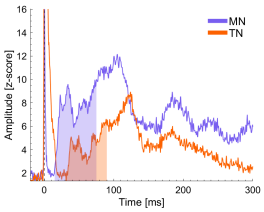

(d) S1 foot area (SH).

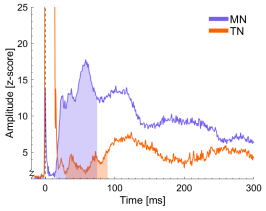

(e) S1 hand area (BS).

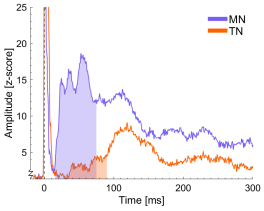

(f) S1 hand area (TO).

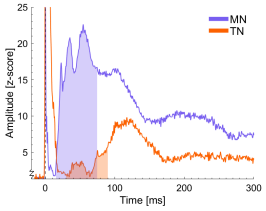

(g) S1 hand area (BU).

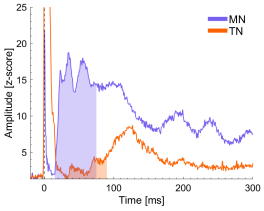

(h) S1 hand area (SH).

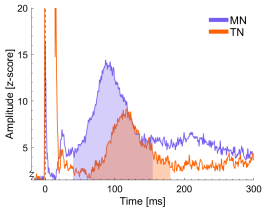

(i) S2 left (BS).

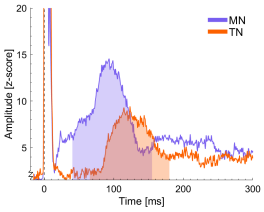

(j) S2 left (TO).

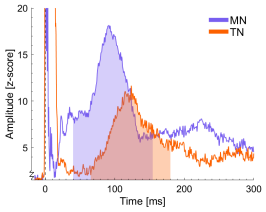

(k) S2 left (BU).

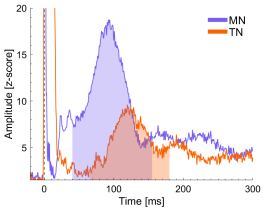

(l) S2 left (SH).

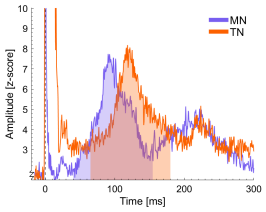

(m) S2 right (BS).

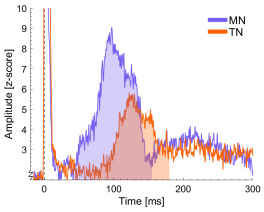

(n) S2 right (TO).

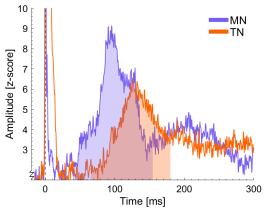

(o) S2 right (BU).

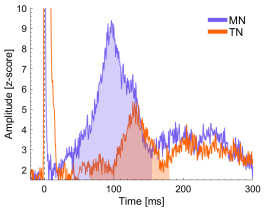

(p) S2 right (SH).

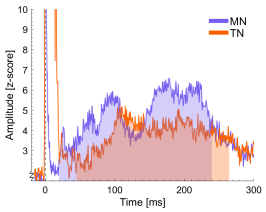

(q) ACC (BS).

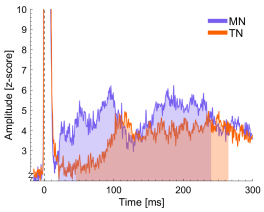

(r) ACC (TO).

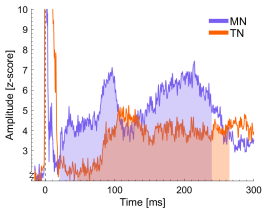

(s) ACC (BU).

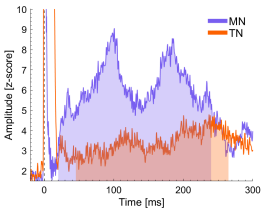

(t) ACC (SH).

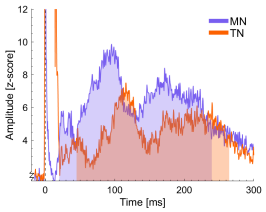

(u) MCC (BS).

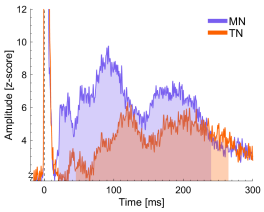

(v) MCC (TO).

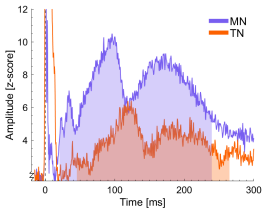

(w) MCC (BU).

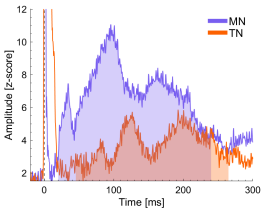

(x) MCC (SH).

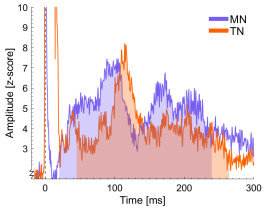

(y) PCC (BS).

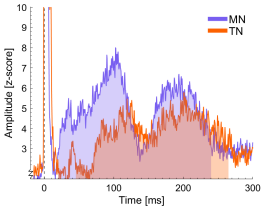

(z) PCC (TO).

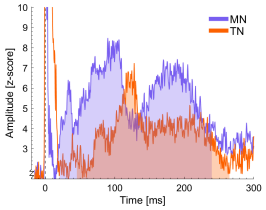

(aa) PCC (BU).

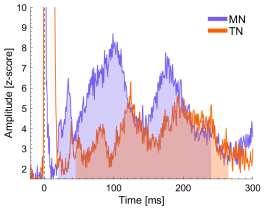

(ab) PCC (SH).

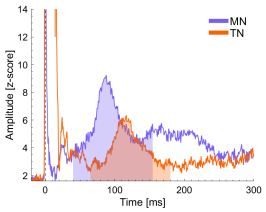

(ac) Left Insula (BS).

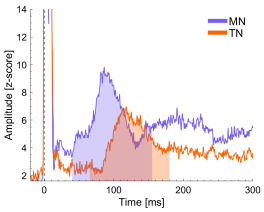

(ad) Left Insula (TO).

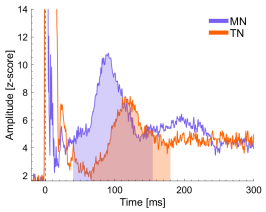

(ae) Left Insula (BU).

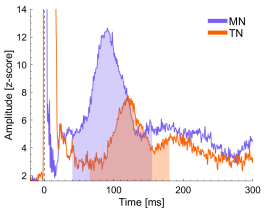

(af) Left Insula (SH).

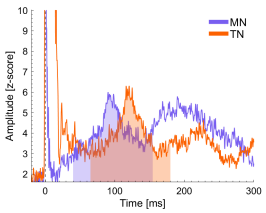

(ag) IC right (BS).

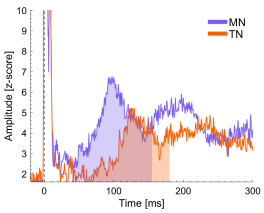

(ah) IC right (TO).

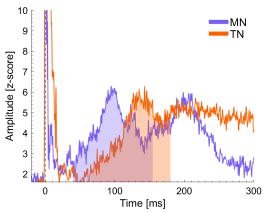

(ai) IC right (BU).

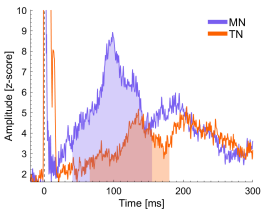

(aj) IC right (SH).

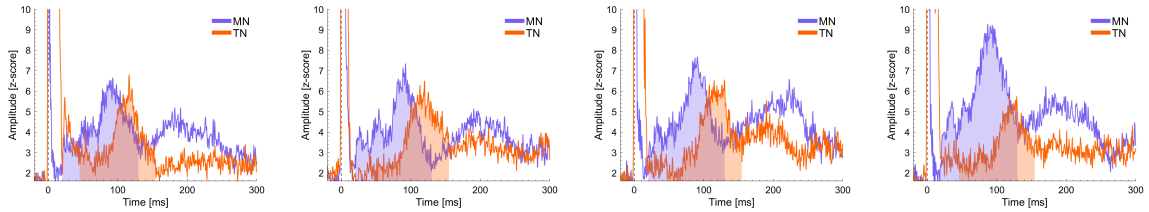

(ak) Thalamus left (BS). **(al)** Thalamus left (TO). **(am)** Thalamus left (BU). **(an)** Thalamus left (SH).

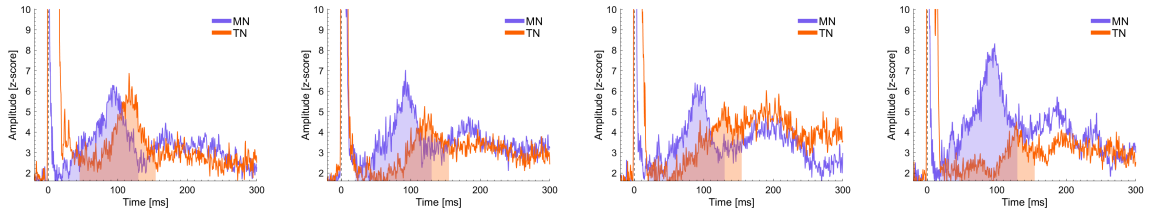

(ao) Thalamus right (BS). **(ap)** Thalamus right (TO). **(aq)** Thalamus right (SH). **(ar)** Thalamus right (SH).

Figure I.3: An overview of the graphs showing the areas under the curves (AUCs) for the somatosensory evoked responses elicited by tibial nerve and median nerve stimulation in all regions of interest, of the patients before spinal cord stimulation treatment (n=4) and of the same patients (n=4) during tonic, burst, and sham spinal cord stimulation. The shaded areas represent the AUCs that were used to determine the AUC ratio for each condition, for each region of interest.
S1, primary somatosensory cortex; S2, secondary somatosensory cortex; ACC, anterior cingulate cortex; MCC, middle cingulate cortex; PCC, posterior cingulate cortex; IC, insular cortex; BS, before spinal cord stimulation treatment; TO, tonic spinal cord stimulation; BU, burst spinal cord stimulation; SH, sham spinal cord stimulation; MN, median nerve; TN, tibial nerve.

I.2.2. All Patients

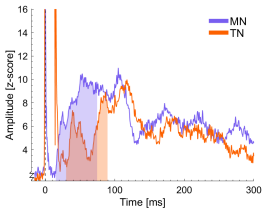

(a) S1 foot area (BS).

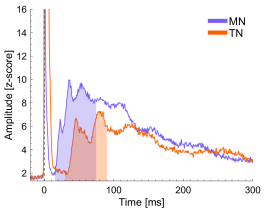

(b) S1 foot area (TO).

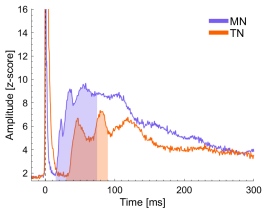

(c) S1 foot area (BU).

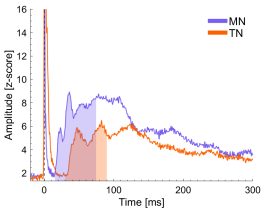

(d) S1 foot area (SH).

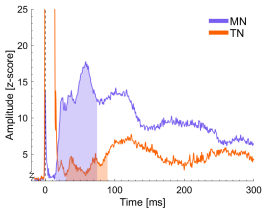

(e) S1 hand area (BS).

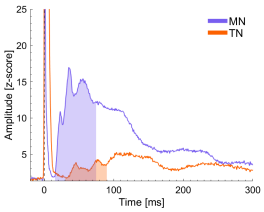

(f) S1 hand area (TO).

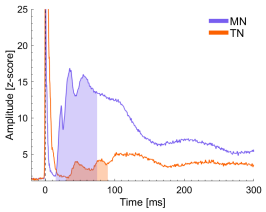

(g) S1 hand area (BU).

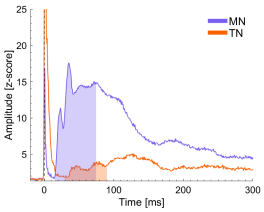

(h) S1 hand area (SH).

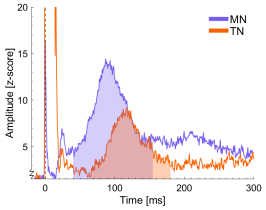

(i) S2 left (BS).

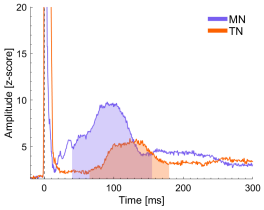

(j) S2 left (TO).

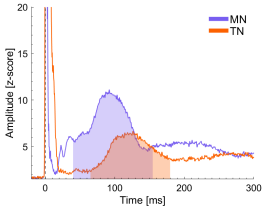

(k) S2 left (BU).

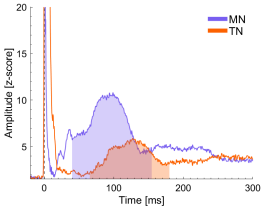

(l) S2 left (SH).

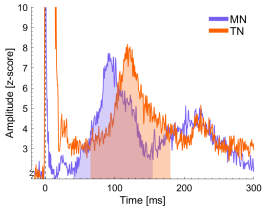

(m) S2 right (BS).

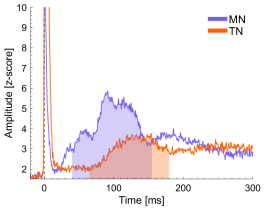

(n) S2 right (TO).

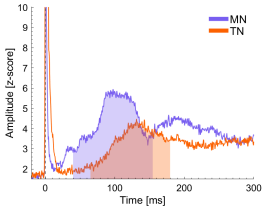

(o) S2 right (BU).

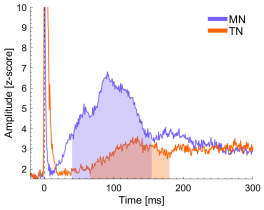

(p) S2 right (SH).

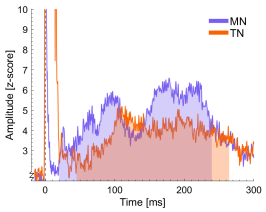

(q) ACC (BS).

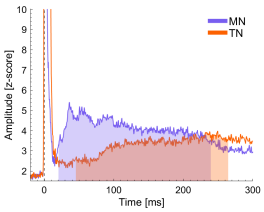

(r) ACC (TO).

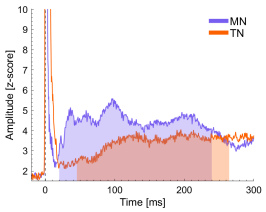

(s) ACC (BU).

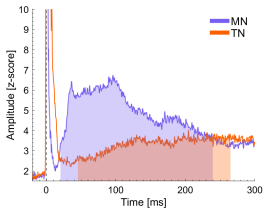

(t) ACC (SH).

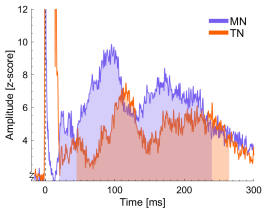

(u) MCC (BS).

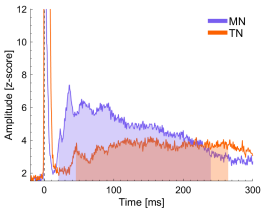

(v) MCC (TO).

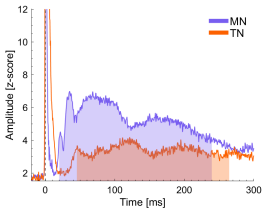

(w) MCC (BU).

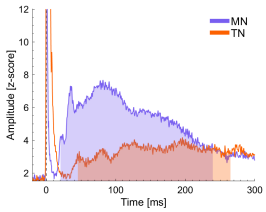

(x) MCC (SH).

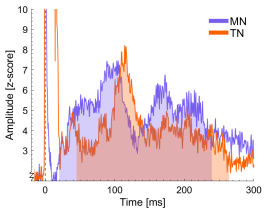

(y) PCC (BS).

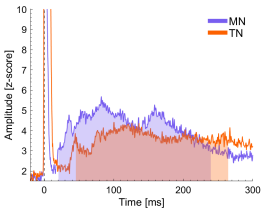

(z) PCC (TO).

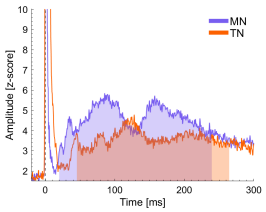

(aa) PCC (BU).

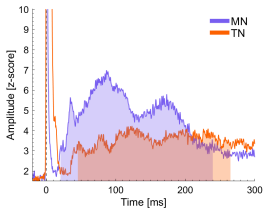

(ab) PCC (SH).

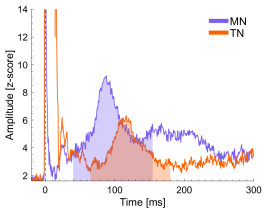

(ac) IC left (BS).

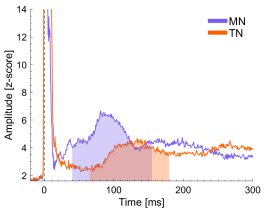

(ad) IC left (TO).

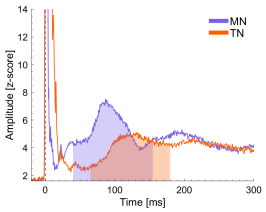

(ae) IC left (BU).

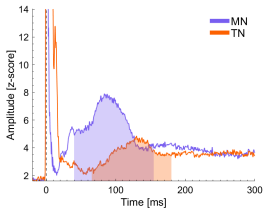

(af) IC left (SH).

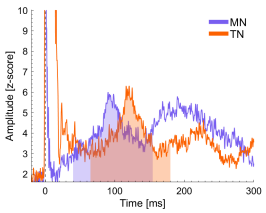

(ag) IC right (BS).

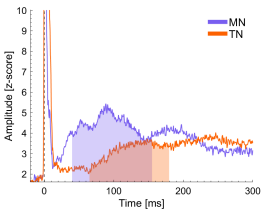

(ah) IC right (TO).

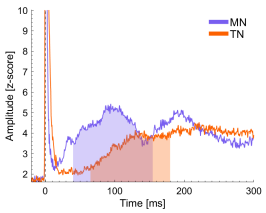

(ai) IC right (BU).

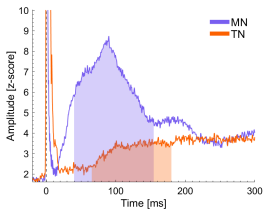

(aj) IC right (SH).

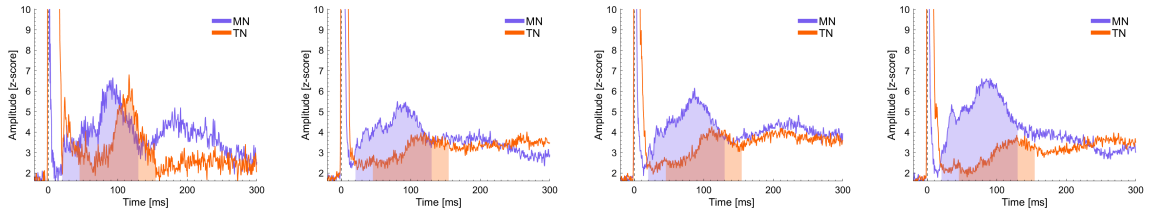

(ak) Thalamus left (BS). **(al)** Thalamus left (TO). **(am)** Thalamus left (BU). **(an)** Thalamus left (SH).

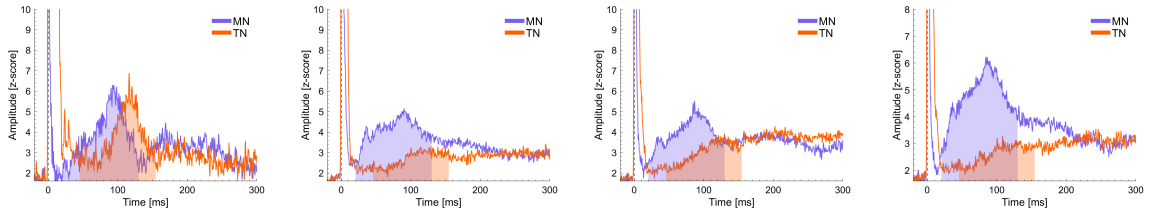

(ao) Thalamus right (BS). **(ap)** Thalamus right (TO). **(aq)** Thalamus right (BU). **(ar)** Thalamus right (SH).

Figure I.4: An overview of the graphs showing the areas under the curves (AUCs) for the somatosensory evoked responses elicited by tibial nerve and median nerve stimulation in all regions of interest, of the patients before spinal cord stimulation treatment (n=4) and of all included patients that were treated with spinal cord stimulation (n=19) during tonic, burst, and sham spinal cord stimulation. The shaded areas represent the AUCs that were used to determine the AUC ratio for each condition, for each region of interest.
S1, primary somatosensory cortex; S2, secondary somatosensory cortex; ACC, anterior cingulate cortex; MCC, middle cingulate cortex; PCC, posterior cingulate cortex; IC, insular cortex; BS, before spinal cord stimulation treatment; TO, tonic spinal cord stimulation; BU, burst spinal cord stimulation; SH, sham spinal cord stimulation; MN, median nerve; TN, tibial nerve.

I.3. Tonic SCS and Burst SCS (Sham)

I.3.1. Tibial Nerve

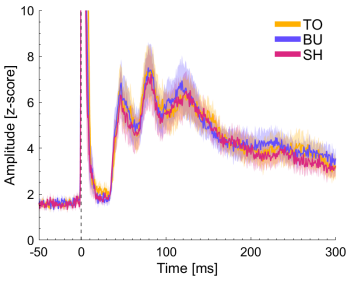

(a) S1 foot area.

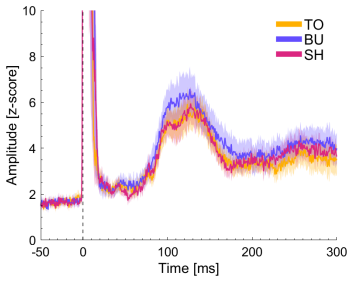

(b) S2 left.

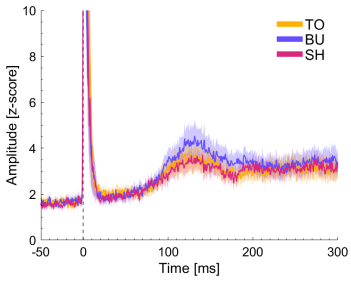

(c) S2 right.

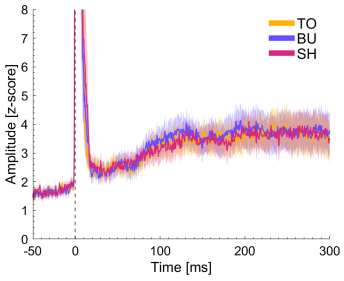

(d) ACC.

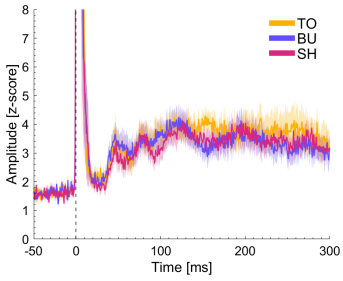

(e) MCC.

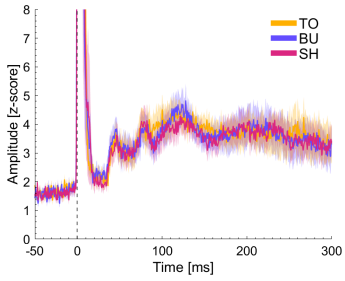

(f) PCC.

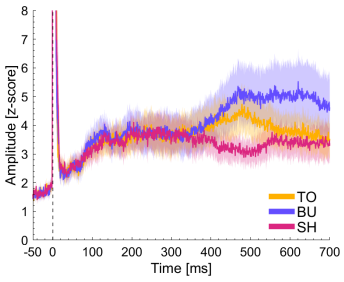

(g) ACC, 700ms.

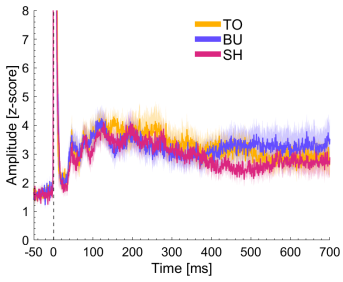

(h) MCC, 700ms.

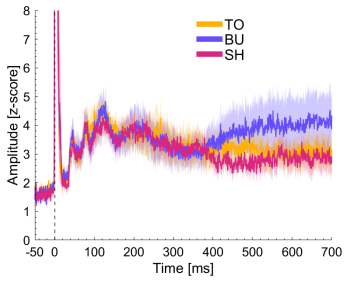

(i) PCC, 700ms.

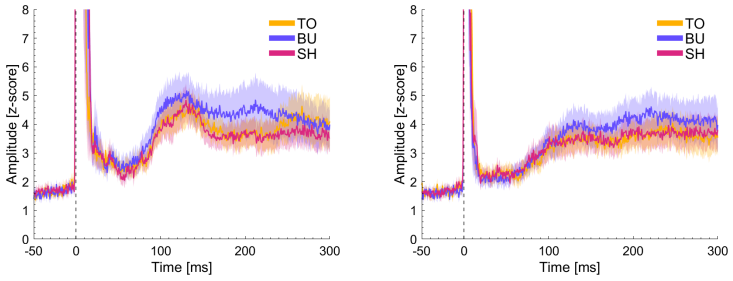

(j) IC left. **(k)** IC right.

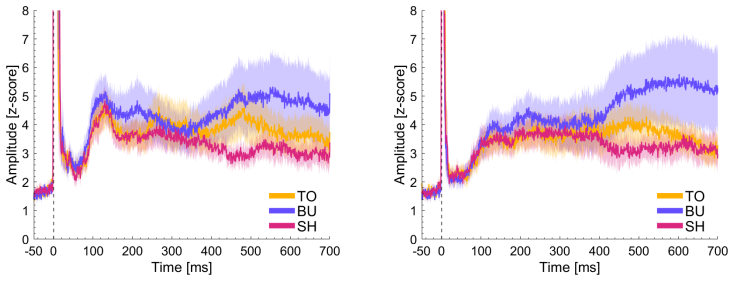

(l) IC left, 700ms. **(m)** IC right, 700ms.

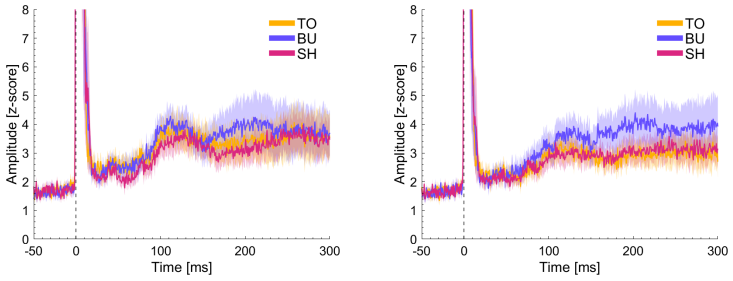

(n) Thalamus left. **(o)** Thalamus right.

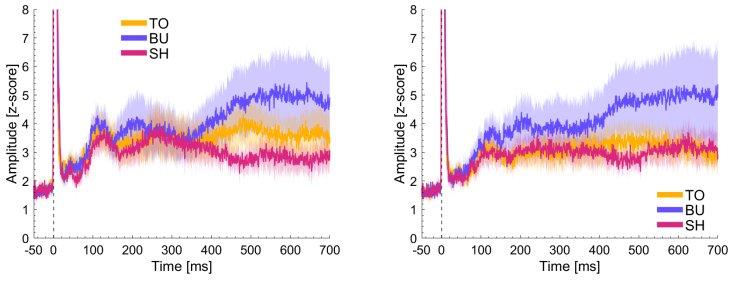

(p) Thalamus left, 700ms. **(q)** Thalamus right, 700ms.

Figure I.5: An overview of the somatosensory evoked responses elicited by tibial nerve stimulation in all regions of interest for the comparison between tonic, burst, and sham spinal cord stimulation. Note the two different ranges of the horizontal axis: either -50 to 300 milliseconds or -50 to 700 milliseconds.
S1, primary somatosensory cortex; S2, secondary somatosensory cortex; ACC, anterior cingulate cortex; MCC, middle cingulate cortex; PCC, posterior cingulate cortex; IC, insular cortex; TO, tonic spinal cord stimulation; BU, burst spinal cord stimulation; SH, sham spinal cord stimulation.

I.3.2. Median Nerve

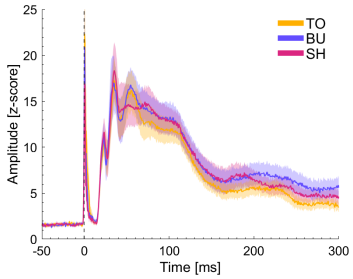

(a) S1 hand area.

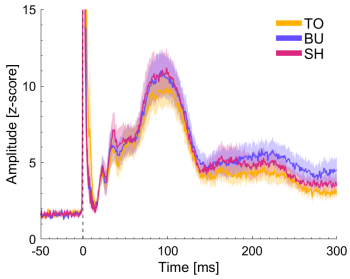

(b) S2 left.

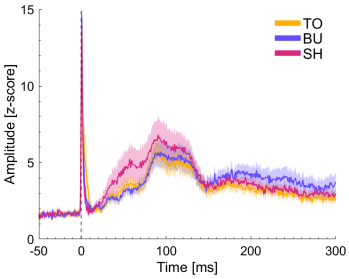

(c) S2 right.

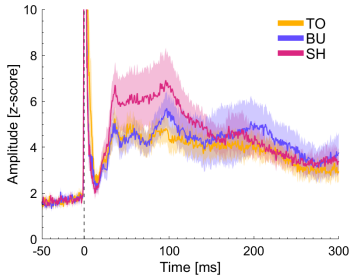

(d) ACC.

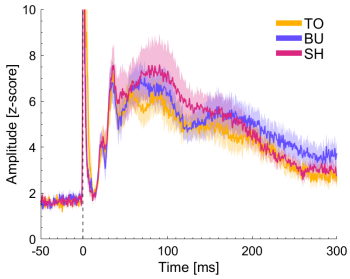

(e) MCC.

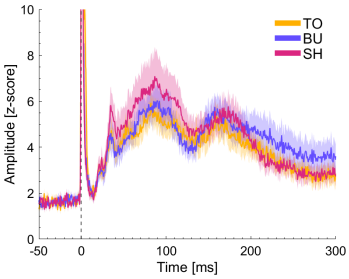

(f) PCC.

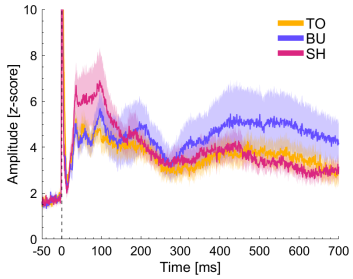

(g) ACC, 700ms.

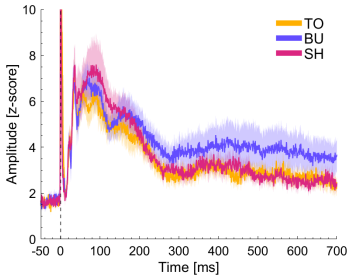

(h) MCC, 700ms.

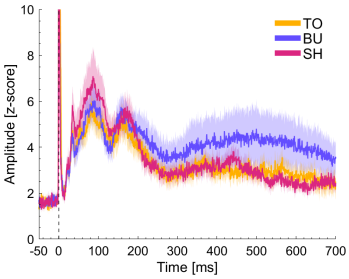

(i) PCC, 700ms.

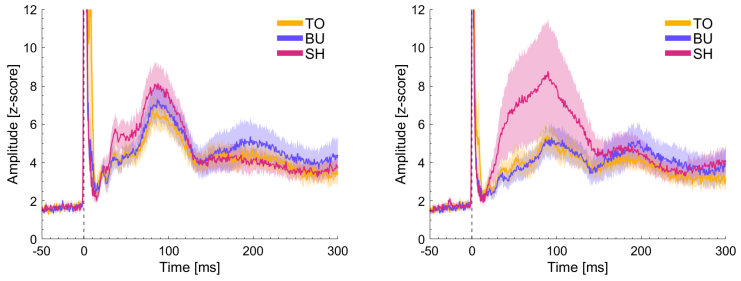

(j) IC left. **(k)** IC right.

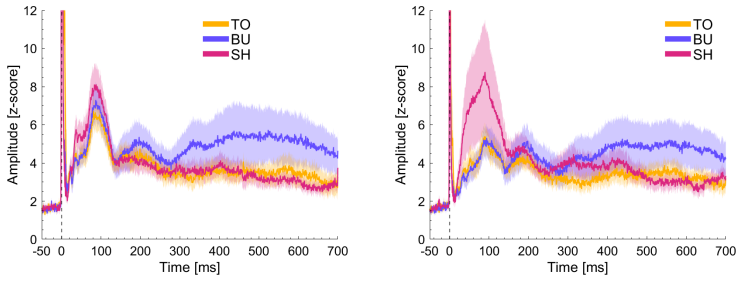

(l) IC left, 700ms. **(m)** IC right, 700ms.

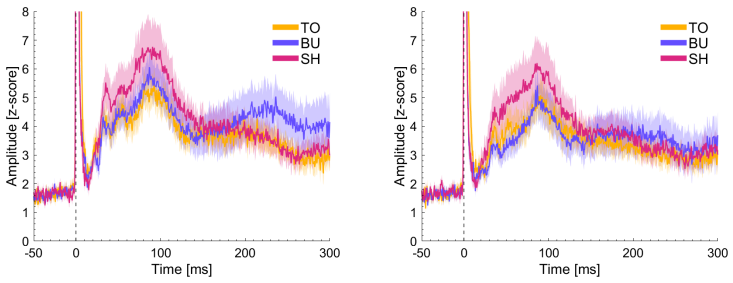

(n) Thalamus left. **(o)** Thalamus right.

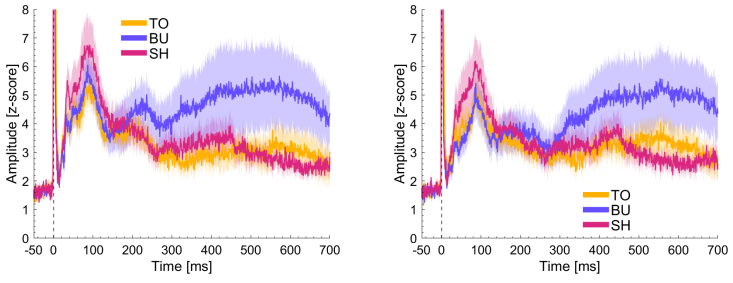

(p) Thalamus left, 700ms. **(q)** Thalamus right, 700ms.

Figure I.6: An overview of the somatosensory evoked responses elicited by median nerve stimulation in all regions of interest for the comparison between tonic, burst, and sham spinal cord stimulation. Note the two different ranges of the horizontal axis: either -50 to 300 milliseconds or -50 to 700 milliseconds.
S1, primary somatosensory cortex; S2, secondary somatosensory cortex; ACC, anterior cingulate cortex; MCC, middle cingulate cortex; PCC, posterior cingulate cortex; IC, insular cortex; TO, tonic spinal cord stimulation; BU, burst spinal cord stimulation; SH, sham spinal cord stimulation.